THE EVALUATION OF THE SUSTAINABILITY OF A MODERN RESIDENTIAL DWELLING IN A HUMID SUBTROPICAL ENVIRONMENT

A Dissertation

by

JAMES FRANCIS SWEENEY

Submitted to the Office of Graduate and Professional Studies of
Texas A&M University
in partial fulfillment of the requirements for the degree of

DOCTOR OF PHILOSOPHY

Chair of Committee,	Robin Autenrieth
Co-Chair of Committee,	Michael Pate
Committee Members,	Ronald Kaiser
	Kelly Brumbelow
	Yassin Hassan
Interdisciplinary Faculty Chair,	Ronald Kaiser

December 2015

Major Subject: Water Management and Hydrological Sciences

ABSTRACT

The objective of this research is the life cycle analysis of a high-performance, above-code home as compared to a more traditionally built home in a humid, subtropical environment. Building energy estimations and environmental impacts analyses were performed, and model development and results were presented. Renewable energy and rainwater collection systems impacts were also investigated.

Annual operational energy was reduced 30% due to decreases in the HVAC energy associated with infiltration and building envelope differences between the 'Reference' and 'As-Built' models. Gas-based heating models embodied energies were 6% and 12% of the total energy and the use phase energy was 93% and 87% for the 'Reference' and 'As-Built' models, respectively. The embodied energy in the 'Reference' model was almost half of the embodied energy in the 'As-Built', but the 'As-Built' model achieved a reduction of life cycle primary energy of 23% compared to the 'Reference' model.

A reduction of 6,314 GJ and 402 metric tons of primary energy and GWP was achieved for the 'Reference' compared to the 'As-Built' model. Total primary energy over the life cycle was 26,216 and 19,983 GJ, with energy intensities of 44.4 and 33.8 GJ/m^2 for the 'Reference' and 'As-Built' models, respectively. The electrical-based heating models followed similar trends as the gas-based model but with a small increase in operational energy. Global warming potential had similar distribution patterns as that of the primary energy and total life cycle global warming potential intensities were

estimated for the ‘Reference’ and ‘As-Built’ models, respectively as 2,835 and 2,166 kg CO_2-eq/m^2.

Solar electric and hot water renewable energy systems decreased the annual operating energy by 12.5% and 15.5% and the total life cycle primary energy by 9.4% and 13.4% for the ‘Reference’ and ‘As-Built’ models, respectively. Finally, with no rainwater harvesting, total water consumption was 29.68 and 31.78 mega-liters for the ‘Reference’ and ‘As-Built’. The use phase dominates both models with 85% and 80% of the use phase for the ‘Reference’ and ‘As-Built’ model, respectively. Rainwater harvesting systems may offset the life cycle use phase and with a Monte-Carlo simulation yielded a 73% demand reduction with a 48% probability.

DEDICATION

This dissertation is dedicated to my mother and father, Patricia Mclean Schwing and James Francis Sweeney for their love that brought me into the world and provided my foundation and for my love, Stacy Ferrell, whose patience, encouragement and love have made this work possible.

ACKNOWLEDGEMENTS

I would like to thank my committee chairs, Dr. Robin Autenrieth and Dr. Michael Pate, for their continued support, guidance and personal advice. I would also like to thank my committee members, Dr. Ronald Kaiser, Dr. Yassin Hassan, and Dr. Kelly Brumbelow, for their guidance and support throughout the course of this research.

Thanks and love to my sister and brother, Piper Ann Sweeney Carrion and Mark Lee Sweeney and their families and my daughter Emma Rose Sweeney for the love and encouragement over the long and winding road that was this work and a final thanks to my friends and colleagues at Texas A&M University and the surrounding community.

I want to thank Kelly Milligan and Christopher Faust, who have been involved with this project from the beginning; their support and passion was essential. To Dr. Peng Yin, who assisted this effort with his incredible productivity with Energy Plus and Wongyu Choi for the help with uncertainty estimations. To Charles Romero, for helping me handle the dissertation template and to Kathy Wadle and all the other staff and students, past and present, at the Riverside Energy Efficiency Laboratory, thank you!

NOMENCLATURE

AFUE	Annual fuel utilization efficiency
AMY	Actual meteorological year
ANSI	American National Standards Institute
AP	Acidification potential
ASHRAE	American Society Heating Recovery Air Conditioning Engineers
BMCC	Building material and component combinations
CFC-11	Chlorofluorocarbons
CFM	Cubic feet per minute
CV	Coefficient of variation
DOE	Department of Energy
DX	Direct expansion
EE	Embodied energy
EIU	Energy intensity
ELA	Effective leakage area
EP	Eutrophication potential
EPRI	Electric Power Research Institute
ERV	Energy recovery ventilator
EUI	Energy use intensity
GJ	Giga Joule
GWP	Global warming potential

HERS	Home energy rating system
HDKR	Hay-Davies-Klucher-Reindl solar radiation model
HVAC	Heating, ventilation and air conditioning
ICF	Insulated concrete form
IE	Impact estimator
IECC	International Energy Conversation Code
ISO	International Organization for Standardization
KW	Kilowatts
kWh	Kilowatthour
LCA	Life cycle analysis
LCC	Life cycle cost
LCEA	Life cycle energy analysis
LCIA	Life cycle impact analysis
LCOE	Levelized cost of energy
LEED	Leadership in Environmental and Energy Design
MBE	Mean bias error
MJ	Mega Joule
NCDC	National Climatic Data Center
NEUI	Net energy use intensity
NPV	Net present value
NREL	National renewable energy laboratory
OE	Operating energy

OSB	Oriented strand board
PE	Primary energy
PM2.5	Particulate matter 2.5 micrometer
PNNL	Pacific Northwest National Laboratory
PSK	Poly-skrim-kraft
PV	Photovoltaic
RE	Renewable energy
RESNET	Residential energy services network
RMSE	Root mean square error
RWH	Rainwater harvesting
RWHS	Rainwater harvesting system
SAM	System Advisory Model
SBIC	Sustainable Buildings Industry Council
SEER	Seasonal energy efficiency ratio
SHGC	Solar heat gain coefficient
SHWS	Solar hot water systems
SP	Smog potential
SPVS	Solar photovoltaic system
TMY	Typical meteorological year
TRACI	Tool for the reduction and assessment of chemical and other environmental impacts
TWDB	Texas Water Development Board
UK	United Kingdom

US	United States
US EPA	United States Environmental Protection Agency
US DOE	United States Department of Energy
US EIA	United States Energy Information Administration
USGBC	United States Green Building Council
VT	Visual transmittance
W	Watt
WPCG	Whole process cradle to grave

TABLE OF CONTENTS

Page

LIST OF FIGURES

Page

LIST OF TABLES

Page

CHAPTER I

INTRODUCTION AND LITERATURE REVIEW

In the summer of 2008, a Houston, Texas homeowner contacted Texas A&M University and began a discussion on the design and construction of a homeowner's future new home. These discussions led to many dialogues that resulted in a research endeavor. The concept of the ultimate high performance home was to be a blend of durability, energy efficiency, safety and security, environmental comfort and air quality and other 'green elements', such as sustainably sourced floors. The philosophy of the home was to build a durable house with lower energy and water costs, lower insurance premiums, low long-term maintenance and impressive resistance to the environment. The dwelling incorporated a durable and robust building envelope (walls, fenestration, roof and slab), efficient environmental control systems, renewable energy systems and an efficient water system, including rainwater collection. The building followed the US Green Building (USGBC 2015) Leadership in Environmental and Energy Design (LEED) guidelines and was built in the latter half of 2009, which led to it being awarded a LEED-Homes Platinum level designation in the fall of 2014.

The building sector is major contributor to socioeconomic development of nations, but it also utilizes a large proportion of energy and available natural resources (Ramesh et al. 2010) while the construction industry is the largest user of materials in the United States (US) (Horvath 2004). In addition to growing concerns over resource consumption and scarcity, climate change is an ever-present geopolitical issue, and the control of greenhouse gases such as carbon dioxide (CO_2) are the focus of mitigation

strategies. Scientific evidence is now overwhelming, climate change presents serious global risks and demands an urgent global response (Stern 2007). In addition, the emission of CO_2 from fossil fuel combustion for the production of electricity, in conjunction with that emitted from cement manufacturing is responsible for more than 75% of the increase in atmospheric CO_2 since the pre-industrial 18^{th} century (Solomon et al. 2007).

In 2014, 41% of total US energy consumption was consumed in residential and commercial buildings, or about 40 quadrillion British thermal units (BTU). Residential heating, ventilation and air conditioning (HVAC) systems alone accounted for 48% of residential building energy consumed in the United States (US EIA 2015), and on average, 40% of the energy consumed in the residences of Texas (US EIA 2015). In the United States, 73% of the thermal loads are derived through the building envelope (non-internal) (US DOE 2009). In this particular study the building envelope was a durable, insulated concrete form (ICF) wall system with a steel roof and a sealed attic space. ICF technology is known to improve the thermal performance of residential buildings by reducing and controlling thermal migration and improving infiltration characteristics (Chasar et al. 2000, Kossecka and Kosny 2002). However, residential concrete form production utilizes more energy and water when compared with typical wood-frame construction (Trusty and Meil 1999).

Heating, ventilating and air conditioning systems (HVAC) mediate the thermal loads not directly controlled by the building envelope. The case study house used in this study has two state-of-the-art, efficient 4-ton heat pumps equipped with energy recovery

ventilators for further climate control. Properly sized and efficient environmental controls are essential to providing the best building strategies that moderate overall life cycle costs.

After heating and cooling, hot water is the second largest consumer of energy in the United States (US DOE 2009). Onsite renewable energy may provide high quality energy while providing lower life cycle costs when compared to conventional systems (Pehnt 2005). Solar thermal is a cost-efficient method for delivering hot water, however appliance upfront costs, efficiencies, installation, and other maintenance issues may dampen performance and should be included in the cost accounting. Approximately 4% of the US electrical demand is for the movement and treatment of water and wastewater (EPRI 2002); additionally, water scarcity in Texas is a concern in some locales (Griffin 2011). Onsite rainwater systems may potentially provide clean water, water storage, and offset costs and demand and may also offset burdened centralized storm water systems. As such, the rainwater harvesting system performance, life cycle impacts and costs are critical elements when reviewing the sustainability of a dwelling.

The over-arching purpose of this research was to evaluate a high-end, high-performance residential dwelling in Houston, Texas from a life cycle perspective. The principles objectives of this research were the study of the building as designed while comparing it to a more traditionally built home and discovering those systems that most impact the life cycle energy, global warming potential and other environmental indicators, an additional objective is to assess the contribution of renewable energy systems and a rainwater collection system. Furthermore, life cycle management can be

applied to the whole construction process, thus making it possible to characterize and improve sustainability indicators and also minimize the environmental loads over the full building life cycle (Ortiz et al. 2009). Understanding modern residential building components impact on life-cycle performance is of value in a climate sensitive and resource-constrained age. Therefore, this study will document a particular building design concept and compare its performance to more traditional construction methods and practices over a 50-year life cycle.

Problem Description and Research Objectives

The residential building market has traditionally embraced the aesthetics and superficialities of the home and while glorifying rapid production, low-cost construction, and mediocre workmanship. The homeowner's attention has rarely been focused on construction components, individual systems and the fabric of the dwelling. Durability was often overlooked for cost savings, and in the current era of increasing resource scarcity, global climate change, environmental hazards, and rising energy and water prices, more attention has been focused on house design and its impacts. Consumer awareness of operation and maintenance costs, environmental impacts, durability and sustainability has increased. These complex issues are compelling individuals, corporations and governments to conserve, harness and manage their resources more acutely. The financial and ecological costs of over-reliance on centralized energy and water have also resulted in a renewed focus on the areas of energy and water efficient homes and renewable forms of energy.

Residential dwellings take a considerable amount of energy and water to build, operate and maintain through their lifetimes. Residential buildings require constant inputs of energy and water to operate and maintain a comfortable environment. The availability and expense of energy and water are of growing concern. Building systems that mediate the external environment, while providing efficient thermal comfort and durability and harvesting their own energy and water, are emerging in the markets of sustainable products. Rapid urbanization is a global phenomenon, resulting in material-use and waste-generation issues being of critical importance to sustainable urban development worldwide (Theis 2005). As Li, et al (2007) suggests, strategies are needed that minimize the environmental impact of expanding urban infrastructure while improving social and economic value. Also, it is essential to evaluate and find comprehensive solutions to manage the development and maintenance of the built environment. Managing urban infrastructures is complex and multi-disciplinary so that it must be done from a 'sustainably' standpoint, which requires the building industry to focus on covering a number of theaters such as energy saving, improved use of materials, including water, reuse and recycling materials and emissions control (Ramesh et al. 2010).

A way to evaluate buildings and their impact is to view the building through the lens of 'building sustainability', and the Sustainable Building Industry Council (SBIC) defines a sustainable building as one in which the site, design, construction, occupancy, maintenance, and deconstruction of the building are accounted for in ways that promote energy, water, and material efficiencies, while providing healthy, productive, and

comfortable indoor environments and long-term benefits to owners, occupants, and society as a whole (SBIC 2012). The assessment of building 'sustainability' is comprised of an evaluation of the buildings energy and resource consumption and associated environmental impacts over the course of the buildings life cycle. For example, life cycle analysis (LCA) is an excellent tool to evaluate the overall environmental impacts of a product because it considers all the inputs and outputs related to the production, use, and end of life along with their potential environmental impacts (Kahhat et al. 2009), therefore, it is the primary method used in this comparative evaluation.

The focus of this research will be to determine the relative contribution of each building component and system to the 'sustainability' of the building through the operational energy phase of the life cycle. Additionally, embodied energy, and other life cycle phases will be estimated with life cycle accounting tools. The principal building systems that will be evaluated are: 1) the building envelope and infiltration, 2) environmental controls (HVAC), 3) the renewable energy systems (photovoltaic and solar thermal system), and 4) the water and rainwater system. System components will be evaluated with embedded real-time monitoring equipment and sensor networks, and various state-of-the-art modeling tools for a comprehensive analysis. The following is a list of overarching objectives for this research.

Research Objectives

1. Review and evaluate the various tools and metrics and modeling systems for dwelling sustainability characterization.

2. Model the dwelling with a publicly available building simulation tool and calibrate the HVAC portion of the model with field data.
3. Estimate the effect of the building envelope design and environmental controls on the cumulative operation energy and embodied energy over a 50-year life cycle through modeling and performance data evaluation.
4. Estimate the effect renewable energy components have on sustainability through modeling and performance data evaluation over a 30-year life cycle.
5. Estimate the effect water system components have on sustainability through modeling and performance data evaluation over a 50-year life cycle.
6. Perform the life cycle analysis on both the a 'Reference' and 'As-Built' buildings and report results that focus on the embodied and use-phase differences along with associated impacts from the renewable and rainwater systems.
7. Make recommendations to improve the performance of the case dwelling by improving and upgrading the various components being evaluated.
8. Perform long and short-term field studies with low-cost instrumentation and sensor networks where feasible.

Literature Review

A building sustainability characterization was performed by performing a building life cycle impact analysis for a 'Reference' and 'As-Built' building design for a 50-year period. This research spanned several areas of relevant research from urban sustainable development, building life cycle analysis, building operational energy, small-scale renewable energy systems and, finally, urban water and rainwater systems research. A sample of relevant literature is dealt with in the following sub-sections.

Building Sustainability Research

In the context of buildings, a sustainability framework is an instrument to compare dwelling optimization capabilities and strategies against other building design alternatives. However, sustainability has moved from a qualitative abstraction to a multidimensional analytical problem. Ortiz et al. (2009) applied life cycle analysis to evaluate environmental loads of a 167 m^2 (1,800 ft^2) residential home in Spain over a 50-year life span. Other accounting practices such as exergy are similar to what Brown and Herenbreen (1996) call energy 'form', with Exergy being the quality of energy utilized. Energy conversions do not affect the amount of energy; it is the quality that is affected (De Meester et al. 2009). Converting high-grade (quality) energy from natural gas to space heating is inefficient. Subsequently, the quality of the energy (exergy) is diminished. In contrast, converting renewable forms of energy into heating is high quality. Exergy accounting methods do not split the energy and material resources, and it may offer decision support options for energy/material optimization problems (De Meester et al. 2009). De Meester, et al. (2009) evaluated 65 optimized Belgian dwellings

in a comprehensive exergetic life cycle approach. De Meester's research took the life cycle assessment one step further and coupled it with an exergy analysis, with the objective of De Meester et al. (2009) being to perform the analysis on the entire building and its construction. Exergy analysis was performed to assess the resource consumption in both the construction phase (embodied exergy) and operational phase (operational phase exergy).

Several researchers have utilized these concepts to evaluate building systems (Brown and Ulgiati, 1997, Chen et al. 2001, Olgyay and Herdt 2004, Pulselli et al. 2007). Operating energy analysis embodied energy, life cycle assessments, and exergy (energy quality) analysis (Brown and Ulgiati 1997, Ortiz et al. 2009, Torio et al. 2009) are typical; however, exergy alone, although suited to evaluate systems that produce and use resources, is less understood and not as widely published in the building life cycle analysis literature (Zargarzadeh et al. 2007, Zhang et al. 2010). Impact oriented approaches such as LCA is the more common approach for considering broader environmental impacts of production processes, and it has been the subject of intense research over the last decade (Buyle et al. 2013, Singh et al. 2010, Zhang et al. 2010).

Life Cycle Analysis

Life cycle analysis is a tool for evaluating industrial products and process and is well utilized by academic, governmental bodies and industry alike. According to the Environmental Protection Agency (EPA 2011), life cycle assessments can be defined as techniques for assessing the potential environmental aspects and potential aspects associated with a product or service by: 1) compiling an inventory of relevant energy

and material inputs and their environmental releases, 2) evaluating the potential environmental impacts associated with identified inputs and releases and 3) interpreting the results to help the user make a more informed decision. Inventory involves data collection and calculation to quantify matter and energy inputs and outputs of the system while impact assessment evaluates the significance of the potential environmental impacts based on the aforementioned inventory (Ramesh et al. 2010). The system boundaries of the analysis typically include the energy and environmental impact of the following phases of the life cycle: 1) manufacture, 2) use, 3) and demolition. The manufacture phase includes manufacturing and transportation of building materials and installations used in the building and renovation of the structure. The use phase encompasses all activities related to the use of the building over it life cycle, including the use, operation, maintenance and repair phases. Finally, the demolition phase includes destruction of the building and transportation of materials to landfill sites and, if included, the recycling of materials.

While the LCA approach has been used to quantify energy and environmental impacts since the 1960's, it was not codified until the 1990's and subsequently in 2006, when the International Organization for Standardization (ISO) published ISO 14040 (Elcock, 2007). LCA is a tool for systematically analyzing environmental performance of products or processes over their entire life cycle, including raw material extraction, manufacturing, use, and end-of-life disposal and recycle. (Ciambrone 1997, Joshi 2000). LCA methods have been used for environmental evaluation of product development processes in other industries for a long time (Cabeza et al. 2014), although application to

the building construction sector has only been state of the art for the last ten years (Buyle et al. 2013, Singh et al. 2010).

Environmental impact measures reported typically in an ISO 14040 compliant form are global warming potential (GWP) (CO_2 equivalent mass), acidification potential (AP) (H^+ ions equivalent mass), human health criteria (PM2.5 equivalent mass), eutrophication potential (EP) (Nitrogen equivalent mass), smog potential (SP) (O_3 equivalent mass), ozone depletion potential (CFC-11 equivalent mass) and fossil fuel consumption (fossil fuel energy in GJ).

Life Cycle Energy Analysis

Life cycle energy analysis is one of the most common of the environmental impact indicators used in literature (see De Meester 2009, Kahhat et al. 2009, Keoleian et al. 2000, Li et al. 2007, Monahan and Powell 2011, Otriz, et al. 2009, Ramesh et al. 2010, Sartori and Hestnes, 2006) primarily because the environmental impacts are strongly correlated with the primary energy utilized for the entire building life cycle (Huijbregts et al. 2006, 2010). Life cycle energy analysis (LCEA) is part of LCA that accounts for all energy inputs to a building in the life cycle (Ramesh et al 2010). Also, LCEA of buildings suggests strategies to achieve reduction in primary energy use of the building, control emissions and is fairly straightforward to compute. Life cycle energy includes (Ramesh et al. 2010), 1) embodied energy, 2) operating energy (use phase), and demolition energy (end-of-life). The embodied energy is the energy content of all the materials used in the building and installations, and energy incurred at the time of new construction and renovation of the building (Ramesh et al. 2010). Finally, demolition

energy is the energy required at the end of the buildings′ service life to demolish it and to transport the material to landfill sites and/or recycling plants. The literature reports that the energy is life time energy, typically in energy over a time frame. However, in some cases, an energy intensity is reported, which is, energy across an area over a defined time period (Citherlet and Defaux 2007, Monahan and Powell, 2011, Ortiz et al. 2009, Ramesh et al. 2010, Sartori and Hestmes 2006).

Utilizing large datasets of office and residential LCA cases from around the world, but mostly from cold climates, Satori and Hestnes (2006) and Ramesh et al (2010) found a linear relationship between total life cycle energy and operational energy. Sartori and Hestnes (2006) also found that buildings with lower total life-cycle energy often had a higher embodied energy but also lower operational energy. Additionally, several "self-sufficient" homes were higher in total life cycle energy than a more, energy-efficient approach due an overuse of embodied energy. Operating energy analysis is typically derived from the energy required to operate a device or process, and it is broadly used to characterize many engineered systems. In terms of total life cycle energy, the operation phase of a dwelling is often a dominant portion of an evaluation (De Meester 2009, Keoleian et al. 2000, Otriz, et al. 2009, Ramesh et al. 2010).

As discussed previously, operating energy for residential dwellings may dominate the energy usage of the building over its lifetime and, as Ramesh et al (2010) suggests, reductions in life cycle energy of designed buildings over their conventional counterparts are proportional to the degree and number of energy saving measures used in the building (where conventional buildings refers to a building built according to the

common practice of a specific country). However, reduced demand for operating and life cycle energy is achieved by an increase in embodied energy of the building due to the energy intensive materials used in technical and other installations. Other researchers have identified this situation as well; Thormark (2002) reported that embodied energy and its share in life cycle energy for low energy buildings is higher than conventional building.

Treloar et al. (2001) presented an evaluation of the embodied energy content of several commonly used construction materials in Australia where the authors argued that embodied energy deserves attention along with the building operational energy. Building envelope thermal properties and permeability have an impact on energy use, and from the literature it can be concluded that environmental impacts correlate closely with primary energy demand of the buildings in their life cycle (Ramesh et al. 2010). From most of the available literature, one can conclude that the operational phase contributes more than a 80-85% share in the total life cycle energy of buildings (Ramesh et al. 2010, Richman et al. 2009, Sharma et al. 2011, Shu-hua et al. 2010), and future efforts should be focused on reducing the operational phase, even at the cost to other less-significant phases.

Though embodied energy constitutes only 10-20% of the life cycle energy, an opportunity for its reduction should not be ignored, and there is potential for reducing embodied energy requirements through the use of materials in the construction that require less energy during manufacturing (Ramesh et al. 2010). Langston and Langston (2008) suggest that operation energy is easy and less complicated in accounting, while

embodied energy is more complex and time consuming, requiring manual takeoffs and robust software.

Other Environmental Impact Indicators

Many authors report other environmental impact indicators and with indicators that are utilized most frequently by the building LCA literature reviewed being total primary energy (PE) and global warming potential, and air (smog, human health respiratory and ozone depletion potentials) and water (eutrophication potential). Adalberth et al. (2001) performed LCA on four multi-family homes and studied different phases of the life cycle of four buildings for the purpose of researching which phase had the largest environmental impact and determining if there were any differences in environmental impact dues to the choice of building construction. Furthermore, their study referred to typical LCA environmental impact indicators such as PE, GWP, AP, EP and human toxicity, and the use phase was estimated to be 70-90% of total environmental impact caused by a building. Atmospheric indicators are the most common indicators reported beside total primary energy (Citherlet and Defaux 2007, Marceau et al. 2006, Monahan and Powell 2011, Ortiz et al. 2009, Ramesh et al. 2010), and some authors report intensity measures as well, such as GWP intensity (Citherlet and Defaux, 2007, Monahan and Powell 2011, Ortiz et al. 2009).

LCA in Building Design Comparisons

As recently suggested, understanding building embodied energy and associated environmental impacts is useful to understand building assembly impacts, and it may lead to informed decision-making based on the values considered, including long term

energy savings or ecologically associated effects such as global warming potential or water consumption. Additionally, the building design effects not only the embodied energy and impacts but also the total life energy, most critically, the operation energy.

Citherlet and Defaux (2007) compared three variants of residential homes in Switzerland, namely, a standard, conventionally design home, a low-energy home and a very low-energy system, while utilizing GWP and AP intensity to illustrate a decrease in GWP as the building efficiency improved. Marceau (2006) compared a two-story single family (2450 ft^2) with a wood-frame structure and with insulated concrete, and the operational energy was found to be lower in the ICF home and determined that the ICF home moderates the load required, requiring less energy. Operating energy was found to be the most significant impact phase through emissions and resource depletion. Kahhat et al. 2009, also addressed a variety of building assembly designs (ICF, concrete blocks, cast-in-place, 2"x6", 24" on center wood frame and steel framed walled systems) and found that the operational energy was 94% of the life cycle energy and that the ICF wall system utilized 5% less energy than the wood-framed system. Additionally, Kahhat et al. (2009) found that the largest pre-use life cycle impact arose from concrete in the building structure. Finally, Monahan and Powell (2011) compared traditional vs. 'modern methods of construction' (MMC) models in the United Kingdom, in with the GWP density indicator and found that MMC achieved a 34% reduction when compared to traditional methods of construction; MMC in this study was a wood-framed wall and the traditional construction was a masonry cavity wall.

Life Cycle Accounting Tools

In the study reported herein, a process-based LCA was performed by using the Athena Sustainable Material Institute's (ASMI) Environmental Impact Estimator (IE), and the models determined the environmental impacts based on current constructions practices and quantified the amount of material in each of the wall systems while covering almost all of the system used in residential buildings (Li et al. 2007). Impact Estimator has been referenced in the literature as tool to estimate life cycle energy of buildings, construction components and their associated environmental impacts based on International Standards Organization (ISO) 14040/140440 and US Environmental Protection Agency's (US EPA) Life Cycle Impact Assessment (LICA) methods (ASMI 2014, Happio and Viitaniemi 2008, US EPA 2011). IE is easy to use and is especially suitable for building construction because it considers various critical factors such as building type, on-site construction, related transportation, maintenance, repair and replacement effects, operation energy emissions, regional variation in energy use and transportation (Kahhat et al. 2009). In general, the life cycle inventory data included second-order system boundaries, that is, primary flows plus energy and material flows including operations (Marceau et al. 2006).

Building Operating Energy Research

The study reported herein seeks to further the residential building life cycle literature by reporting a comparative study of an actual energy-efficient residential building and a modern IECC 2012 code equivalent home in a hot and humid climate by utilizing the US DOE Energy Plus building simulation software to determine the annual

operational energy. The HVAC model in the Energy Plus simulation was based on a calibrated model from performance data measured in the field. Other non-HVAC end-use loads were determined based on Pacific Northwest National Laboratory simulation guidelines and International Energy Conservation Code (IECC) 2012 code minimums. Gas and electric water and space heating models were also presented. Additionally, the study reported on water consumption over the life cycle for both cases, and finally, the study also addressed the impact of renewable energy and rainwater collection system on the associated life cycle indicators.

Building Envelope

The building envelope mitigates the building from the affects of the external environment and is fundamental to many of the critical design criteria such as energy efficiency, environmental control, security, and hurricane/tornado resistance. The design strategy employed several novel design strategies compared to typical residential building construction. The building envelope is critical in maintaining thermal comfort and many studies have reviewed the building envelope's effects on minimizing heating and cooling loads (Antonopoulos and Koronaki 1999, Henze 2005, Kossecka and Kosny 2002, Kosny et al. 1998, Siddiqui and Fung 2009). The building envelope maintains thermal comfort by providing structure and minimizing air filtration/loss. Building structure heat transfer characteristics such as control of radiation (surface emissitivies), conduction (R-value) and convection processes are the main mechanisms of heat flow in and out of a building.

The research seeks to evaluate the 'As-Built' building envelope compared to a traditional wood-frame home 'Reference' case in terms of infiltration and overall building envelope affects as reported in annual operation energy consumption. The 'As-Built' case building wall system is (from the outside to inside): 1) stucco and/or brick, 2) an air gap (maintained by 1x1.5" battens every 6 inches), 3) a combined radiant/vapor barrier, 4) an ICF wall (2.5" of polystyrene, 6" concrete, 2.5" polystyrene), and 5) a 5/8th inch fire rated drywall. The total thickness of the ICF wall system is 14-16 inches. The 'Reference' case is the more a conventional 2"X4" wall of International Energy Conservation Code (IECC) complaint (2012). The 'Reference' building envelope assumed the same geometry and new constructions for fenestration, exterior and interior walls, roof, ceilings, and floors were implemented. All constructions followed IECC code and are adopted directly from US DOE-PNNL 'Reference' code (Mendon et al. 2013). The 'Reference' home was based on the 'As-Built' geometry but incorporated a more typical building construction that met IECC 2012 code and the envelope model descriptions of both buildings models are listed in Chapter 2.

Building envelope designs may incorporate strategies that have high-mass walls that contain high density and high capacity materials such as concrete. These types of walls can produce thermal storage that can store energy (hot or cold), thus resulting in a dynamic capacitance characteristic of the building that has been shown to offset energy loads (Antonopoulos and Koronaki 1999, Henze, 2005, Kosseecka and Kosny 2002, Siddiqui and Fung 2009, Reddy 2000). The dynamic effect of thermal capacitance is well characterized and primarily performed with simulation tools and modeling (Kosny

et al. 1998, Kosseecka and Kosny 2002). Even though little field information exists it has been found that increasing thermal capacitance leads to maximizing heat/cool storage, reducing peak loads and smoothing energy fluctuation (Antonopoulos and Koronaki 2000).

In Houston, a passively ventilated attic is typical. Houston attics reaching temperatures over 130 degrees F and nearly 100% humidity on summer days. This heat input to the building envelope affects the air conditioning systems by reducing product lifetimes, efficiency, and may creep into leaky ducts, leaky ceilings and other penetrations into the conditioned space. Additionally, heat conducts through the framing system via thermal bridging. The project incorporated a sealed attic with a durable and heat-rejecting boundary. The roof system is a radiant-vapor barrier installed below a shingle-based steel roof that has a wind rating of 130+ mph. This was installed on top of a classic rafter support structure that was insulated with open-cell foam.

Utilizing building simulation software, this study evaluated the building system's environmental control capabilities compared to the 'Reference' case based on building envelope and infiltration effects. An inherent property of the As-Built model (ICF construction and sealed attic) is low effective leakage area. The interconnectedness of the foam block and the monolithic nature of the concrete yield a wall system with little infiltration crevices or gaps in the wall system. To separate the effects of the infiltration from the building envelope, thermal and infiltration modeling control may be performed to isolate the effects.

Environmental Controls

The owner installed two high efficiency (17 SEER), four-ton air-sourced heat pumps. The size of the house required that two zones be established, one for each floor. Ducting was located in a sealed highly insulated attic space. Fresh air intake into the building environment is important to maintain air quality in an airtight building. Various devices maintain the environmental comfort in the building including: 1) air-sourced heat pump, 2) bathroom ventilators, and 3) energy recovery ventilators. Houston, Texas is often hot and humid and the fresh humid air intake can be mitigated with an Energy Recovery Ventilator (ERV), especially during cooling season. ERVs contain cross-flow heat exchangers that provide enthalpy transfer by exposing incoming and outgoing air to each other across a conductive matrix core and ERV application and optimum control strategies in different climatic regions have been performed (Rasouli et al. 2010, Zhou et al. 2007). Zhou has documented (2007) that ERVs capable of moisture recovery may reduce annual cooling load by 20% if the ERVs are properly controlled. ERV system controls will be evaluated and control strategies will be suggested to optimize heat and cooling. All environmental controls operating energy will be monitored to calibrate the As-Built operational energy model.

Renewable Energy Research

Hot water is critical to the house system for traditional residential uses and potentially for space heating via ducted hot water coils. The dwelling utilizes flat-plate collectors, thermo-siphon heat exchanger mated with an 80-gallon water storage tank. In addition, an on-demand hot water heater backs up the solar hot water system (SHWS).

The house is also equipped with a 3.5 kW, 20-panel polycrystalline solar photovoltaic system (SPVS) installed on the southeastern roof at a 42-degree tilt, and the system is grid-tied with no battery storage. The potential of renewable energy systems to offset operating energy can be significant, however, installation and operational issues may plague their performance. Additionally, product efficiencies may be overstated and simulation tools such as National Renewable Energy Laboratory's Solar Advisory Model and TRYNSYS have been used to optimize and study solar thermal systems in residential applications (Hobbi and Siddiqui 2009, Kalogirou 2009). Additionally, Kalogirou (2009) presents thermal performance with life cycle evaluation of a thermosiphon solar hot water system and a similar approach will be conducted to estimate the impact of these systems installed at this location. This research utilized NREL's SAM because of combination of solar modeling with a robust solar radiation database, life cycle energy and economic features and is public-availably (Blair et al. 2014). SAM's PV models have been verified and validated against measured data (Blair et al. 2012, Freeman et al. 2013, Rudie et al. 2014, Thevenard and Pelland 2011). In addition, Blair et al. (2012) and Freeman et al. (2013) compared model versus quality-controlled measured performance data for nine PV systems. Blair et al. (2012) found ± 3% or less annual errors for all the systems at and monthly errors varying ± 6%, while Freeman et al. (2013) concluded that combinations of SAM mode errors fell within an annual error range of 8.5%. SAM was utilized to verify existing residential renewable energy systems performance to perform optimizations and to estimate life-cycle energy production and costs in the context of a building life-cycle analysis.

Onsite Water Systems Research

As water resources become more stressed, higher water pricing and regulation will be implemented. Many municipal water supplies, while safe, have documented levels of high chlorine, deposit forming minerals, heavy metals and other unregulated contaminants. Alternate water sources, such as rainwater harvesting, are becoming more attractive options to handle ever-increasing demands and costs. According the Li et al. 2010, motivation for these alternate water system lies in several factors: 1) consumer cost of water and wastewater will rise, 2) climate change may alter rainfall, 3) population growth and standard of living increasing, 4) high-quality water used of low quality purposes, and 5) runoff and wastewater handling reductions.

Rainwater harvesting can supply high quality water. Rainfall in Houston ranges from three to six inches per month affording ample opportunity to catch and store water. The home's system is able to harvest water from approximately 75% of the roof, passing water through covered gutters to a macro-filtering system and then into an underground cistern. Potable water can be accessed from the cistern or domestic supply and all water domestic water is passed through an advanced water filtration system utilizing reverse osmosis and ultraviolet radiation. Approximately four people could use this supply at 80 gallons-per-day for 24 days.

In order to evaluate the utility of a rainwater system, a life cycle approach must be utilized and several authors have reported using this approach for specific situations and applications (Basupi 2013, Farreny et al. 2011, Ghimire et al. 2014, Roebuck and Ashley 2006, Ward et al. 2008). In particular, Roebuck and Ashley (2006) demonstrated

verified life cycle software tools that will be used in the study reported herein. Using a macro-enabled spreadsheet, hydraulic simulation and life cycle analysis production and costs were performed on an urban rainwater system.

This study will analyze the rainwater system costs and benefits in the life cycle context for 50-years, and it will offer alternative redesigns for similar conditions in more competitive constraints. The simulations are constrained by input parameters such as on-site water demand data, historical rainfall analysis and other site-specific information and financial inputs.

Scope and Organization

This dissertation is split into three primary sections, excluding introduction, conclusion and appendices; the first, chapter two, focuses on the energy consumed and embodied in two different building design scenarios and environmental impacts associated with their life cycles, the second section, chapter three, focuses on the impact of the onsite renewable generation system and the economics sensitivities of their implementation and the fourth chapter, focuses on the rainwater collection system and its estimated life cycle performance and economic sensitivities. The third and fourth chapters focus on the life cycle performance of the individual systems in the context of design optimizations, economic considerations and model-parameter sensitivities. Each section focuses on quantifying the energy and water consumed or produced and analyzing alternate scenarios and their associated impacts. Finally, chapter five summaries the outcomes of the researched report herein and suggests future opportunities for research.

Contributions

The aforementioned building components and systems will be integrated to evaluate the building system sustainability. Monitored data and building simulation programs will be used to simulate the energy usage of the dwelling. Specific data that is gathered from the building component studies will provide more intrinsically valid parameters for the simulation and secondary data sources were used otherwise. Simulations were performed to assess the relative impact of each component on the operation phase of the dwelling life cycle. This work explored available literature, monitored data and current analysis techniques applicable to each building system and evaluation of the whole building are presented.

Research Contributions

1. Developed and validated a residential building operational energy model for a building in a hot and humid climate with Energy Plus, a publicly available building energy simulation program.
2. Evaluated the impact of a low-infiltration (ACH1.5) insulated concrete form building envelope design ('As-Built') compared to a higher infiltration (ACH5), wood-framed, IECC-based (2012) 'Reference' case had on the annual building operational energy use.
3. Performed annual and total life cycle energy differences and life cycle environmental impacts estimated over a 50-year life cycle of both building models with Impact Estimator, ASMI's publicly available building life cycle analysis tool.

4. Evaluated the impact of renewable energy components, and water systems on the dwelling's sustainability performance over the life cycle.
5. Performed solar photovoltaic and solar hot water field studies and modeling validations in a hot and humid climate with System Advisory Model, a public available renewable energy simulation platform. In addition, system design and economic considerations were performed through life cycle costing and sensitivity analysis.
6. Performed rainwater harvesting system field studies and modeling validations in subtropical Texas. In addition, system design and economic considerations were performed through life cycle costing and sensitivity analysis.
7. Utilized sensor networks and instrumentation to verify model parameters, inputs and outputs.

CHAPTER II

OPERATIONAL AND EMBODIED ENERGY

Synopsis

The availability, expense and environmental impact of energy and water utilization are a growing concern in a resource constrained and environmentally sensitive age, and life cycle accounting tools can provide sustainability indicators of buildings to assist in the design and understanding of the impact of building systems. Residential buildings require constant material and energetic inputs to operate and maintain a comfortable and secure indoor environment; however, operating energy for these dwellings may dominate the energy usage and associated environmental impact of the building over its lifetime. An operational energy and environmental impact simulation of an energy-efficient, high-end residential house built in hot and humid climate (International Energy Conversation Code Region 2A) was performed. The energy-efficient home was a LEED for Homes Platinum designated home, and it incorporated a durable and robust building envelope and efficient, lighting, environmental controls and renewable and rainwater systems. An 'As-Built' model was developed, and additionally, a 'Reference' case was developed based on the same geometric design and location but with 2012 International Energy Conservation Code building requirements. The objectives of the research were to estimate the life cycle impact (energetic and environmental emissions) of the 'As-Built' dwelling compared to the 'Reference' from a life cycle analytical framework, incorporating both an operational and embodied energy component. The results of the study are presented in two parts; Part 1, the development

and analysis of the building energy models, including calibration and annual operation estimates, and Part 2, the development of the embodied energy model and total life cycle impact analysis. Specifically, Part 1 describes the model development and implementation in the US Department of Energy's Energy Plus building energy simulation software to estimate annual operational energy over the lifetime. The building simulation was performed in Energy Plus, and it was calibrated and verified with existing field data and actual meteorological year (AMY) weather data, and projections of operational annual energy were estimated with typical meteorological year data (TMY). Additionally, a reference home was modeled to characterize the difference in the actual house design and the reference case. Part 2 presents the life cycle accounting (LCA) estimation of the energy demand and environmental impact of the dwellings over a 50-year life cycle. LCA was performed on the 'As-Built' case, and it was compared to an IECC 2012 based 'Reference' case. Material energy estimations and impacts were performed with the Impact Estimator, LCA software publicly available from the Athena Sustainable Materials Institute. The model development is reviewed and the results are presented.

The annual operational energy was reduced by 31.2% and 28.9% for the gas and electrical space and water heating models respectively, these reductions were due to the decrease in HVAC energy, and they were determined to be from infiltration and building envelope differences in the 'Reference' and 'As-Built' models, with infiltration impacting the reductions more than twice the amount as the building envelope effects alone. For the gas space and water heating models the embodied energy phase (product

production, construction, transportation) was 6% and 12% of the total energy while the use phase (operational and maintenance) lifetime energy was 93% and 87% for the 'Reference' and 'As-Built' models, respectively. The electrical space and water heating models followed similar trends with a slightly more (1-2%) energy being utilized in the operational phase.

The embodied energy in the 'Reference' model was almost half (48%) of embodied energy in the 'As-Built', but the 'As-Built' model achieved an overall reduction of total primary energy of 23-24% compared to the 'Reference' model and over 50-year life cycle, which corresponded to an approximate reduction of 6,314 GJ (1.75 E06 kWh) and 402 metric tons of primary energy and GWP, respectively (gas and electric space and water heating models averaged). Renewable energy systems were reported to decrease the annual operating energy 12.5% and 15.5% for the 'Reference' and 'As-Built' models, respectively. Additionally, over the life cycle with a 0.5% degradation factor, the total life cycle primary energy was reduced by 9.4% and 13.4% for the 'Reference' and 'As-Built' models, respectively.

With no rainwater harvesting considered, total water consumption was 29.68 and 31.78 mega-liters (ML) for the 'Reference' and 'As-Built' models, respectively, Additionally, the 'As-Built' model contained 49% more water consumption in the product phase, 46% more in the construction phase, and 7% more overall compared to the 'Reference' model. The end-of-life phase had no water consumption. The use phase dominates both models total life cycle water consumption and was 85% and 80% of the total for the 'Reference' and 'As-Built' models, respectively. Although stochastic in

nature, rainwater-harvesting systems may dramatically offset the life cycle use phase, and the studies presented herein, based on a Monte-Carlo simulation, yielded a 73% demand reduction with a 48% probability. This reduction in demand was approximately equivalent to the corresponding embodied water in the 'As-Built' alone.

Introduction

The assessment of building sustainability in a life cycle impact context is comprised of analyzing operating energy and embodied energy of the building life cycle (Brown and Ulgiati 1997, Ortiz et al. 2009, Torio, et al. 2009). Life cycle accounting of a building generally consists of the production phase, the operating and maintenance phase and the demolition phase. The operation phase may account for a large portion of the life cycle energy and associated environmental impact. In the United States (US), 73% of the thermal loads are derived through the building envelope (non-internal) (US DOE 2009), and heating, ventilating and air conditioning systems (HVAC) control the thermal loads not mediated by the building envelope. Residential HVAC systems accounted for 48% of energy consumed in the United States (US EIA 2015), and on average, 40% of the energy consumed in the residences of Texas (US EIA 2015). Properly sized and efficient environmental controls are essential operational strategies that moderate indoor climate and overall life cycle costs. After heating and cooling, hot water is often the second largest consumer of energy in the United States (US DOE 2009); however, in recent assessments, appliances, electronics and lighting have gained a larger share, and as much as 40 to 41% of the household energy load in the West-South-Central US and Texas may be attributed these types of loads (US EIA 2015).

The building envelopes in this investigation are a durable, insulated concrete form (ICF) wall system with a steel roof and a sealed attic space, along with a more traditionally constructed wood-frame building and attic built to 2012 code standards. ICF building envelope technology is known to improve the thermal performance of residential buildings (Chasar et al. 2000, Kossecka and Kosny 2002, Kosny et al. 1998); however, due to the large consumption of concrete, residential ICF construction utilizes more energy and water when compared with typical, wood-frame construction (Marceau and Van Geem 2006, Kahhat et al. 2009, Trusty 1999). Life cycle analysis is a method to investigate the energy and resources utilized and emitted during the life cycle of the building.

Life cycle studies of buildings analyze several aspects of energy and environmental impacts, and as Kahhat et al. (2009) suggests, typically focus on the effects of energy efficient strategies, and green house gas emissions involved in the construction and production of the building, along with variances in the different types of buildings, both commercial and residential. Some studies focus on the embodied phase (Monahan and Powell 2011) while others focus on the entire life cycle (Citherle and Defaux 2007, Marceau and Van Geem 2006, Monahan and Powell 2011, Kahhat et al. 2009, Keoleian et al. 2000, Ortiz et al. 2009, Sartori and Hestnes 2006, Stek et al. 2011, Ramesh et al. 2010). Life cycle studies of buildings consistently reveal the embodied phase of the building to be less than the operational phase. As a percentage of life cycle energy, 9-10% for the embodied fraction is typical (Keoleian et al. 2000, Kahhat et al. 2009, Ortiz et al. 2009, Ramesh et al. 2010). Most studies report the

operational-use phase as the dominant phase of the life cycle unless the building is a self-sufficient building (Monahan and Powell 2011, Sartori and Hestmes, 2006).

This study seeks to further the residential building life cycle literature by reporting a comparative study of an actual energy-efficient residential building and a modern (IECC 2012) code equivalent home in a hot and humid climate by utilizing the US DOE Energy Plus building simulation software to determine the annual operational energy, along with the Sustainable Materials Institute's Athena Impact Estimator to perform the life cycle impact analysis. The HVAC model in the Energy Plus simulation was based on a calibrated model from performance data measured in the field. Other non-HVAC, end-use loads were determined based on Pacific Northwest National Laboratory (PNNL) simulation guidelines and International Energy Conservation Code (IECC) 2012 code minimums. Gas and electric, along with water and space heating models were also presented. Additionally, the study reported on water consumption over the life cycle for both cases, and finally, the study also addressed the impact of renewable energy and rainwater collection system on the associated life cycle indicators.

Background and Methodological Approach

In the summer of 2008, a Houston, Texas homeowner contacted Texas A&M University and began a discussion on the design and construction of residential buildings and the homeowner's future new home. This discussion became a research endeavor and each component of the building was meticulously discussed resulting in the concept of an innovative home was made up of a blend of durability, energy efficiency, security, safety, comfort and air quality design elements (Thompson 2010). The philosophy of the

home was to build a durable house with lower energy and water costs, lower insurance premiums, low long-term maintenance and resistance to the environment. The building followed the US Green Building Leadership in Environmental and Energy Design (LEED) guidelines, and it was built in late 2009 and occupied in 2010. In the fall of 2014 it was awarded platinum level designation.

The methods used in this study involved a combination of field research, component modeling, building simulation and material and energy life cycle accounting. Operational energy was determined by modeling the building in US Department of Energy's Energy Plus building simulation software, an industry standard, well-documented, and tested simulation software, including several HVAC system tests (Neymark and Jodkoff 2002, US DOE 2014a) and multiple building simulation program tests such as NREL's and the International Energy Agency BESTest that utilizes ANSI/ASHRAE 140-2011 Standard (ASHRAE 2011, Neymark and Jodkoff 1995).

The building geometry was constructed from building plans, interviews of the builders and first-hand knowledge of the components and systems. Once model calibrations were performed on the 'As-Built' system, a 'Reference' case was also constructed and simulated with the same geometry but with different materials and system configurations based on the International Energy Conservation Code (IECC) 2012 benchmarks used in IECC code comparison studies for the US Department of Energy and executed by Pacific Northwest National Lab (US DOE-PNNL), see Mendon et al. (2013) for more details.

The embodied energy and environmental impacts of the building envelope were also estimated with the Athena Institute's Impact Estimator, a publicly available building life cycle assessment tool. Impact Estimator has been referenced in the literature as a tool to estimate life cycle energy of buildings, construction components and their associated environmental impacts based on International Standards Organization (ISO) 14040/140440 and US Environmental Protection Agency's (US EPA) Life Cycle Impact Assessment (LICA) methods (ASMI 2014, Happio and Vitaniemi 2008). Life cycle analysis is a tool for evaluating industrial products and buildings. It is well applied by industrial, academic, and governmental bodies alike, and, according to US EPA (2011) life cycle assessments it can be defined as techniques for assessing potential environmental aspects, along with potential aspects associated with a product or service by: 1) compiling an inventory of relevant energy and material inputs and their environmental releases, 2) evaluating the potential environmental impacts associated with identified inputs and releases and 3) interpreting the results to help the user make a more informed decision. A building life cycle illustrates many of the forces and components that comprise the resource utilization, energy and environmental impact of residential buildings, and Figure 1 illustrates a typical building life cycle, the activities involved and the phases the building material undergoes including preconstruction, transport, construction, use (operation), maintenance, dismantling, recycling and disposal (Ortiz et al. 2009). Life cycle analysis attempts to approximate, with the best available databases and estimates, the material and activities comprising all phases of dwelling life. Typically life cycle analyses have boundary conditions established to

clearly define the limits of the phases and assumptions in the analysis.

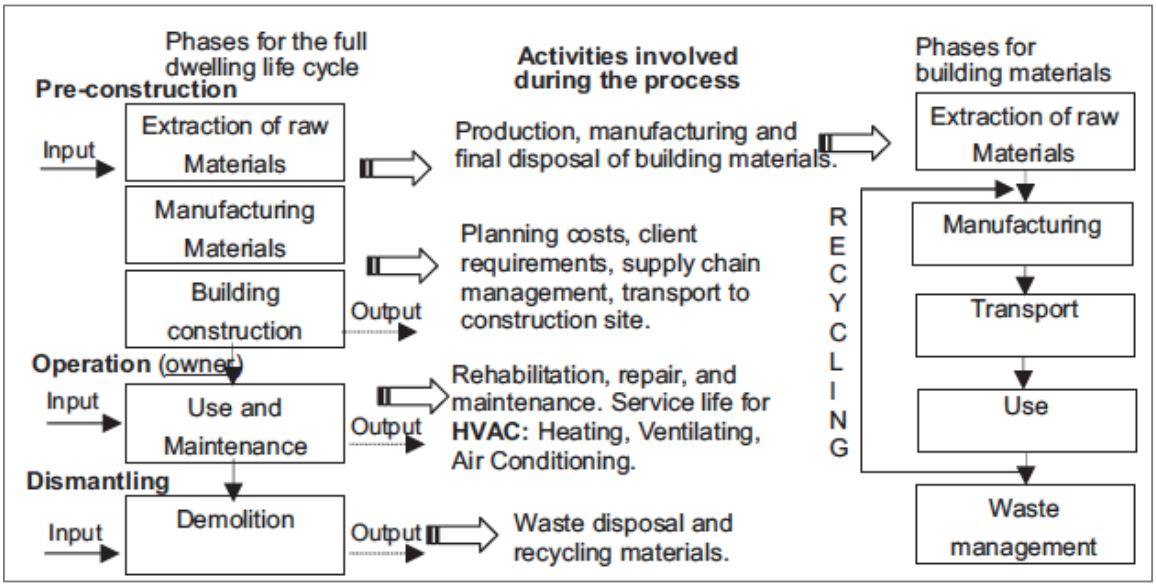

Figure 1. A schematic representation of the building life cycle (Ortiz et al. 2009)

The majority of the data from this portion of the study was estimated based on secondary data, primarily from life cycle databases. Data for the operational phase of the building will be estimated in the building performance section of the research, and demolition impacts will be estimated from secondary life cycle databases.

In this research, the LCA 'As-Built' model was constructed based on building plan takeoffs and design information, and the 'Reference' model was also constructed based on the same geometry but with different materials that are common practice for the region while maintaining IECC 2012 compliance. The embodied energy analysis for both cases incorporated the building envelope (walls, fenestration, roof), the foundation

and the interior walls. No equipment, mechanical or otherwise was included in this part of the analysis and no interior finish was modeled.

Building System, Components and Characteristics

The 'As-Built' home was built by a local builder who specialized in energy-efficient buildings and ICF construction. Additionally, and the building was a large, two and half story, urban home in humid, sub-tropical Houston, Texas (IECC Zone 2A) with 5 bedrooms, 5 bathrooms, and a conditioned floor area of 591 m^2 (6,363 ft^2). The 'As-Built' home details are listed in Table 1.

Table 1. General dwelling details

Type	Description
Builder Name	Durable Residential Builders, LLC
General Information	Energy efficient, durable, noise resistant, urban, custom home in Houston, Texas.
Building type	Large custom house with, 4 bedrooms, exercise room, and 5 bathrooms
Building location (city, state, gen lat, long)	Braes Heights, Houston, Texas Lat: 29.696, Long: -95.434, Altitude: 49 ft. (14.93 m)
Climate	Hot and humid, IECC Zone 2A
Year of construction/Year of occupancy	2009/2010
Conditioned floor area	591 m^2 (6,363 ft^2)
General schedule	Typical residential family oriented household. Maid activity on Monday, Wednesday, Friday.
Days occupied in a year	2 weeks unoccupied
Home type	Single family detached, two and half story
Attic	Unvented, insulated with open cell insulation installed on the roof deck
Walls	Stucco, brick and rock facades and radiant barrier, on 11-inch foam and concrete block wall. Drywall finish inside.
Roof	Durable metal roof, composite shingle look
Windows	Low-e, two-layer, hurricane impact windows
Foundation	Slab on pier and beam

The design strategy was comprised of several strategies compared to typical residential building construction, including a building envelope with a durable, low-infiltration, 10-inch wide ICF wall system with a steel roof and a sealed attic space. The home was tested and audited by a certified Residential Energy Services Network (RESNET®) Home Energy Rating System (HERS) rater and the building achieved a 1.5 air changes per hour (ACH) at 50 Pa, which was smaller than an IECC 2012 minimum of 5 ACH. In addition, impact resistant, low-emissivity windows balanced out the advanced building envelope.

The dwelling had two state-of-the-art high efficiency (17 SEER) 4-ton heat pumps equipped with energy recovery ventilators (ERV) for makeup air energy recovery and the maintenance of air quality. The environmental comfort in the building is maintained by various devices including: 1) air-sourced heat pump, 2) bathroom ventilators, and 3) energy recovery ventilators with the fresh humid air intake being mitigated with ERVs. Table 2 lists the major mechanical systems installed in the home.

Table 2. Dwelling mechanical systems overview

Type	Description
Heating	Two four-ton, 17 SEER heat pumps, Lennox XP21-048-230-02), gas backup furnace), 13.63 kW (46,500 BTU/hr)
Cooling	Two four-ton, 17 SEER heat pumps, 8.7 HSPF, Lennox XP21-048-230-02, 13.92 KW (47,500 BTU/hr)
Domestic hot water	Solar hot water with efficient natural gas demand heater (0.86 EF)
Leakage/Infiltration	Air changes per hour (ACH): 1.52
Ventilation	Balanced with 2, energy recovery ventilators (ERV) (one for each unit) running at low speed (80 CFM each) , 10” inline kitchen vent with makeup air, bathroom vented with inline fans, UV filtration
Controls/automation	Seven day programmable thermostats

To round out the features of the home, the residence also had a 3.5 KW photovoltaic and 1.7 KW solar hot water systems as well as a modern rainwater collection system and they are the subject of chapters three and four, respectively.

Dwelling Operational Energy Model

The operational energy for the 'Reference' and 'As-Built' models for this study were developed in building simulation software, and their primary purpose was the determination of the annual heating and cooling energy utilized by the models. The additional energy demands for the house, such as lighting and miscellaneous plug loads and hot water, were estimated utilizing standard methods and simulation tools where applicable. The energy for hot water usage was determined by estimating the average hot water used per day by utilizing the standard method prescribed in ASHRAE 90.2, and NREL's System Advisory Model simulation tool was used to estimate the annual hot water energy consumption. See chapter three for more detail on the hot water demand estimations. Appliance, plug-loads and lighting schedules, power and internal loads were estimated by utilizing US DOE code home methods developed by PNNL (Mendon et al. 2013).

The 'As-Built' calibrated model was developed to verify the model, and then it was adapted to a generalized HVAC model TMY weather data, HVAC auto-sizing and continuous availability. Occupancy, appliance, plug-loads, lighting schedules and non-mechanical internal heat gains were held constant from model to model. The foundation insulation level was also held constant. The building envelope and HVAC systems operation and infiltration were modified to develop the 'Reference' case; specifically,

the systems altered were the heat pump, infiltration and ventilation (ERV presence/absence).

The general method was as follows:

1. Generate the geometry of the building and its constructions
2. Generate the mechanical systems
3. Update infiltration and ventilation characteristics
4. Apply occupancy and schedules
5. Calibrate the model to achieve ASHRAE Guideline 14 for annual HVAC energy demand (AMY 2012 data driven model results with field measured data)
6. Determine heating and cooling operational energy for the 'As-Built' case utilizing TMY weather data and auto-sized HVAC systems
7. Adjust model to create a 'Reference' case and perform simulation
8. Determine heating and cooling operational energy for the 'Reference' case utilizing TMY weather data and auto-sized HVAC systems
9. Add-in hot water, appliance, plug-load and lighting energy
10. Analyze differences in energy consumption and load differentiation

Building Geometry

Three floor plans, two elevation plans and one site plan were used for building geometry development. The whole house was divided into five thermal zones: first, second, and third floors (bedroom and bath) were treated as conditioned zones while the garage and attic were taken as unconditioned zones. The whole building is shown in Figures 2 and 3. The IECC 'Reference' case used the same dimensions and geometry of the 'As-Built' case.

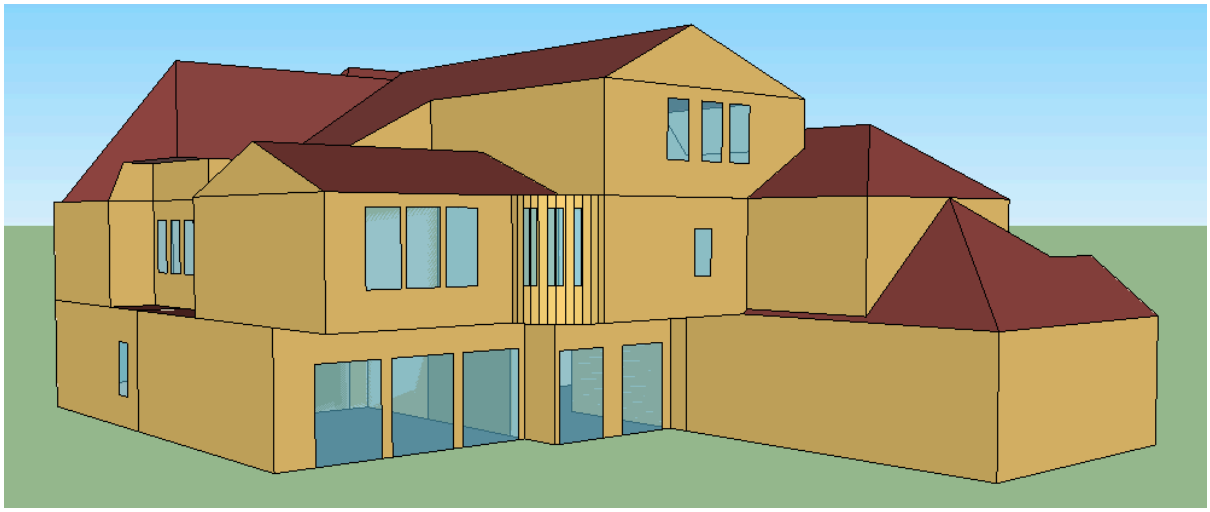

Figure 2. Rendered building geometry (southeast view)

Building Envelope

The building envelope was composed of standard and customized simulation objects for doors, windows, walls, floors, ceilings and the roof, and it was derived from the 'As-Built' system. The 'Reference' building envelope assumed the same geometry, and new constructions for fenestration, exterior and interior walls, roof, ceilings, and floors were implemented. All constructions followed IECC code and are adopted directly from US DOE-PNNL 'Reference' code (Mendon et al. 2013).

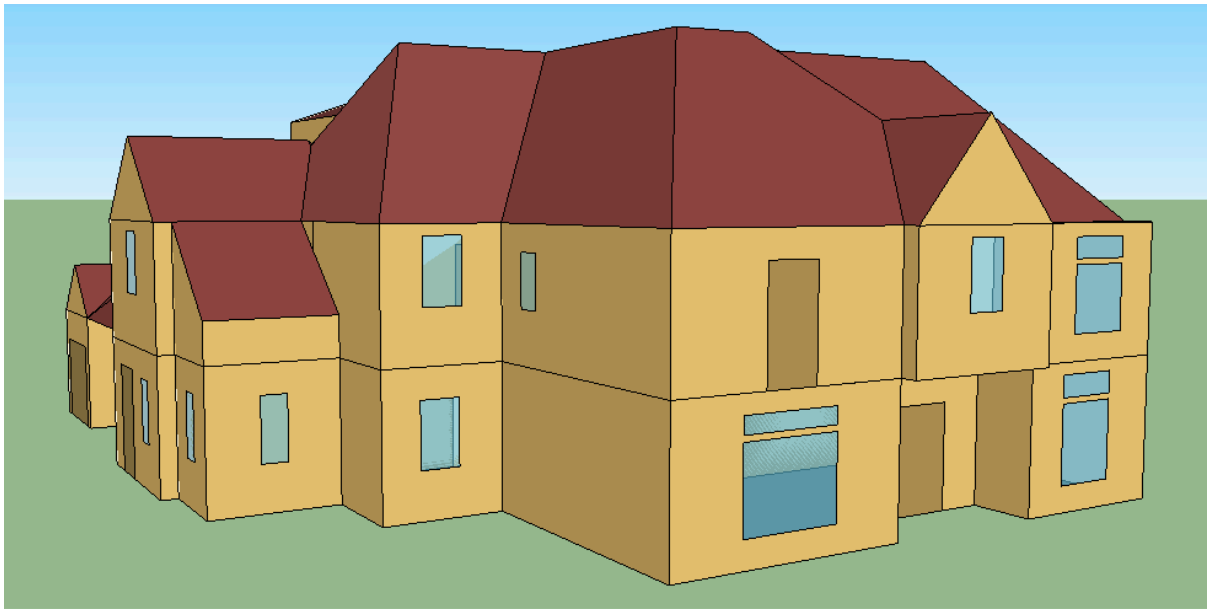

Figure 3. Rendered building geometry (northwest view)

The 'Reference' home was based on the 'As-Built' geometry, but it incorporated a more typical building construction that met IECC 2012 code. The envelope model descriptions are listed in Table 3. The 'As-Built' building exterior wall system was a composite of components that were modeled as constructions and made of the following materials: 1) stucco and rock facades, 2) an air gap, 3) insulation board (polystyrene), 4) concrete, 5) insulation board, and 6) gypsum board (sheetrock). The exterior reference wall system was based on a typical 2"X4" 16" O.C. stud wall consisting of a stucco facade, felt paper, and gypsum board and with an estimated R-value of 13. The ceiling and floors were also approximations of actual built conditions. The bottom floor consisted of subflooring with the second and third floor consisting of 5/8" plywood. The ceilings are modeled as sheetrock (gypsum board) in both models.

Table 3. Building envelope model detail 'As-Built' and 'Reference' model details

Model detail	'Reference' case	'As-Built' case
Exterior walls		
Exterior wall construction	Wood-frame walls (2" x4" 16" O.C.),1" Stucco, Building Paper Felt, Insulating Sheathing (if applicable), 5/8" Oriented Strand Board, Wall Insulation,1/2" Drywall,	Wall system - Facade, air gap, radiant barrier, 2.5" EPS, 6" concrete, 2.5" EPS, 5/8" dry wall
U-factor (Btu / h-ft^2 * °F) and/or R-value (h-ft^2 °F / Btu)	Exterior wall IECC 2012: R-13	Composite estimated: R-21, HERS rater estimate: R-33
Roof and Ceiling		
Roof Construction	Asphalt Shingles, ½" OSB, on rafter roof deck	Metal roof, air space, battens, radiant barrier, 5/8" plywood, rafter roof deck with 6" polyurethane foam
U-factor (Btu / h ft^2 °F) and/or R-value (h ft^2 °F / Btu)	IECC 2012 residential ceiling: R-38 Roof: R-1.0	Composite estimated: R-22
Window		
Glass-type and frame	Glass, vinyl framed window with IECC U-factor and SHGC	Advanced glass film low-E, Argon filled, wood clad, aluminum framed window
U-factor (Btu/h -ft^2°F), SHGC	IECC 2012 residential glazing requirement: SHGC 0.25, U-Factor 0.4	Low-E window: SHGC 0.27, U-Factor .35
Foundation		
Insulation level	R-13	Same as 'Reference' case

Fenestration

The Energy Plus model window object was derived from Aratesh, D. et al. 2009, and it was transformed from commonly available properties of composite window

systems, such as the solar heat gain coefficient (SHGC), the thermal transfer expressed as a U-factor and the visual transmittance (VT), to the glazing properties required by Energy Plus. The material properties of the advanced window were SHGC of 0.27, U-factor of 0.35, and a visual Transmittance of 0.47. A model was performed in a spreadsheet to estimate a composite glazing material. The window model for the reference was based on IECC 2012, and consisted of a double-pane Argon insulated model with a SHGC of .25 and a U-factor of 0.4.

Roof and Slab System

The 'As-Built' roof system developed in the model was a multilayer roof construction of the following materials: 1) metal surface, 2) air space, 3) 5/8" plywood and a 6-inch layer of polyurethane (open-cell foam), and the 'Reference' case was modeled with typical roof consisting of asphalt shingles on ½" oriented strand board (OSB). The 'As-Built' and 'Reference' model slabs were modeled as floors with an R-value of 13, and the ground temperature were derived from the 1-ft below-grade monthly temperature reported by Reddy (2000), a regional expert on local, monthly ground temperatures (see Appendix A-7 for a listing of the monthly ground temperatures used in the simulation).

Mechanical Systems

A high efficiency heat pump was utilized for both the 'As-Built' and 'Reference' models with supplemental heating provided. The supplemental heating was modeled with both gas and electric. Thermostats were held constant in both models at 76°F and 71°F, for cooling and heating, respectively, and a two-week vacation was modeled in the

summer at a 85°F set point. The thermostat set points were consistent with other studies such as US DOE-PNNL study previously mentioned (cooling 75°F, heating 72°F) and ASHRAE Standard 55-2013, *Thermal Environmental Conditions for Human Occupancy* (ASHRAE 2013a) (cooling 76°F, heating 71°F). Table 4 presents a full list of the mechanical and infiltration attributes for the models presented.

Table 4. Mechanical systems properties for the 'As-Built' and 'Reference' models

Model detail	'Reference' case	'As-Built' case
Heating type	Heat pump, electric and gas supplemental heating modeled	Heat pump, electric and gas supplemental heating modeled
Cooling type	Central DX heat pump	Central DX heat pump
Heating sizing	Field data to calibrate model and auto-sized to design day for operational energy evaluation	Field data to calibrate model and auto-sized to design day for operational energy evaluation
Cooling sizing	Field data to calibrate model and auto-sized to design day for operational energy evaluation	Field data to calibrate model and auto-sized to design day for operational energy evaluation
Cooling efficiency	Co-efficient of performance: 4.5	Co-efficient of performance: 4.5
Heating efficiency	Co-efficient of performance: 3.5, Gas heating efficiency: AFUE 78%, Electrical efficiency 1	Co-efficient of performance: 3.5, Gas heating efficiency: AFUE 78%, Electrical efficiency: 1

Table 4. Continued

Model detail	'Reference' case	'As-Built' case
Thermostat set point	76°F Cooling/71°F Heating ASHRAE Standard 55-2013	76°F Cooling/71°F Heating ASHRAE Standard 55-2013
Thermostat set back	No setback weekly setback, 2 weeks in Summer cooling setback to 85 °F	No weekly setback, 2 weeks in Summer cooling setback to 85 °F
Ventilation/Infiltration	IECC 2012: 5 Air Changes/Hr (ACH) @ 50 Pa, Utilized Energy Plus ELA mode, ELA = 284.8 in^2	ERV @ 80 CFM, 54% Total recovery eff., 76% Sensible recovery eff., 50% Fan total eff., 90% motor eff., 1.52 ACH @ 50 Pa with blower door test (HERS). Utilize ELA model in Energy Plus ELA = 86.68 in^2
Fan schedule	Utilized field to calibrate model and always available for operational energy evaluation	Utilized field to calibrate model and always available for operational energy evaluation
Fan Efficiencies (%)	Total fan efficiency 25%, Motor efficiency 65%	Total fan efficiency 25%, Motor efficiency 65%

Fan schedules and efficiencies were held constant from model to model. The major mechanical component in the Energy Plus model included two heat pump systems (coils and air handlers), two energy recovery ventilators, and supplemental heating. A generic air loop system with a heat pump system was utilized and is illustrated in Appendix A-8. Supplemental heating coils were required for the heat pump simulation, and there was no outside air inlet connected to the air loop, as the fresh air is provided by infiltration, bathroom fans as well as the energy recovery ventilators previously

mentioned. The mechanical systems modeled were tuned with system specification and with field verified data for the calibrated model. No ducting system or duct leakage was modeled.

Two four-ton air-source heat pumps were used to provide cooling and heating, with one serving the first floor and the other serving the second and third floor (one bedroom/exercise room and bath). The air handler unit models a constant air volume fan that cycles on and off with a cooling or heating system. The availability schedule of the fan was set to always-on and the fan was simulated as blow-through. Also the motor heat loss was modeled to enter the airstream. The single-speed DX coil model uses performance information at rated conditions along with curve fits for variation in total capacity, energy input ratio and part-load fraction to determine performance at part-load conditions. Performance curves are required to determine the coil performance, and the default Energy Plus performance curves were used in the simulation. The auto-sizing function of the Energy Plus simulation program was utilized to auto size the heating and cooling systems for the purposes of developing the appropriate response to the different loads presented by the building envelope, leakage, and ventilation.

Two energy recovery ventilators were installed to provide fresh air to the first floor and the second floor, and they were independent of the heat pump system. The ERVs were modeled as a heat exchanger object with supply and exhaust fans. The heat exchanger object modeled the operation of an air-to-air heat exchanger from the supply and exhaust air streams and operates whenever the unit was available and when the supply/exhaust airflow were present. The performance data was set at 0.76 sensible and

latent heat recovery and the nominal flow rate and electric power were set at 80 CFM and 82W, respectively. Due to a larger infiltration rate (5 ACH), the 'Reference' model contained no ERV.

Scheduling and Occupancy

The model was developed with four occupants occupying the space and the occupant's schedule was based on the US DOE PNNL method previously mentioned (Mendon et al. 2013) and the 24-hour fractional schedules for lighting, occupancy, appliances, and plug –load electrical are depicted in Appendix A-9, A-10, and A-11, respectively.

Appliance, Lighting and Miscellaneous Plug-Loads

Utilizing a method similar to PNNL (Mendon et al. 2013) for the IECC studies, appliance, plug-load and lighting different end-uses were split out to resemble the Building America research benchmark (Hendron and Engebrecht 2009) and to account for the approximate differences between the internal gains specified by the IECC. The sum of lighting and appliances from the Building America benchmark consisted of an adjustment factor being added in as an additional load (Mendon et al. 2013). Additionally, annual-energy internal-heating gains from general loads, lighting, and occupants were estimated based on Table 5, and a listing of the annual energy consumption and associated internal heat load gains for the appliances, and other equipment utilized in the simulation can be found in Appendix A-12.

Lighting was modeled as installed, plug-in and garage lighting. Following Mendon et al. 2013. The lighting characteristics and energy consumption were based on

the Building America Simulation Protocols (Hendron and Engebrech 2010), which utilized a baseline calculation formulation based on lighted area and applies a fractional portion to different lighting types (incandescent, compact fluorescent and high efficiency). The 2012 IECC required seventy-five percent of all lighting to be high efficacy. These formulas are presented in Appendix A-13.

Table 5. Internal gains and load model details

Model detail	'Reference' case	'As-Built' case
Lighting - Average interior power density (W/ft^2)	Living space: Lighting Power Density 2012 IECC, 2010 Building America House Simulation Protocol. Appendix A-13	Same as 'Reference' case
Interior lighting schedule	Lighting schedule (IECC 2009), Appendix A-14	Same as 'Reference' case
General internal gain load (Btu/day)	IECC 2006 and US DOE PNNL Item listed in Appendix A-12	Same as 'Reference' case
Internal gains Schedule(s)	Internal gain schedule (US DOE PNNL)	Same as 'Reference' case
Occupancy	4	Same as 'Reference' case
Occupancy schedule	Occupancy schedule (IECC 2009). Appendix A-9	Same as 'Reference' case

Table 5. Continued

Model detail	'Reference' case	'As-Built' case
Exterior lighting Annual energy (KWh)	347 kWh/yr for the IECC 2006, 2010 Building America House Simulation Protocol	Same as 'Reference' case
Exterior lighting Schedule	Exterior lighting schedule, 2010 Building America House Simulation Protocol	Same as 'Reference' case
Garage lighting	40 kWh for the IECC 2006, 2010 Building America House Simulation Protocol	Same as 'Reference' case

Model Calibration

Utilizing the aforementioned 'As-Built' model, a calibration of the model was performed by assessing HVAC equipment demand profiling, monthly HVAC energy demand and comparing measured data with AMY-based simulation results from the same year. Heating gas energy was estimated based on utility bills with a based load disaggregation. The 'As-Built' calibrated model utilized air handler flow rates that were estimated based on field measurements, and the field determinations of air handler airflow were made with an Energy Conservatory plate flow meter with a manufacture's stated accuracy of 7%. Figure 4 illustrates the operational energy modelling, calibration and analysis performed in this study.

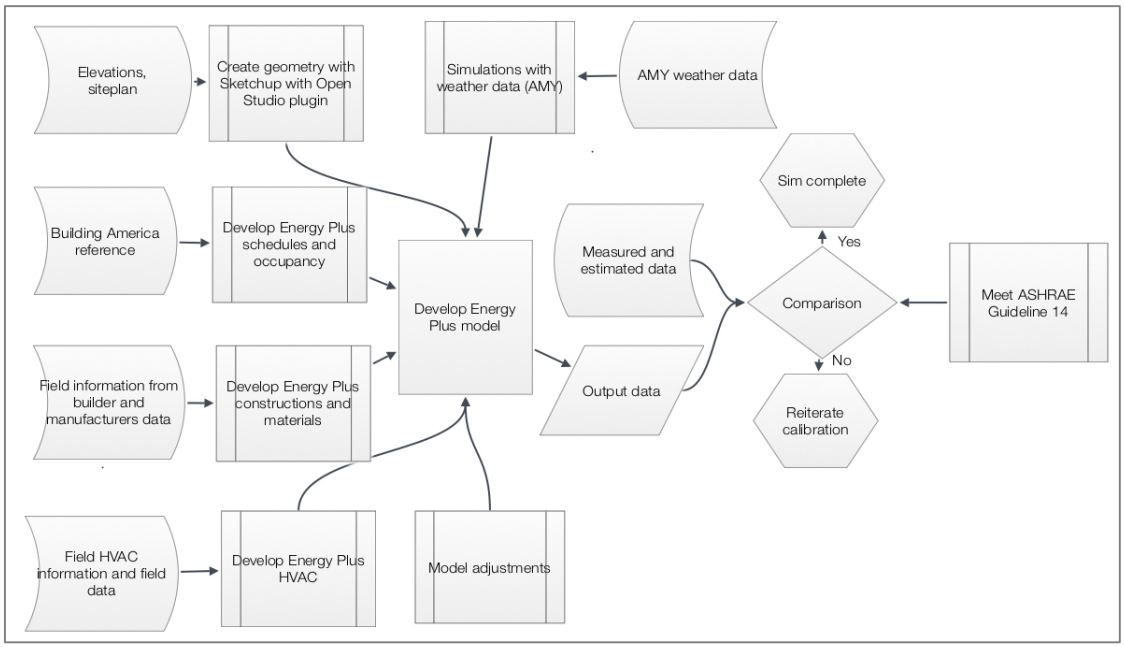

Figure 4. HVAC operational energy modeling, calibration and analysis process diagram

Calibration targets were established based commercial building simulation practices and AHSRAE Guideline 14-5.3.2.4, *Whole Building Calibrated Simulation Performance Path*. Section 14-5.3.2.4 suggests an annual mean bias error (MBE) of 15% and a coefficient of variation of the root-mean-squared error CV(RMSE) of 5% or less (ASHRAE 2014a) for a well-calibrated model. Measured data and utility gas meter data were used for calibrations that included monthly energy consumption for both heat pump systems, ERVs, and monthly whole house gas consumption. In addition, indoor air temperature and humidity were monitored on each floor to verify thermostat settings and to assess the overall comfort (see Appendix A-15 through A-20). System parameters and availability schedules were adjusted for calibration, and an annual MBE of 21% and CV (RMSE) of 4% for the year 2012. Figure 5 depicts the HVAC monthly energy

consumption for both the measured and simulated data.

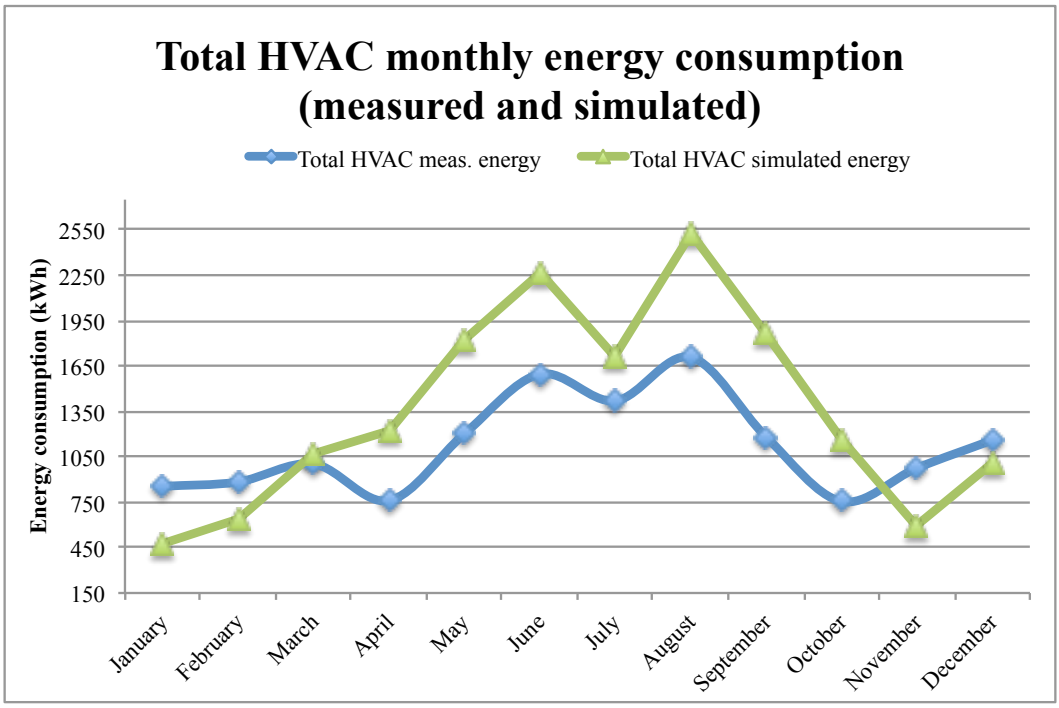

Figure 5. Total HVAC energy calibration results illustrating measured and simulated monthly energy profiles

Operational Energy

Once calibration was achieved the model was adopted and the HVAC systems were auto-sized to design-day data for Houston, Texas, and simulations were run with TMY data with the HVAC availability set to 'always available'. Figure 6 illustrates the operational energy modeling process flow diagram and associated inputs, processes, and outputs for the generation of operation energy of the models. Operational energy models

were performed for both electric and gas supplemental heating (AFUE 78%), and model annual energy and associated end-use for each of the model are presented in Figure 6.

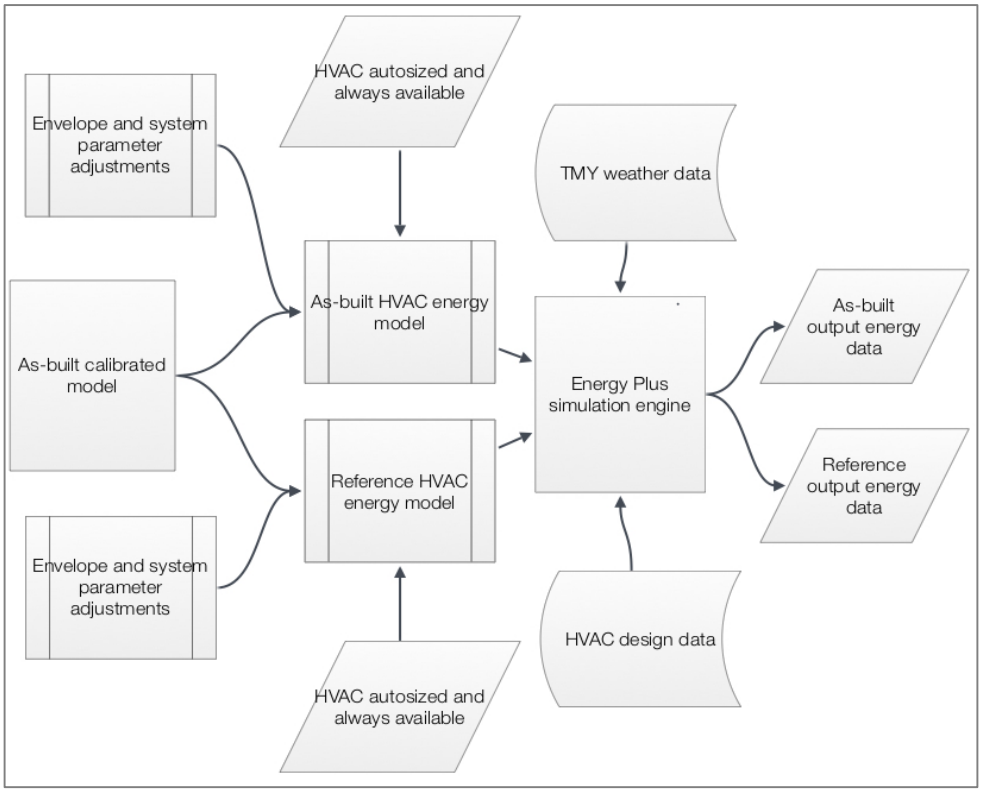

Figure 6. Operational energy modeling process diagram

Monthly summations of the building energy were summed over the year to arrive at the annual energy for each model. Building energy was estimated based on the following equations.

$$Energy_{Building} = \sum_{1}^{\#of\ zones} Energy_{Zone} + Energy_{HVAC} + Energy_{Exterior}$$

Where $Energy_{Exterior}$ was the exterior lighting and plug-loads, $Energy_{Zone}$ was defined as the summation of the non-HVAC energy present in each zone, or:

$$Energy_{Zone} = Energy_{Appliances} + Energy_{Lighting} + Energy_{Plug-loads}$$

The energy utilized by the HVAC systems, $Energy_{HVAC}$, was also defined with its individual components and described as follows:

$$Energy_{HVAC} = Energy_{HVAC\ cooling} + Energy_{HVAC\ heating} + Energy_{Air\ handler} + Energy_{ERV}$$

Operating Energy Results

The 'As-Built' model achieved a 31.2% and 28.9% reduction in total building energy when compared to the 'Reference' model for gas and electrical supplemental heating, respectively. This was due to the reduction in the total HVAC energy, as the average HVAC energy (electrical and gas models averaged) total was 48.4% of the annual building energy for the 'As-Built' model and 60.2% of the annual energy for the 'Reference' model. The 'As-Built' models had a 42% and 45.3% reduction compared to the 'Reference' model for gas and electrical supplemental heating, respectively. Figure 7 is a stacked bar chart of each model, and the relative contributions of the end-uses and cumulative annual energy.

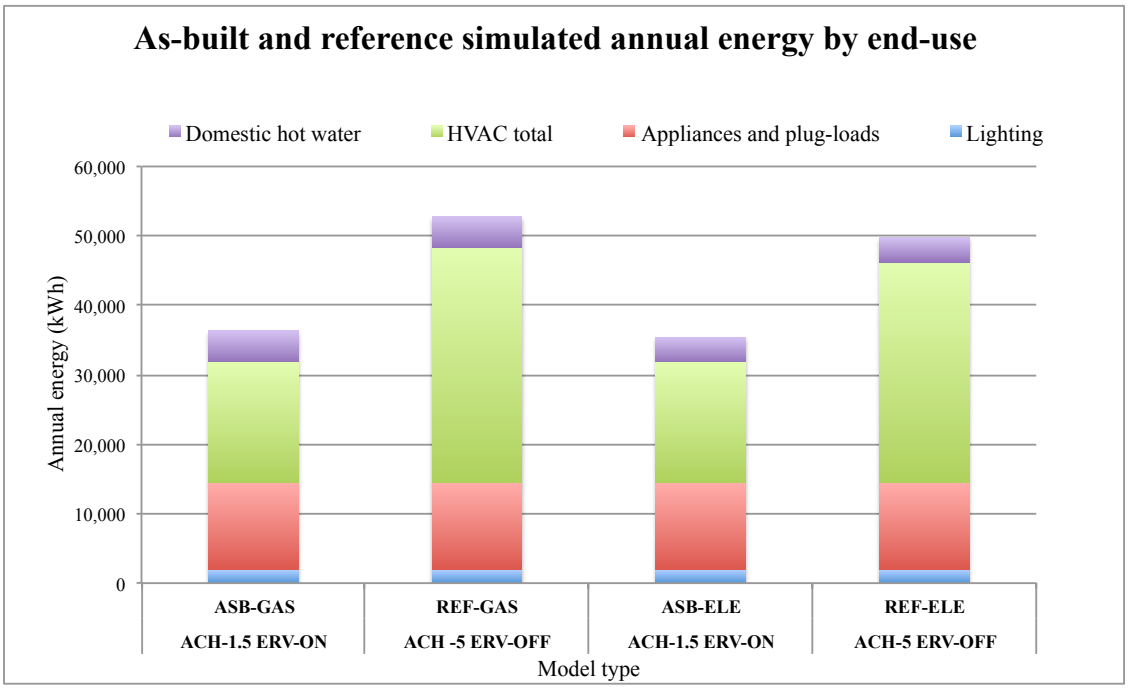

Figure 7. Annual operation energy of 'As-Built' and 'Reference' model by end-use

Lighting represented an average (electrical and gas models averaged) of 5.4% and 3.8%, and the appliances and plug-loads were an average of 35.1% and 24.6% of the annual energy for the 'As-Built' and 'Reference' model, respectively. Finally, domestic hot water energy consumption was an average 11.2% and 7.8% of annual energy for the 'As-Built' and 'Reference' model, respectively. The gas supplemental heating was approximately 3% higher compared to the electric only system for the 'As-Built' model and 6% higher for the 'Reference' case.

HVAC Energy

The primary contributor for the HVAC energy consumption increase for the 'Reference' model was determined to be infiltration. An inherent property of the 'As-

Built' model (ICF construction and sealed attic) is low effective leakage area as measured by a blower-door test. Comparative models for the 'Reference' and 'As-Built' model with gas supplemental heating were run to isolate the effects of the building envelope from the infiltration effects. The building model was held constant and the infiltration was adjusted to assess the relative impact of both the 'Reference' and 'As-Built' case, and the infiltration (ACH) was held constant and the building envelope was changed ('As-Built' to 'Reference'). Table 6 presents the findings for adjusting the 'As-Built' and 'Reference' models.

Table 6. Impact of infiltration and building envelope design on total and HVAC simulated energy

MODEL DETAILS/ ENERGY	**INFILTRATION REDUCTION ACH5 to ACH1.5**		**BUILDING ENVELOPE REDUCTION REF to 'AS-BUILT'**	
CONSTANT VARIABLE	'AS-BUILT'	'REFERENCE'	ACH1.5	ACH5
BLDG TOTAL ENERGY	23.7%	23.4%	10.2%	9.8%
HVAC TOTAL ENERGY	39.2%	36.5%	19.2%	15.6%

With the models presented, the impact of infiltration is substantial and reducing an IECC 2012 code-based building with infiltration of ACH 5 to ACH1.5 decreases the building HVAC total energy an average of 37.85%. Achieving an ACH 1.5 in residential building construction is considered a tight house (Sadineni et al. 2011), and infiltration and ACH control is due to the builiding envelope type and construction practice, and ICF construction is known to mimnimize infiltration and effective leakage area (Kosny

et al. 1998, Thompson 1995). Penetrations to the ICF wall systems such as windows and doors need to be sealed appropriately, but the rest of the wall system is air tight once assembled. A spray-foam insulated attic, achives a low-leakage roof and attic system from the outset. Infiltration is important to control annual operational energy and associated life cycle impacts.

The building envelope effects are observed by comparing constant infiltration rates for each mode and an average reduction in HVAC energy of 17.4%. Building energy reduction of about 10.2%. This observation was consistent with reported reductions of energy consumption by ICF building envelopes compared to typical framing construction (Marceau and VanGeem 2006, Kossecka and Kosny 2002). This is due to the ICF's higher R-value and thermal mass ability to moderate temperature swings and peak loads (Marceau and VanGeem 2006, Kosny et al. 1998, Kossecak and Kosny 2002).

Non-HVAC Energy Burden

Of the non-HVAC energy loads, the appliances and plug-loads are the largest, with domestic hot water second; however, the appliance and plug-load estimates are conservatively based on the PNNL and Building America estimates for a standard home. Additionally, a home of this size may have luxury or 'lifestyle' items such as multiple refrigerators, central vacuum cleaners, spas and pools, and other items that may yield appliance and plug-load electrical demand well beyond the benchmark. US national averages indicate a trend in the reduction of overall HVAC energy as a percentage of building total energy, but despite energy efficiency improvements and governmental

programs such as Energy Star, appliances and miscellaneous plug-load energy footprint grows (US EIA 2013).

Impact of Solar Energy Systems

Annual operating energy for life cycle calculations were estimated for the models based on the addition of an average renewable energy (solar photovoltaic and solar hot water system) contribution and were estimated based on annual simulations with a 0.5% annual degradation factor from work presented in chapter three. Fifty-year average annual energy contributions of 3,757 kWh/yr and 1,637 kWh/yr (ele)/2,023 kWh/yr (gas), for the solar photovoltaic and solar hot water, respectively, were subtracted from the building energy demand to estimate the annual building energy with renewable energy. The renewable energy systems contributed an annual average of 15.5% and 12.5% reduction to the 'As-Built' and 'Reference' operational energy, respectively. Figure 8 is a graphical depiction of the annual energy of the models with and without solar energy systems.

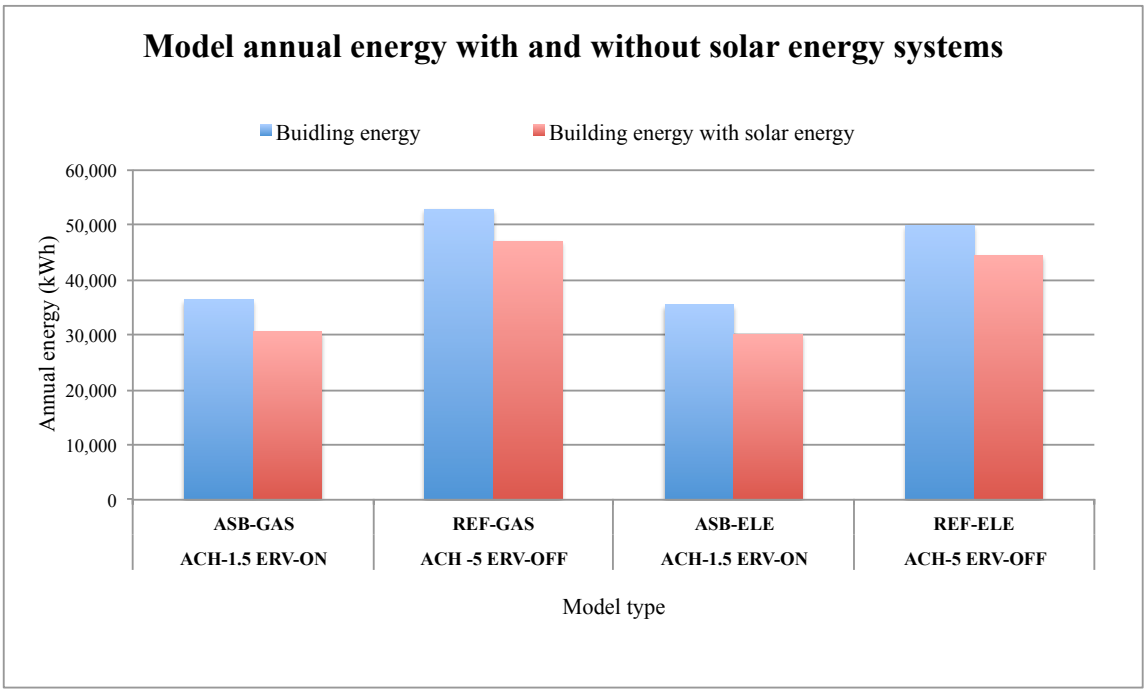

Figure 8. Model annual energy with and without solar energy systems

Energy Use Intensity

Building Energy Use Intensity (EUI) is an index that can be used to describe the amount of energy a building uses per year, and formally it is a ratio of the total annual energy used onsite over the building area not including spaces typically not conditioned or outside (walkways, porches, verandas, etc...) (ASHRAE 2014b). The EUI may take into account source or site energy, and in this study, site energy is considered. Additionally, renewable energy generation may be characterized by a similar index that subtracts generated renewable energy from the building site energy and produces a building Net Energy Use Intensity (NEUI). These ratios are formally presented as follows:

$$Total\ Energy\ Use\ Intensity\ (EUI) = \frac{TotalAnnualEnergyUse}{GrossFloorArea}$$

and

$$Total\ Net\ Energy\ Use\ Intensity\ (NEUI) = \frac{NetAnnualEnergyUse}{GrossFloorArea}$$

where

$$TotalAnnualEnergyUse = \sum_{1}^{12} Energy_{monthly}$$

and

$$GrossFloorArea = \ Area\ of building\ excluding\ major\ unconditioned\ areas$$

Building EUIs and NEUIs are useful in comparing buildings in a standardized way and setting performance goals. Additionally, they are currently being used by both governmental agencies, such as the US Energy Information Administration, and building industry associations, such as ASHRAE (ASHRAE 2010 and US EIA 2015). The building models presented in this study achieved the following results presented in Table 7.

Table 7. EUI and NEUI indices for the 'As-Built' and 'Reference' models

MODEL	ASB-GAS	REF-GAS	ASB-ELE	REF-ELE
VENTILATION/INFILTRATION	ACH-1.5 ERV-ON	ACH -5 ERV-OFF	ACH-1.5 ERV-ON	ACH-5 ERV-OFF
EUI kWh/m^2	61.4	89.3	59.9	84.2
EUI kBTU/ft^2	19.5	28.3	19.0	26.7
NEUI kWh/m^2	51.7	79.5	50.8	75.1
NEUI kBTU/ft^2	16.7	25.2	16.1	23.8

EUI as the energy intensity per square area is highly dependent on the type of building and as such needs to be taken in the context to the type of building evaluated. Residential buildings have been categorized with EUIs by Architecture 2030's Challenge and the Passivhaus program to assess typical buildings and to assign targets (Architecture 2030 2015, Straube 2009). Architecture 2030 provides an analysis of the US EIA residential building energy database and sets reductions based on US regional averages. These reductions are based on 50%, 60%, 70%, 80% and 90% from the regional average EUI. Single-family buildings, both detached and attached garages, in the southern region of the US were reported to have an average EUI of 41.8 and 38 EUI kBTU/ft^2-yr, respectively (Architecture 2030 2015).

The 'Reference' model achieved a EUI below the US EIA average and the 'As-Built' model is essentially at the 50% reduction target of EUI 19.4. Additionally, the EUI for the gas and electrical heating models achieved similar EUI and NEUI, with gas having a bit higher number due to extra energy usage as a s result of process efficiency differences. The EUI for both the 'As-Built' and the 'Reference' model were both smaller (higher performing) when compared to the South-regional national averages, and with renewable energy systems, the results were even smaller; however, the lowest NEUI attained, at 16.1, did not meet the 60% reduction target of the Architecture 2030 (EUI 15.5) or the high achieving, Passivhaus standard of an EUI of 15.

Dwelling Life Cycle Embodied Energy

In order to characterize the embedded energy and environmental flows of the buildings construction, operation, and end-of-life, a life cycle analysis approach is required. The Impact Estimator (IE) from the Athena Sustainable Materials Institute (ASMI) is a publicly available whole-building, environmental life cycle decision support tool that takes comprehensive life cycle inventory databases and makes it accessible in a software-based accounting tool. The model provides a cradle-to-grave life cycle inventory (LCI) for a whole building over a user-selected life cycle service life and inventory results are flows in the form of energy and raw material as well as emissions to the environment (air, water and land) (ASMI 2014). The tool supports life cycle assessment measures based on the US EPA's Tool for the Reduction and Assessment of Chemical and Other Environmental Impacts (TRACI v2.0) and in accordance with ISO 1440/14044 (LCA - Principles and Framework/ Requirements and Guidelines) and ISO 21930/31 (Environmental declarations on building products) (ASMI 2014). In addition, IE's database is comprised of ISO 14040/14044 compliant unit process and LCI data related to basic materials, building products, and components, fuel use and transportation (ASMI 2014). The Impact Estimator version utilized in this research study was 5.0.0125.

Environmental measures reported in IE include 1) global warming potential (CO_2 equivalent mass), 2) acidification (H^+ ions equivalent mass), 3) human health criteria (PM2.5 equivalent mass), 4) eutrophication potential (Nitrogen equivalent mass), 5) smog (O_3 equivalent mass), 6) ozone depletion (CFC-11 equivalent) and 7) fossil fuel consumption (fossil fuel energy in GJ) (ASMI 2014). These measures are midpoint life

cycle impact assessment indicators based on US EPA TRACI. The tool provides the capability of inputting annual operational energy by fuel type, and it is able to calculate pre-combustion energy (extraction, refining and delivery energy). Finally, it takes into account building system demolition and end-of-life disposition of materials (ASMI 2014). The bill of materials takeoff estimates based on the IE's model components have been compared against detailed manual takeoff and have been found being within ± 10% with results within measured differences of 15% are to be considered insignificant (ASMI 2014). Materials are grouped by assembly and are divided into the following major categories: 1) foundation, 2) walls, 3) beam and columns, 4) floors and 5) roofs. An additional extra basic material category provides for other materials that may not fit in the defined categories. The Athena's tool has been used in building and construction lifecycle impact studies reported in the literature (Kahhat et al. 2009, Perez-Garcia et al. 2005, Steck et al. 2011) in technical briefs (Bushi and Meli 2014) and in LCA tool reviews (Haapio and Viitaniemi 2008).

Assumptions and Boundary Conditions

The lifecycle impact study was constrained to building operation energy performance and embodied energy of the building roof, exterior walls, fenestration, foundation and interior walls. Operating energy included all the energy used by the building, including, HVAC energy, lighting, appliances, and plug-loads. Gas and electrical energy are input separately to account for operational energy effects. The embodied energy model was developed in IE and follows standard LCA methods

previously outlined and conforming to the EN15804/15978 (category and calculation definitions) system boundary and reporting formats (ASMI 2014).

Lifecycles stage are typically divided into four stages, each conceptual module labeled A1 through C4; an additional module "D" accounts for benefits outside the system boundary of the object of assessment, and includes the benefits of recycling and reusing materials at end of life as illustrated in Figure 9. The system LCA boundary for this study was set to the end-of-life stage (life cycle stages A1-C4). Figure 9 illustrates the typical life cycle stages used in LCA and a typical EN15978 system boundary (A1-C4) depicting the product production, construction, use and end-of-life phases.

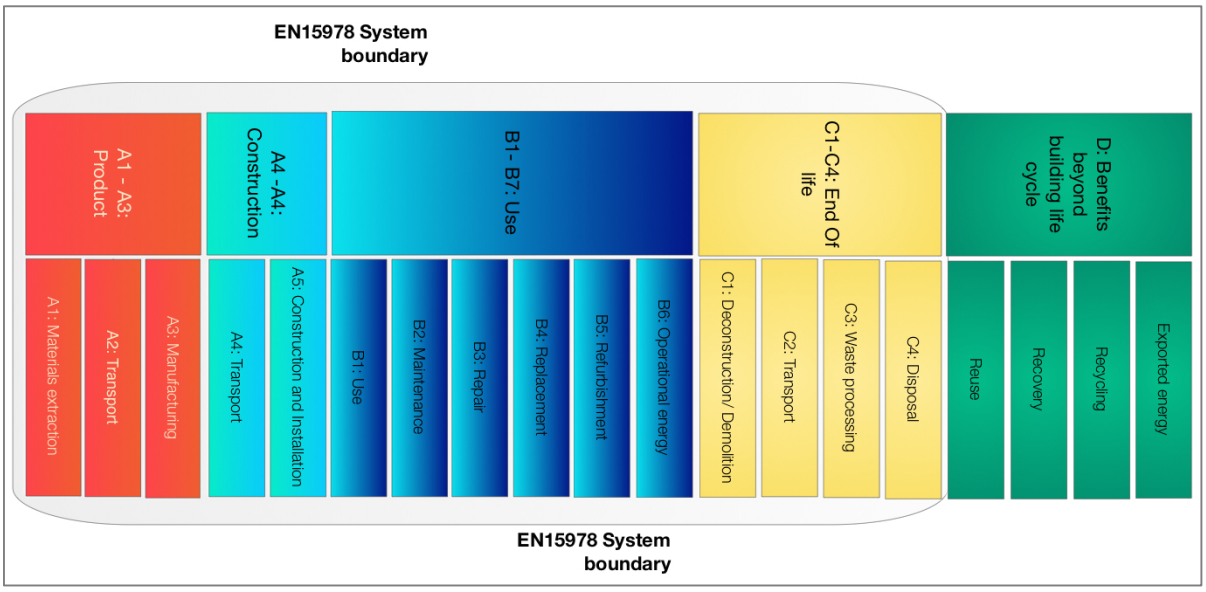

Figure 9. Building life cycle stages (A-D), EN15978 system boundary (A-C)

The product stage involves modules A1-A3, namely, primary resource harvesting and mining (A1), all transportation of material up to manufacturing plant gate (A2) and the manufacture of raw materials into products (A3). The construction stage (A4-A5) is divided into two modules, namely transportation to the site (A4) and construction equipment energy use and effects of construction waste (A5). The use stage contains modules B1-B7 and includes, installed product use (B1), maintenance (B2), repair (B3), replacement (B4), refurbishment (B5), operational energy use (B6), and operation water user (B7). Finally, the end of life contains modules C1-C4. The end of life stage is comprised of de-construction/demolition energy (C1), transport (C2), waste processing (C3) and disposal (C4) of the buildings materials. Stage D is supplemental information and flow beyond the building life cycle such as reuse, recovery, and recycling potential. This stage was not included in the analysis. The study conducted herein, utilized the boundary (A-C) identified in Figure 9 (EN15978 system boundary).

Regional Specifics and Conditions

IE facilitates regional specificity to support the activation of the appropriate electric grids, transportation modes and distances, and product manufacturing technologies applicable to the product mix for the selected region (ASMI 2014). Electricity supply is especially important due to various types of generators and grids available to a region. With this approach, electricity-related impacts associated with manufacturing materials, products and components, as well as construction, operation and maintenance energy are accounted for at the regional level.

Environmental Indicators

Table 8 lists a review of some LCA of residential building and the life cycle environmental indicators utilized by the authors reviewed; not surprising, the primary energy (PE) and global warming potential (GWP) are heavily used and air (smog, human health respiratory and ozone depletion potentials) and water (eutrophication potential) effects in less numbers.

Table 8. Environmental indicators commonly used in the LCA literature

Authors and year	**Primary energy cons.**	**Global warming potential**	**Smog potential/HH respiratory effects**	**Acid-ification potential**	**Eutro-phication potential**	**Ozone depletion potential**
Units	Mega-Joule	CO_2 equiv. mass	O_3 / $PM_{2.5}$ equiv mass	H^+ equiv. mass	N equiv. mass	CFC-11 equiv. mass
Monahan and Powell 2011	X	X				
Stek et al. 2011	X	X	X			
Ramesh et al. 2010	X					
Kahhat 2009	X	X	X		X	
Ortiz et al. 2009		X		X		X
Citherlet and Defaux 2005		X		X		X
Utilized in this study	**X**	**X**	**X**	**X**	**X**	**X**

Each of the indicators may be associated with its relevant scale. Global impacts include global warming potential (GWP), ozone depletion potential (ODP), and resource depletion and regional impacts are typically associated with smog and acidification

potential (SP, AP). Human health respiratory potential (HHRP) and eutrophication potential (EP) are local in their impacts. All of the indicators listed in the residential building LCA studies were investigated in the study and water resource consumption was also included in the analysis. A description of each environmental indicator is provided in the Appendix and tabulated in Appendix A-22.

Model Development of Embodied Energy

IE was used to estimate the life cycle energy of two building models, namely a 'Reference' and an 'As-Built' model, and operational energy was determined from the calibrated Energy Plus models previously discussed. The building plans and Energy Plus building geometry was utilized to organize and group the takeoffs for the IE model. Figure 10 illustrates a process diagram of the life cycle modeling and analysis, and it includes the inputs, sub-processes, processes, databases, and outputs involved in the method.

Over 160 and 190 individual objects and associated components were input into the 'Reference' and 'As-Built' models, respectively; the majority of the objects being wall and roof surfaces. IE divides building construction into primary assemblies such as: foundation, walls (interior and exterior), roof, floors and extra basic materials. All objects have a range of materials that are specific to the object type (i.e. wall object: wood-stud wall, concrete block, etc.) of specific, user-defined dimensions.

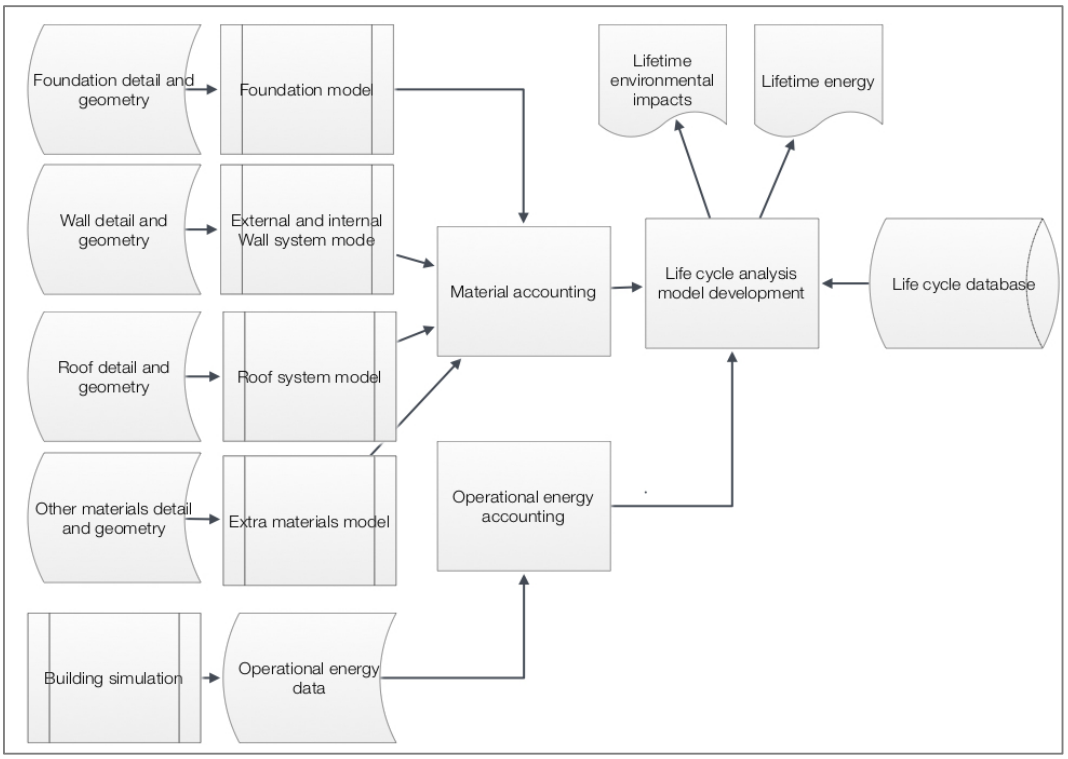

Figure 10. Life cycle modeling and analysis used in this study

Other attributes of the object are included, such as interior and exterior walls specified as load bearing or non load bearing. Fenestration is built into the exterior wall, objects, as well as, outer and inner envelope materials (insulation, paint, drywall, etc.). Other materials that do not fit into predefined objects need to be included in extra basic materials.

Model Details

'Reference' and 'As-Built' models were similar with the exception of a few major assemblies and components. The 'Reference' model construction was based on IECC 2012 code and regional building practices. The building envelope was constructed from a traditional framed house with fiberglass insulation and with a standard vented

attic with fiberglass insulation on the top floor ceiling. The roof was constructed of standard asphalt shingles, a vapor barrier, 1/2" of OSB roof decking on top of roof trusses. The vapor barrier was modeled as polypropylene-scrim kraft (PSK) material. The building rested on a post-tension slab model, which is common for the clay soils of the South-Houston, Texas. All concrete in the 'Reference' model utilized average (9%) fly ash content.

The 'As-Built' building envelope provides a more durable and thermal resistive wall system compared to the Reference building. It achieved these measures by utilizing an ICF exterior wall system and a durable roof system with a sealed, insulated attic. Two-by-six framing and spray foam insulation was utilized in the wall system where the ICF was not appropriate or feasible. The roof system was a durable 26-gauge metal exterior on top of a multi-layer thermal boundary that was comprised of radiant barrier, ice and water shield, 5/8" plywood roof decking with 5 ½" of spray foam, all on top of a truss system. The radiant barrier was modeled with a two-layer PSK barrier while the ice and water shield was modeled as bitumen membrane. The underside of the roof deck was insulated with spray foam. Concrete in the 'As-Built' system was 25% fly ash.

All floors were modeled the same for the 'Reference' and 'As-Built' models. The first floor was modeled as a 2"X4" stud screed on top of a slab pad, and is typical for wood floors installed on top of concrete. The second and third floors were modeled with web-truss assemblies and ¾" plywood as a sub-floor. The final "finish" layer of the floors was not part of the assemblies of any of the floors. Fenestration was modeled the same in both models with standard doors and aluminum cladded, wood-framed, double-paned windows. Interior wall construction was standard 2"X4" stud wall with the 'Reference' case utilizing 1/2" sheetrock and the 'As-Built' 5/8" fire-rated sheetrock. Other known support and structural members (composite wood beams and iron posts) in the interior of the house were modeled to the same detail. Table 9 presents description and model details for 'As- Built' and 'Reference' building assemblies.

Table 9. Construction and model details by building assembly

CONSTRUCTION		MODEL	
IECC reference	**As-built**	**IECC reference**	**As-built**
EXTERIOR WALLS			
Latex paint	Latex paint	Latex paint	Latex paint
Stucco	Stucco	Stucco (includes wire mesh underlayment)	Stucco (includes wire mesh underlayment)
OSB sheathing	Radiant barrier	OSB sheathing	2 layers of PSK
2"X4" stud wall	ICF or 2"x6" wood stud	2X4 wall assembly	ICF assembly or 2X6" wall assembly, concrete has 25% flyash
Wood wall has fiberglass inulation	Wood wall has open cell foam	3.5" of Fiberglass insulation	2X6" wall assembly has 5 1/2" of polyiscyurante
1/2" interior sheetrock	5/8" interior fire-rated sheetrock	1/2" regular gypsum board	5/8" fire-rated gypsum board
ROOF			
Asphalt shingles	Metal shingles	Standard asphalt shingles	Metal shingle 26 gauge
No battens	2"X"2 battens	No battens	2"X"2 battens
Roof felt #15	Radiant barrier and water shield	Roof felt #15	2 layers of PSK with bitumen membrane (2ply)
1/2" OSB roof deck	5/8" plywood roof deck	1/2" OSB roof deck	5/8" plywood roof deck
Truss of rafters with joists	Truss of rafters with joists	Light frame wood truss assembly	Light frame wood truss assembly
	Open cell foam insulation		5 1/2" of polyisocyurante
FENESTRATION			
Aluminum clad, wood frame	Aluminum clad, wood frame	Aluminum clad, wood frame	Aluminum clad, wood frame
Double pane windows	Double pane windows	Double pane glazed and operable	Double pane glazed and operable
Standard door	Standard door	Standard door	Standard door
FOUNDATION			
Post-tension slab	Concrete pier and beam	Post-tension model composed of:	Pier and beam model composed of:
All concrete is average (9%) flyash content	with voidboxes	36"X12" perimeter and 24"X12" interior beams	42"X12" perimeter and 24"X12" interior beams
	All concrete has 25% flyash content	4" Slab pad	4" Slab pad
		Interior beam and tensioning tendons in EBM	Piers and interior beam in EBM
INTERIOR FLOORS			
1st - wood screed on slab with plywood floor	1st - wood screed on slab with plywood floor	1st - wood screed in EBM	1st - wood screed in EBM
2nd - web truss with plywood floor	2nd - web truss with plywood floor	2nd - web truss with 3/4" plywood	2nd - web truss with 3/4" plywood
3rd - web tuss with 3/4" plywood floor	3rd - web tuss with plywood floor	3rd - web tuss with 3/4" plywood	3rd - web tuss with 3/4" plywood
3rd floor ceiling has 10" of fiberglass	5/8" ceiling fire-rated sheetrock	3rd floor/ceiling has 10" of fiberglass insulation	5/8" fire-rated gypsum board
1/2" ceiling sheetrock		1/2" regular gypsum board	
INTERIOR WALLS			
Standard 2"X4" interior wall	Standard 2"X4" interior wall	2"X4" wall assembly	2"X4" wall assembly
1/2" interior sheetrock on both sides	m	2" X1/2" sheetrock	2"X 5/8" sheetrock
EXTRA BASIC MATERIALS			
Conrete for the beams and slab	Concrete for the pier	Concrete, 20 M Pa, Average flyash content	Concrete, 20 M Pa, 25% flyash content
Rebar, ligature and tendons	Rebar and ligature for the foundation beams and piers	Rebar	Rebar
Materials for the 1st floor screeds	Materials for the 1st floor screeds	2"X4" soft pine screeds	2"X4" soft pine screeds
Material for structural steel supported columns	Material for structural steel supported columns	5"X5" square iron tubing	5"X5" square iron tubing
Material for GULAM beams	Material for GULAM beams	GULAM beams	GULAM beams
	Material for roof battens		2"X2" soft pine

Dwelling Life Cycle Energy Results

The dwelling life cycle energy results are divided into two sections, with one entailing the distribution and effects of the building assembly and the other, a discussion of the whole life cycle, its phases and the distribution of impacts.

Building Impact Simulation Results

The primary energy distribution by assembly group identifies those assemblies consuming maximum energy and causing the greatest emissions. Figure 11 below presents the primary energy consumption by various assembly groups and different building models.

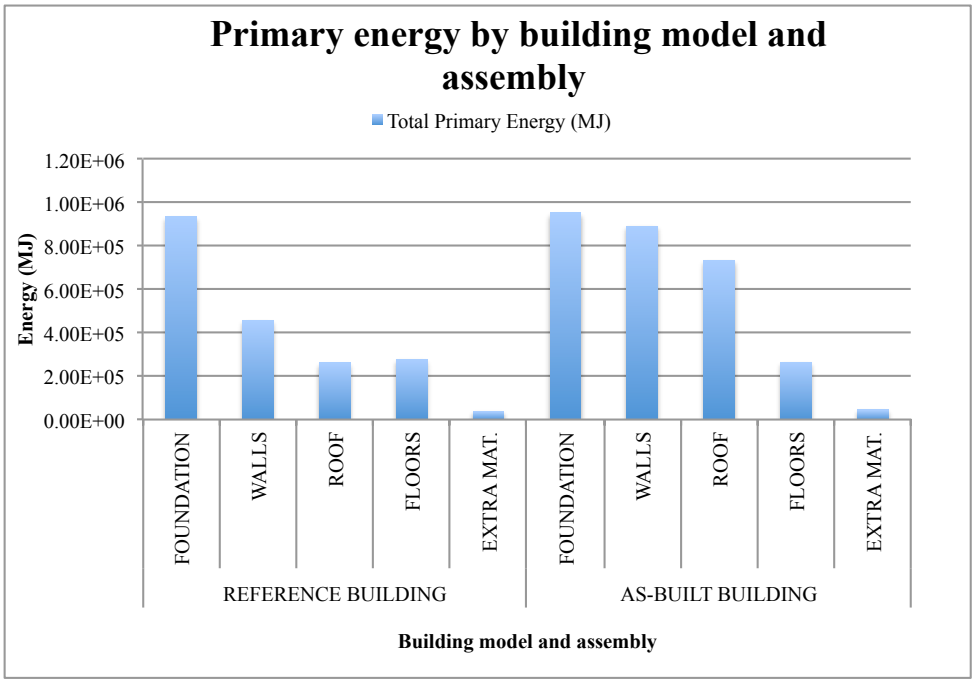

Figure 11. Primary energy by building model and assembly

By category, the foundation, walls and the roof have a substantial impact and differences in the 'Reference' and 'As-Built' cases are due to the large amount of concrete and steel in the walls and slightly larger amounts of concrete in the foundation. It can be observed from Figure 11 that the foundation accounts for the highest percentage of primary energy for both the 'Reference' and the 'As-Built' model with the 'As-Built' model slightly leading the 'Reference'. The second largest impact was the wall assemblies with the 'As-Built' primary energy double the amount of the 'Reference' model. The roof assembly is the third largest consumer of primary energy and the 'As-Built' model is over double the amount of primary energy compared to the 'Reference' model. The floors and extra basic materials are the same for both cases and as such have the same primary energy.

The relative reduction from the 'Reference' to the 'As-Built' model for all environmental indicators is illustrated in Figure 12. Due to the less concrete in the walls, and steel in the roof, along with more wood utilization, the 'Reference' model environmental impact categories were 60 to 20% less than the 'As-Built'.

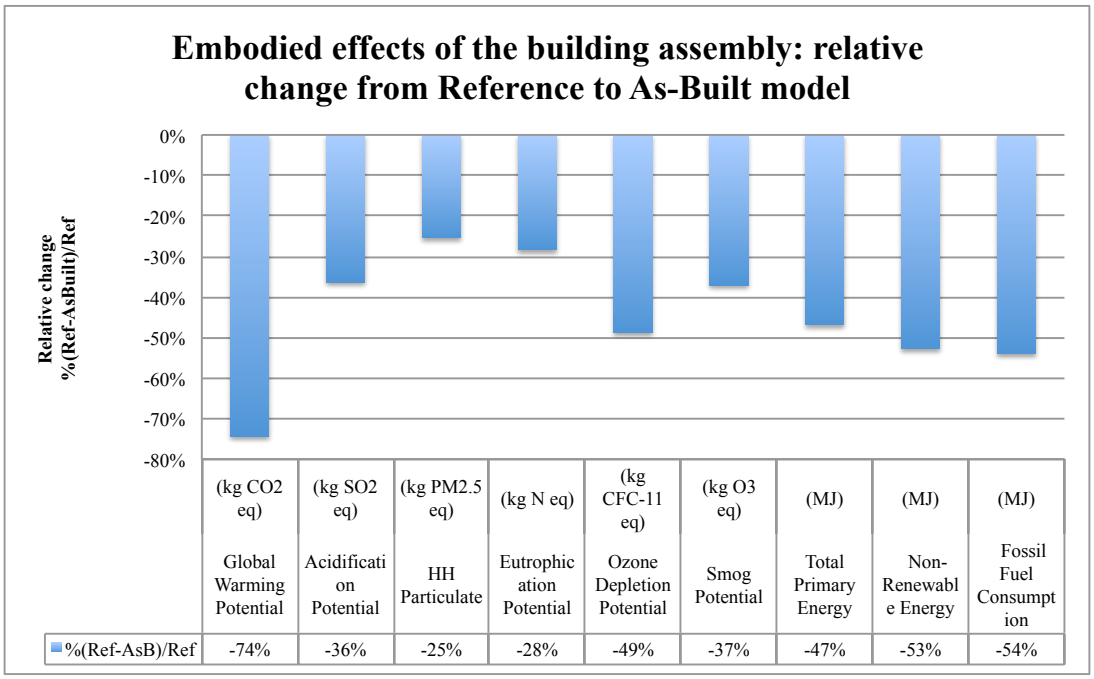

Figure 12. Building embodied environmental impact relative change from 'Reference' to 'As-Built' model

Global warming potential was reduced 74% and the total primary energy reduction was 47% from the 'Reference' to the 'As-Built' model. The total primary energy for the 'Reference' model was 1.74 E+06 MJ and the 'As-Built' model was 2.66 E+06 MJ. The increased impact of the building envelope is substantial on the amount of material required and subsequent environmental emissions. However, as discussed in the next section, in life cycle terms, this amount of initial primary energy is modest in comparison to the overall life cycle impact. Although the building envelope is expensive upfront in terms of materials, energy and emissions, it achieves impressive reductions in filtration and thermal control and as such reduces life cycle energy and emissions overall.

For reference, Figures A28-A33 in the Appendix illustrate the environmental impact factor distributions in the building assembly and with this type of assembly analysis, design trade-offs can be identified by inspecting and comparing alternative assemblies such as walls and roofs for the purpose of assisting future designs that may offer lower consumption of resources and energy, subsequently minimizing environmental emissions to the air and water. The assembly distribution values are tabulated in Appendix A-24.

Life Cycle Analysis

Operational energy was added to the analysis with space and water heating with gas and electric energy being modeled for both the 'Reference' and the 'As-Built' models. Additionally, renewable energy offsets to the gas space and water heating was performed to predict the impact of the renewable energy systems. Figure 13 displays the total primary energy by life cycle phase for each building model and for space and both water heating energy types. Comparing the gas and electrical space and water heating energy models the differences in the operational primary energy use was 4.1 and 4.6% for the 'Reference' and 'As-Built', respectively. The slight difference in operational energy was due to conversion efficiency differences.

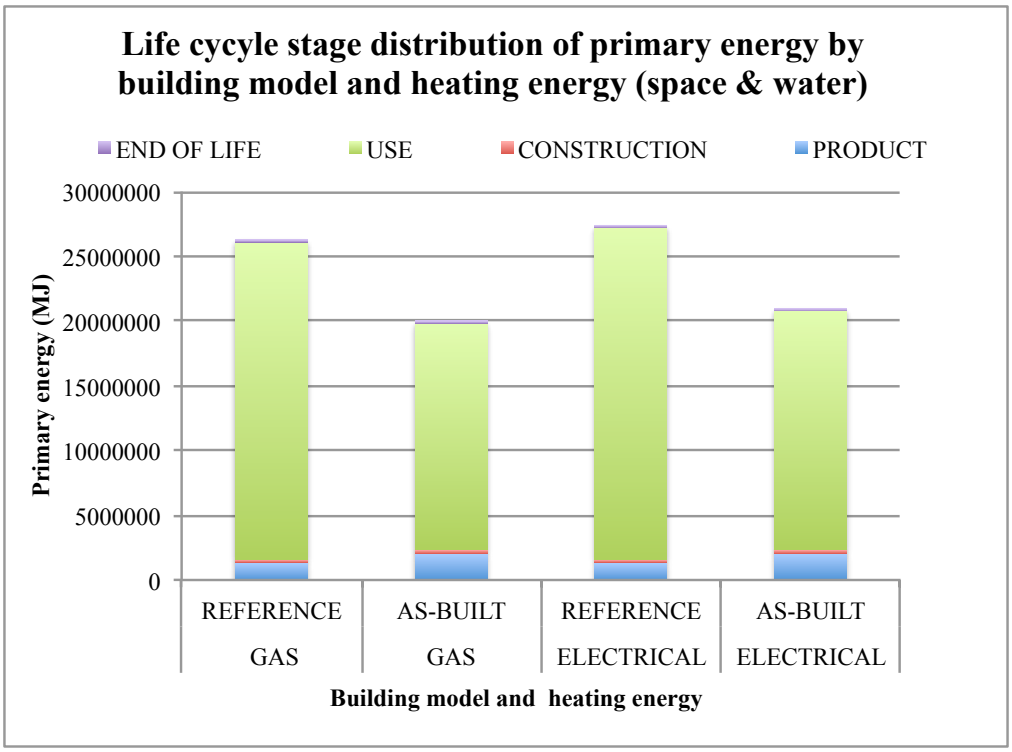

Figure 13. Life cycle phase distribution of primary energy by building model and heating energy (space and water)

All models showed similar trends. For example, the use phase (B1-B7) of the space and water gas energy model accounted for 93.7% ('Reference') and 88.3% ('As-Built') of life cycle primary energy. The product phase (A1-A3 accounted for 5% for the 'Reference' and 9.8% for the 'As-Built' while the construction phase (A4-A5) was 0.9% and 1.5%, respectively. Finally, the end of life phase (C1-C4) was determined to be 0.5% for the 'Reference' model and 0.8% for the 'As-Built' model. The gas model percentages were close to the electric model and were as follows ('Reference', 'As-Built'): use phase: 93.4%, 87.3%, product phase: 5.2%, 10.3%, construction phase: 0.9%, 1.6%, end-of-life phase: 0.5%, 0.8%. For the 'Reference' model the use phase is

14.12 times larger than the other phases combined, with the ‘As-Built’ model being 6.87 times all the other phases combined.

Figure 14 displays the relative increase and decrease in the environmental emissions and energy for the ‘Reference’ and ‘As-Built’ mode by life cycle stage.

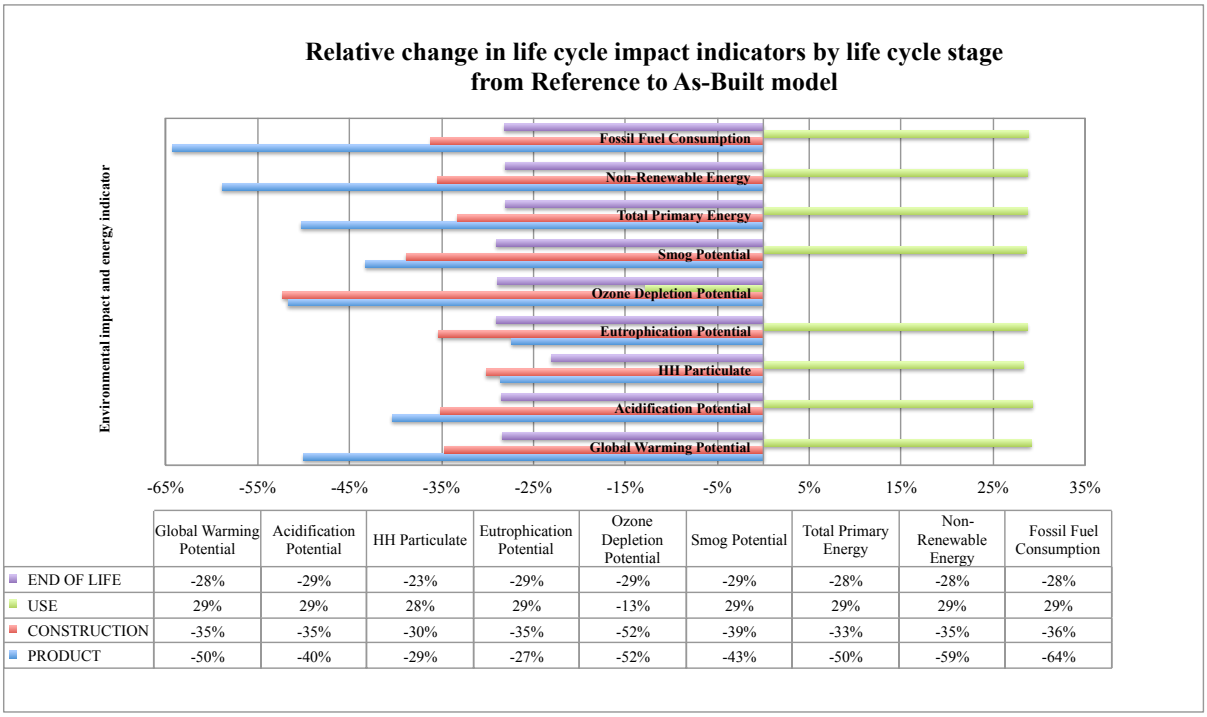

	Global Warming Potential	Acidification Potential	HH Particulate	Eutrophication Potential	Ozone Depletion Potential	Smog Potential	Total Primary Energy	Non-Renewable Energy	Fossil Fuel Consumption
END OF LIFE	-28%	-29%	-23%	-29%	-29%	-29%	-28%	-28%	-28%
USE	29%	29%	28%	29%	-13%	29%	29%	29%	29%
CONSTRUCTION	-35%	-35%	-30%	-35%	-52%	-39%	-33%	-35%	-36%
PRODUCT	-50%	-40%	-29%	-27%	-52%	-43%	-50%	-59%	-64%

Figure 14. Relative change in life cycle indicators by life cycle stage ('Reference' to 'As-Built') for gas energy model

For all life cycle phases, except the use phase, there is less impact for the ‘Reference’ model; however, the use phase overwhelms the product and construction phases for each category and combining the life cycle phases results in a different pattern emerging. Figure 15 illustrates the entire life cycle relative change from the ‘Reference’ to the ‘As-

Built' model by each environmental and energy impact category. All categories achieved positive improvements from the 'Reference' model except oxygen depletion potential, which occurred because of the use of foam insulation instead of fiberglass insulation. Total primary, non-renewable and fossil fuel energy consumptions were reduced 24% over the life cycle. Global warming potential and acidification potential were reduced 24% and 25%, respectively, while other atmospheric emissions such as human health particulate potential and smog potential were reduced 18% and 11%, respectively.

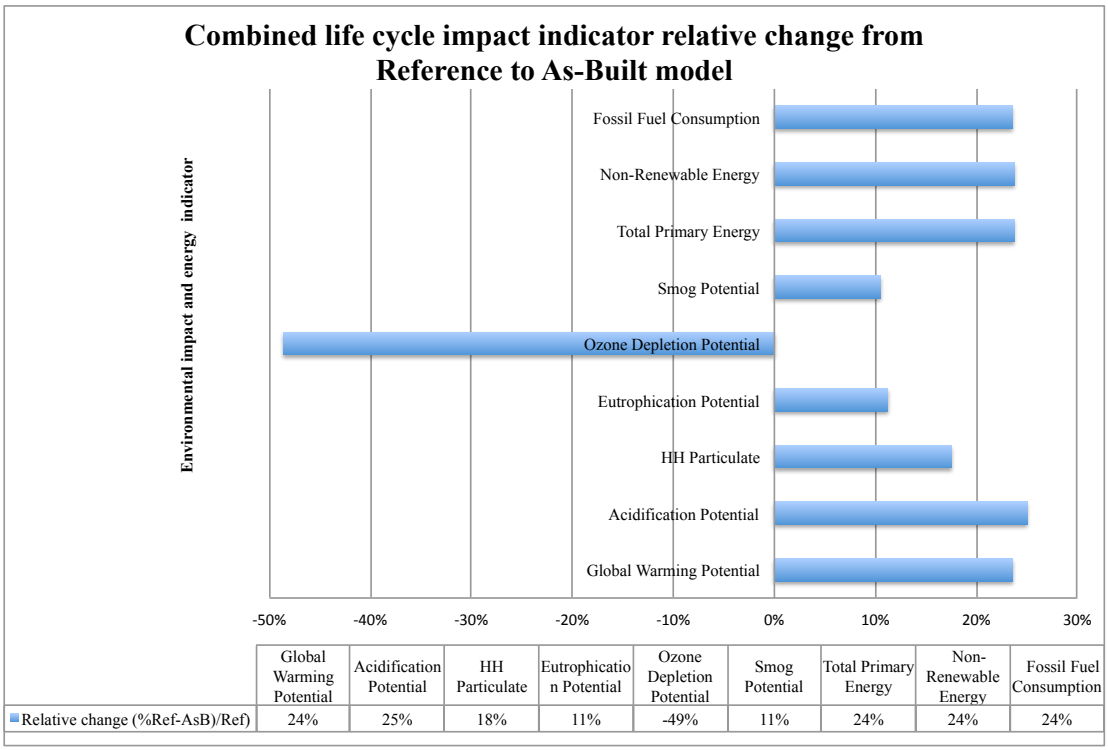

Figure 15. Life cycle impact indicators relative change from 'Reference' to 'As-Built'

Eutrophication potential was reduced by 11% in the analysis. Life cycle environmental impact indicators by life cycle stage for gas and electric space and water heating are tabulated in the Appendix A-25and 26, respectively. Additionally, Figure A-34 through A-39 illustrates graphical representation of the life cycle stage contribution of each of the reported environmental indicators for the gas space and water-heating model.

An investment in the initial phases of the building life cycle trade up for less life cycle impact in the long run. Operational energy variables such as the primary building electrical demands, consisting of HVAC, lighting, appliances and plug-loads, and domestic hot water usage, dominate the life cycle energy profile and subsequent environmental impacts in all categories except ozone depletion potential.

Renewable Energy Impact

Operational energy inputs for the life cycle model were augmented with the renewable energy reductions discussed previously in chapter three for gas water heating only. The renewable energy systems were combined, and they offset the annual operational energy that was input into Impact Estimator. Table 10 tabulates the results of the reduction percentage of the impact indicators for the use-phase of the building. The reduction is calculated by the relative change from the use phase primary energy without renewable energy compared to the use-phase primary energy with renewable energy.

Table 10. Renewable energy systems (SPVS and SHWS) life cycle environmental impact indicators as a reduction percentage

Building Model	Global Warming Potential	Acidification Potential	HH Particulate	Eutrophication Potential	Ozone Depletion Potential	Smog Potential	Total Primary Energy
REFERENCE	9.4%	9.5%	8.8%	9.5%	0.2%	9.1%	9.4%
AS-BUILT	13.4%	12.3%	13.3%	13.3%	0.2%	12.7%	13.2%

Primary energy and global warming potential were reduced 9.4% and 13.4% and acidification and smog potential were reduced by 9.1% and 9.5% for the 'Reference' and 'As-Built' model respectively. The eutrophication potential decreased 9.5% and 13.3% for the 'Reference' and 'As-Built' models and finally, the ozone depletion potential decreased by a small fraction of 0.2% while electric space and water heating numbers were slightly larger by 1 and 2% for the 'Reference' and 'As-Built' model in all categories except for the ozone depletion potential, which stayed the same. Appendix A-27 tabulates the use phase for the 'Reference' and 'As-Built' gas water and space-heating models with and without renewable energy input.

Water Resources

Water consumption was estimated in the life cycle analysis of the building and was determined based the consumption in the product, construction and a small fraction of the use phase for maintenance and replacement in Impact Estimator. Additionally, operational use was determined based on direct water consumption estimations utilized in chapter four while water consumption derived from electrical generation was estimated in the water use phase. Rainwater effects on the operational use of the water were also estimated based on assumptions and on a stochastic simulation presented in

chapter four. Figure 16 presents the water consumption of the different building models by life cycle stage and their associated consumptive values in liters and the rainwater building use with and without RWH.

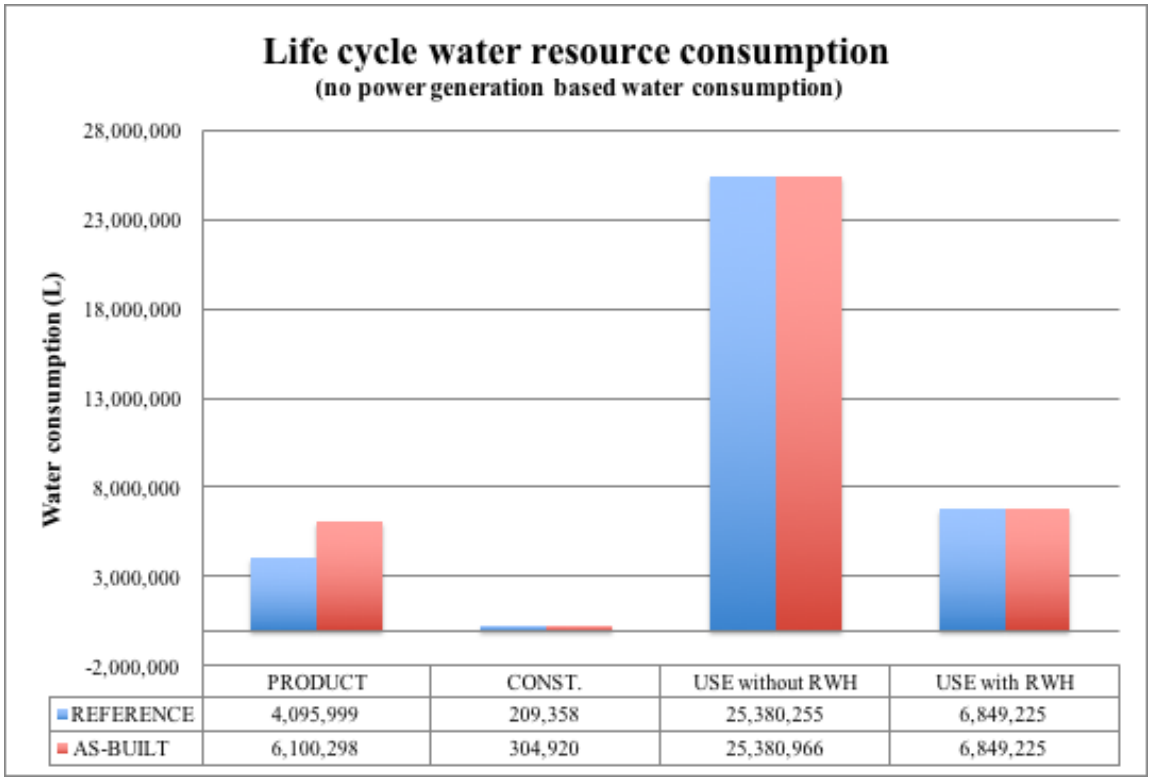

	PRODUCT	CONST.	USE without RWH	USE with RWH
REFERENCE	4,095,999	209,358	25,380,255	6,849,225
AS-BUILT	6,100,298	304,920	25,380,966	6,849,225

Figure 16. Life cycle water consumption with and without rainwater harvesting

With no rainwater harvesting considered, total water consumption was 29.68 and 31.78 mega-liters (ML) for the 'Reference' and 'As-Built' models, respectively. The 'As-Built' model contained 49% more water consumption in the product phase, 46% more in the construction phase and, finally, 7% more overall compared to the 'Reference' model. The end-of-life phase had no water consumption. The use phase

dominates both models with 85 and 80% of the use phase for the 'Reference' and 'As-Built' model, respectively.

Utilizing the results of the Monte-Carlo simulation reported in chapter four, the rainwater catchment was estimated based on a 75 % fraction of the annual demand being met by the rainwater so that the annual water consumption would be reduced from an estimated 507 m^3/year to 127 m^3/year. Additionally, the probability of this occurrence was estimated to be 45.8%. The operational use phase of the water consumption was estimated at 6.36 ML over a 50-YR life cycle, and this consumption was close to the product phase water consumption of the 'As-Built' model. With operational water use at these levels, the life cycle water consumption was reduced 64% and 60% for the 'Reference' (10.672 ML) and 'As-Built' (12.77 ML) model, respectively.

Summary and Conclusions

Operational Energy Analysis

The 'As-Built' model achieved a 31.2% and 28.9% reduction in total building energy when compared to the 'Reference' model for both that gas and electrical supplemental heating, respectively. Total HVAC energy was 48.4% of the annual building energy for the 'As-Built' model and 60.2% of the annual energy for the 'Reference' model. The 'As-Built' models had a 42% and 45.3% reduction from the 'Reference' model for the gas and electrical supplemental heating, respectively. The lighting represented an average (electrical and gas models averaged) 5.4% and 3.8% and the appliances and plug-loads were an average of 35.1% and 24.6% of the annual energy for the 'As-Built' and 'Reference' model, respectively, in addition, domestic hot water

energy consumption was an average 11.2% and 7.8% of annual energy for the 'As-Built' and 'Reference' model, respectively.

Approximately 23% (average of the models) of total building energy reduction was attributed to an infiltration reduction from ACH5 to ACH1.5 (holding building envelopes constant) while a 10% (average of the models) reduction in building energy was due to building envelope effects. However, as discussed previously, these reductions are linked in that infiltration is impacted by the building envelope materials and construction type and quality.

Finally, the renewable energy systems contributed an annual average of 12.5% and 15.5% reduction for the 'Reference' and 'As-Built' operational energy while the life cycle primary energy was reduced 9.4% and 13.4%, respectively.

EUI as an Operational Energy Indicator

Building Energy Use Intensity (EUI) and Net Energy Use Intensity (NEUI) are indices that can be used to describe the amount of operational end-use energy that building uses per year. Also they are useful in comparing buildings to other buildings in a standardized way and to set performance goals currently being used by governmental agencies. EUI/NEUI are highly dependent on the type of building as the energy intensity per square area, and as such, needs to be taken in context to the type of building evaluated. When compared to Architecture 2030 goals based on US EIA residential building regional statistics), the 'Reference' model achieved a EUI below the US EIA average and the 'As-Built' model is essentially at the 50% reduction target of EUI 19.4 with the EUI for the gas and electrical heating models achieving similar EUI and NEUI

values, with gas having a bit higher number due to extra energy usage due to process efficiency differences. The EUI for both the 'As-Built' model and the 'Reference' model were both strong achievers when compared to the US southern regional average and with renewable energy systems the results were even stronger; however, the lowest NEUI attained, at 16.1, did not meet the 60% reduction target of the Architecture 2030 (EUI 15.5) or the high achieving, Passivhaus standard of an EUI of 15.

Life Cycle Impact Analysis

The results of the life cycle analysis for all phase are consistent, for both the 'Reference' and 'As-Built' models, with the use (operation and maintenance) stage clearly being the most dominant, and by assembly group, wall and foundation assemblies have been shown to yield the maximum emissions. For the 'As-Built' case the roof assembly was also a major contributor.

For the gas space and water heating, the embodied energy was 1,608 GJ and 2,376 GJ over the 50-year period for the 'Reference' and 'As-Built' models, respectively, while embodied energy intensities (GJ/m^2) being 2.7 and 4.0, respectively for the 'Reference' and 'As-Built' cases. Operational energy was 24,483 and 17,226 GJ, with energy intensities of 41.4 and 29.5 GJ/m^2 over the 50-year period for the 'Reference' and 'As-Built' models, respectively. Total primary energy over the life cycle was 26,216 and 19,983 GJ, with energy intensities of 44.4 and 33.8 GJ/m^2 for the 'Reference' and 'As-Built' models, respectively. The embodied phase was 6% and 12% and the use phase was 93% and 87% of the total primary energy for the 'Reference' and 'As-Built' model, respectively. Primary energy life cycle totals and intensities are

tabulated in Appendix A-40. The electrical space and water heating models followed similar trends as the gas modes with the operational energy and total energy slightly higher (see Appendix A-41 for more details).

Global warming potential followed similar distribution patterns as that of the primary energy and with the gas space and water heating models, GWP intensities (kg CO_2-eq/m^2) being 193 and 286, respectively for the 'Reference' and 'As-Built' cases. Use phase GWP intensities were 2,626 and 1,861 kg CO_2-eq/m^2 over the 50-year period for the 'Reference' and 'As-Built' models, respectively. Total life cycle GWP intensities of 2,835 and 2,166 kg CO_2-eq/m^2 for the 'Reference' and 'As-Built' models, respectively. The embodied phase was 7% and 13% while the use phase was 93% and 86% of the total primary energy for the 'Reference' and 'As-Built' model, respectively. Again, the electrical space and water heating models followed similar trends as the gas modes with the operational energy and total energy being slightly higher (see Appendix A-40 and A-41 for more details).

The results from inventory analysis and impact assessment either compared one life-cycle stage with the other or one assembly to another so as to help to identify the building design components that have the largest impact with respect to total energy load and environmental impact. Improving the design of the building envelope to minimize the initial embodied energy footprint while maintaining the high operational performance attributed to low infiltration, minimal thermal transmission and efficient HVAC systems are of the highest concern. Identifying wall and roof system alternatives that can simultaneously reduce the upfront environmental burden and minimize the use

phase energy burden is the forefront in building design. Additionally, renewable energy systems can appreciable impact not only reductions in building energy demand but also reductions in environmental emissions to the air and water. Finally, rainwater collection systems and their output, although highly dependent on rainfall, may have a significant impact on life cycle water consumption. For example, in this study a 22.6 m^3 rainwater collection system yielded, with a 45.8% probability, approximately the same use-phase water consumption as the 'As-Built' model product and construction phase alone.

LCA is a quantitative, but approximate approach to evaluate building design and to explore the systems and relationships that impact design goals. Life cycle understanding assists and influences building and system designs and attributes, and it may influence the over-arching decision-making process in the building sector, such as influencing building codes and their emphasis. By exposing the critical parameters influencing environmental emissions and resource conservation, life cycle analysis studies of buildings are desirable to evaluate design alternative in the built environment.

CHAPTER III

RENWABLE ENERGY SYSTEMS

Synopsis

Hot and humid climates with high solar radiation have the potential to offset residential building energy consumption with the application of solar hot water and photovoltaic electricity generation, both of which are the subject of this paper. However, the costs, lack of incentives for the systems and more importantly, the unfulfilled need for proof-of-concepts continue to limit market penetration. Although, solar energy use and production has grown in the United States, regional economics coupled with a need for incentives continue to keep many solar abundant regions underdeveloped. For example, the surplus of natural gas in certain areas of the United States, particularly Texas, continues to keep gas and electricity production economical compared to solar alternatives. However, ecologically minded consumers, trends that demand lower energy homes and finally, a desire for local energy independence, which is the hallmark of net-zero energy buildings (NZEB), continue to fuel solar energy systems penetration. To support solar use, this research was performed to evaluate and analyze the real-world life cycle energy and costs of a solar photovoltaic and solar hot water system installed on a high-end residential home in Houston, Texas (IECC Zone 2). The house was a well-insulated, low-infiltration, large urban home with two renewable energy systems installed; a 3.5 kW solar photovoltaic system and a 1.71 KW solar hot water system. Analyses were part of a larger study performed to investigate the contributions of the solar energy offsets on the operational energy of the building over a life cycle of 30-

years. Field measurements of energy production were compared to solar energy simulations based on typical meteorological year and the National Solar Radiation Database (NSRDB) data. NSRDB provided the basis for a probabilistic interpretation of annual energy production in terms of exceedance probability measures, P50/P90. It was found that field estimates were within simulation uncertainties and P90 predictions were within 2.5% of TMY3 results for both the solar photovoltaic system (SPVS) and solar hot water system (SHWS). Additionally, optimizations in the system design and life cycle costs were investigated to determine annual optimal performance for the solar energy systems. The SHW system was installed at a less than optimum azimuth of 270° instead of 180°. The SPVS was installed at optimal design conditions of 180° azimuth and 42° tilt. Additionally, payback and LCOE could have been minimized with the addition of another solar hot water collector with a minimal impact to overall cost. Cost sensitivity analysis on the LCOE and NPV were also performed and over a 30-year lifecycle, TMY3 based simulations predicted a NPV of $796 (21.8-year payback) and -$1246 (29.2-year payback) for the SHWS and SPVS, respectively. The SHWS achieved a LCOE of 8.1 ¢/kWh while the value for the SPVS is 12.29 ¢/kWh. For the SPVS, the photovoltaic module and collector costs were the largest determinant in life cycle costs, and of special note, a reduction in module cost by 67% reduces the LCOE to the regional electric price. Finally, the combined renewable energy systems, as installed in the residence, generated a estimated 30-year life-cycle energy production of 184,814 kWh, with auxiliary gas provided for additional hot-water heating.

Introduction

The zero-energy home trend has gained momentum in recent years (Marszal et al. 2011, Li, D. H. et al. 2013) and The United States Department of Energy sponsorship of the 'Zero-Energy Ready Home' program promotes high performance homes that are so efficient that the installed renewable energy systems can offset all or most of its annual energy consumption (US DOE 2014b). In these types of buildings two design principles figure prominently, energy efficiency measures and renewable energy systems (Li, D. H. et al. 2013). Advanced building envelope designs and efficient heating, air conditioning and ventilation systems (HVAC), efficient lighting and appliances, all contribute to energy efficiency. In all cases achieve the zero-energy status the buildings require renewable energy systems which are typically photovoltaic systems; however, hot water provided by solar thermal systems can offset energy as well. In some regions throughout the world, solar hot water is common for traditional domestic water uses, and in some climates, it may even be used for space heating. In the case study evaluated and analyzed herein, hot water was provided by a solar hot water system (SHWS) incorporating flat-plate solar collectors, and a thermo-siphon heat exchanger mated with an 80-gallon water storage tank. In addition, a natural gas fueled on-demand hot water heater backs up the solar thermal system. As noted previously, the house was also equipped with a 3.5 kW, 20-panel polycrystalline solar photovoltaic system (SPVS) installed on the southeastern roof at a 42° tilt and is grid-tied with no battery storage.

The potential of using renewable energy systems to offset residential operating energy can be significant. However, system costs, along with installation and operational

costs and other issues may hinder system penetration and performance. Simulation tools such as TRYNSYS and the National Renewable Energy Laboratory's (NREL) System Advisory Model (SAM) have been used to optimize and study solar electric and thermal systems in residential applications (Blair, et al. 2014, Hobbi and Siddiqui 2009, Kalogirou 2009). Additionally, Kalogirou (2009) presents thermal performances with life cycle evaluations of thermosiphon solar hot water systems. A similar approach utilizing NREL's SAM was used in the study reported herein to estimate the impact of the two solar systems installed at this location. The background of SAM is that it is in ongoing development with NREL, Sandia National Laboratories and in partnership with the US Department of Energy since 2006 (NREL 2014). Also, SAM is an energy performance and economic modeling tool, which enables users to analyze a wide variety of financial models and renewable energy system types, and it contains verified product databases and models for numerous commercially available products. Verification of SAM models with field data has been conducted in past studies with positive results (Freeman et al. 2013, 2014). To summarize, SAM provides a comprehensive suite of analysis tools and it is publicly available (Blair et al. 2014).

Energy production from the solar energy resource is dependent on the variability of weather, particularly the solar radiation. Typical meteorological year data is constructed from "typical" months that represent normalized weather data for a given site (Wilcox and Marion 2008) and is often used to perform solar and building simulations. The filtered aspect of this meteorological data can obscure worst-case situations that may, in fact, impact life cycle energy production and costs (Dobos and

Gilman 2012, Vignola et al. 2012). However, the variability of solar resources and its impact on the energy production can be analyzed by using exceedance probabilities based on large solar radiation datasets, such as the NSRDB. The NSRDB dataset provides input to SAM statistical analysis capabilities and provides P50/P90 exceedance probability calculations. P50/P90 analysis is an analysis performed to estimate system performance based on variable inputs such as weather (Dobos and Gilman 2012, Vignola et al. 2012). In the study reported herein SAM was utilized to verify existing residential renewable energy systems, perform optimizations and to estimate life-cycle energy production and costs in the context of a building life-cycle analysis.

System Characteristics

Solar Photovoltaic System

The solar photovoltaic array for the case study was installed on the southeastern roof at installed design conditions of 180° Azimuth and a 42° tilt. The solar photovoltaic panels, along with the solar hot water system panels are shown in the Figure 17 satellite image.

Figure 17. Renewable energy systems building roof placement (Google Maps 2014)

The SPVS is comprised of 20 individual 175 W modules with associated micro-inverters that have a certified efficiency rating of 94.5%. The PV system has a peak Standard Test Conditions (STC) DC size of 3.5kW and with a design estimated electrical generation of 4,346 kWh per year. The array consists of 20, 175W modules that individually connect directly a micro-inverter. Two hundred and forty volt output power passes through a utility disconnect and ties into a breaker located in the main service panel. The utility disconnect is mounted on the wall within 5ft of the utility meter. Figure 18 illustrates the PV system installed on a south facing roof.

Figure 18. Street (left) and close-up (right) views of the solar photovoltaic system (SPVS)

The PV modules have micro-inverters that provide AC power and data communications via the power-line interconnects to the building circuit breaker. A data acquisition gateway is also connected to the service panel and polls the micro-inverter status information, including power data. Figure 19 is an illustration of the photovoltaic system, grid connection and associated data system. Voltage and current information is monitored by the data acquisition gateway and posted to a centralized, Internet-based, data monitoring service.

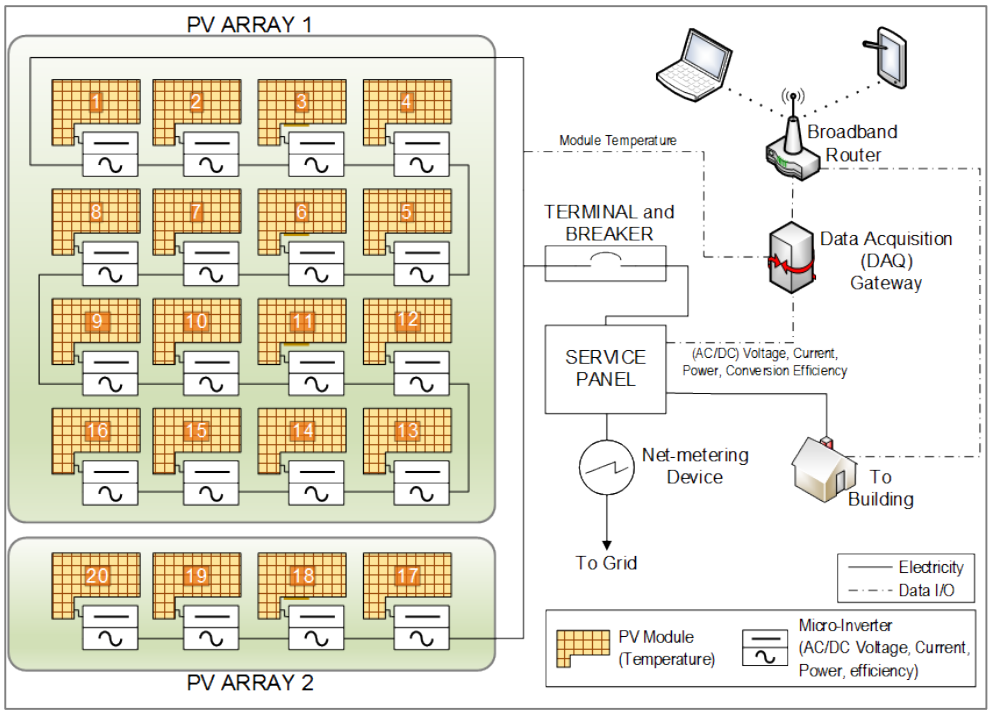

Figure 19. Solar photovoltaic system and monitoring system diagram

Solar Hot Water System

A 2.97 m^2 flat-plate collector and thermosiphon heat exchanger with a 0.3 m^3 (80-gallon) water storage tank provides solar hot water. The flat-plate collector is on a 22° tilt facing west as originally specified by the renewable energy contractor. A diagram of the solar hot water system is presented in Figure 20. The SHWS features a high performance coating to maximize absorption of the solar radiation. A low-power (24 W) gear pump operating at 0.02 kg/sec circulates heated water from the solar panel into a flat-plat heat exchanger. The flat-plate heat exchanger provides heat to the hot water tank by thermosiphon flow, whereby the hot water passively circulates in the

system. In addition, an on-demand, efficient gas-fueled hot water heater backs up the solar thermal system as a booster.

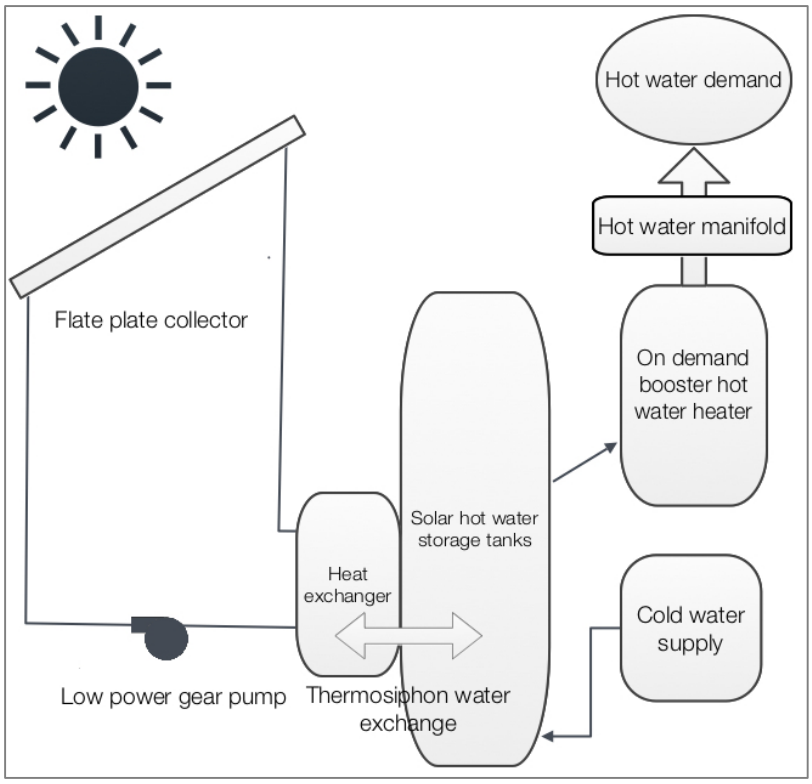

Figure 20. Illustration of the solar hot water system and its major components

The solar hot water appliance provides protection against overheating and stagnation, thus preventing damage to the collector and fluid, finally, the installed solar water heat collectors are low profile. Figure 21 is a photograph of the solar collector, heat exchanger and thermal storage tank, while Table 11 lists the detailed specifications of the SHWS.

Table 11. Solar hot water system specifications

Specification	Description of item
System Type	Domestic hot water (DHW) heating only
Collector Loop	Liquid (polypropylene glycol), 1.219 m x 2.438 m (4X8 ft) , 7.6 cm) (3 in) deep, 50 kg (110 lb) each, Absorber: copper tube on aluminum sheet; absorptance of 94% (± 2%) and emittance of 5% (± 2%)
Collector Type	Glazing: Low-iron, patterned, tempered glass with side edge guard Single glazing,
Collector Area:	2.973 m^2 (32 ft^2)
Storage Volume	0.3 m^3 (80 gallons), glass lined, ASHRAE 90.1 certified
On-demand hot water heater	86% efficiency conversion, Hot water capacity: 0–78.7 LPM (0-26 GPM), Gas input rate MAX/MIN : 69.16/13.92 KWh (236,000/47,500 BTU)
Pump	Low power (24 W) gear pump, 0.02 kg/sec (0.32 gpm/sec) flowrate

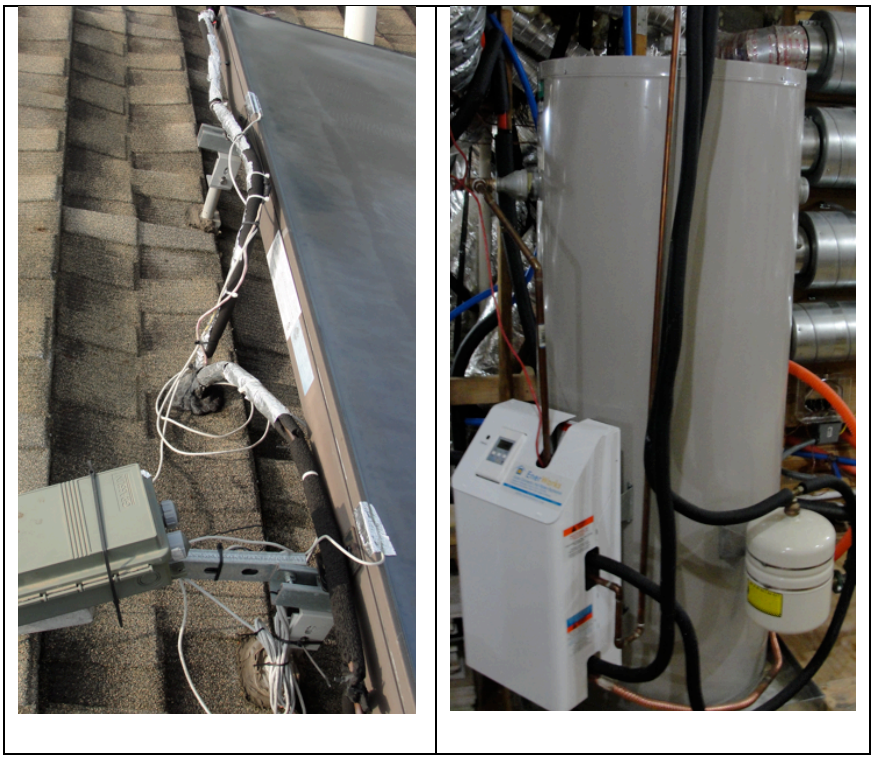

Figure 21. Solar thermal collector, heating appliance and hot water storage tank

Solar Energy Simulation

Renewable energy production was assessed with monitoring equipment and simulation tools. The PV system power was monitored with direct power measurements. Additionally, the thermal characteristics of the solar thermal system were monitored with a sensor network to estimate the heat delivered from the solar system to the solar storage tank. Onsite measurements were used to verify the simulation programs predictions. NREL's SAM was utilized further to analyze the solar thermal and electric systems to assess performance and estimate life cycle production. Table 12 details many of the top-level details of the systems to be simulated.

Table 12. Relevant system parameters for the simulations performed

System parameter	Solar photovoltaic system	Solar hot water system
Rated system size	3.5 KW	1.71 KW
Panel tilt	42°	22°
Azimuth	180° (South)	270° (West)
Weather and radiation data source	TMY3 Hobby Airport, Houston, TX	TMY3 Hobby Airport, Houston, TX
Longitude and Latitude	29.9833 °N, -95.3667 °E	29.9833 °N, -95.3667 °E
Installed cost	$26,500	$6,350

SAM predictions are based on weather and solar irradiance for a typical metrological year (TMY3) and the NSRDB dataset for Houston, TX, in addition to detailed parametric specifications of the SPVS and SHWS. SAM facilitates an integration of multiple databases and models for renewable energy systems, including PV modules and inverters and solar hot water collectors and has been extensively validated against measured data and other similar tools (Blair et al. 2012, Freeman et al.

2013, Rudie et al. 2014, Thevenard and Pelland 2011). SAM integrates the California Energy Commission's (CEC) PV module database, which contains model parameters for the eligible photovoltaic modules maintained by the CEC for the California Solar Initiative. SAM also integrates Sandia's model for grid-connected PV inverters, which is an empirical model of inverter performance based on parameters of commercially available inverters maintained by the CEC (NREL 2015). Additionally, SAM has solar thermal collector performance datasets verified by the SRCC and models based on published solar flat-plate thermal collector concepts and models (Burch and Christensen 2007, Duffie and Beckman 2013, NREL 2015).

The simulation was run in conjunction with TMY3 and NSRDB data for the area nearest to the location (Hobby airport, Houston, TX). Other notable site position and radiation data are listed in Table 13.

Table 13. Simulation site, temperature, wind and irradiance parameters

Site parameters		
Location	Hobby Airport, HOU,TX	
Data Source	TMY3	
Elevation	13	meters
Lat	29.65	° N
Long	-95.283	° E
Weather Station ID	722435	

Table 13. Continued

Annual irradiance and temperature and wind summary		
Global horizontal	4.28	$kWh/m^2/day$
Direct normal	3.68	$kWh/m^2/day$
Diffuse horizontal	2.01	$kWh/m^2/day$
Average temperature	21.1	° C
Average wind speed	3.5	m/s

Solar Photovoltaic System Simulation

SAM was used to model the grid-connected PV system that consists of a 20-module photovoltaic array and associated inverters. Models for the modules and inverter are used in SAM, which facilitates the choosing of either Sandia, CEC or manually input performance data for PV modules, and in addition to choosing either the Sandia or single-point efficiency models for inverters (NREL 2015). The user specifies the module and inverter characteristics, array design, AC and DC derating factors, shading, costs and temperature correction models (NREL 2015). The photovoltaic module used in this simulation is based on the CEC performance model and predicts module performances based on a database of module characteristics determined from module ratings of the system deployed. The inverter CEC database calculates the systems AC voltage output by using parameters from SAM's CEC database of parameters with the Sandia inverter mode (NREL 2015). The inverter model calculates the voltage DC to AC conversion efficiency, based on the DC power input of the photovoltaic array. Also, the model limits the inverter's output to the inverter's maximum AC power (NREL 2015).

SAM's PV models have been verified and validated against measured data (Blair et al. 2012, Freeman et al. 2013, Rudie et al. 2014, Thevenard and Pelland 2011). In addition, Blair et al. (2012) and Freeman et al. (2013) compared model versus quality-controlled measured performance data for nine PV systems. Blair et al. (2012) found ± 3% or less annual errors for all the systems at and monthly errors varying ± 6%, while Freeman et al. (2013) concluded that combinations of SAM mode errors fell within an annual error range of 8.5%. Rudie et al. (2014) ran performance analysis of SAM PV models for 100 sites with measured data and found a mean bias error of 0.8% and a mean absolute error of 13.7%. Thevenard and Pelland (2011) concluded SAM's combined uncertainty was approximately 8.7% for the first year of operation and a lifetime energy error of 7.9%. Uncertainties may be derived from radiation and climatic variability, and from other site characteristic deviations such as shading and system derating factors. For the study reported herein, the combined uncertainties of the parameters used in the simulation were estimated to be ± 6.26% and in Appendix A-42 are tabulations of the uncertainties along with their assumptions.

Solar Hot Water System Simulation

SAM has a closed-loop flat-plate collector model that transfers energy from the transfer fluid to the external heat exchanger and the solar storage tank (NREL 2015). In SAM, the solar tank is filled with water from the mains, pumped through the heat exchanger and returned to the top of the tank (NREL 2015). The system installed, evaluated and reported herein operates in the same fashion. In addition, the solar thermal energy output of the system was predicted based on incident solar radiation and solar

collector properties and coefficients (Duffie and Beckman 2013, NREL 2015), additionally SAM used the system ratings tested and reported by the SRCC in accordance with ISO 9806, *Solar thermal collector test methods*. The collector in this study was assumed to be flat-plate and plumbed in parallel with uniform flow. Additionally, the collector was characterized by the linear form of the collector efficiency and incident angle modifier, the parameters were corrected for the flow rate, heat exchanger, and pipe losses using relations in Duffie and Beckman (Duffie and Beckman 2013, NREL 2015). The collector was configured in a location with TMY and NSRDB meteorological and geographic data and the collector orientation, tilt, flow-rate, fluid type, number of collectors, model type, albedo and collector area were also configured. In addition to collector data and weather conditions, other site-specific data was required, with all of these inputs and configurations then being used to generate the simulations. The solar heat exchanger is external to the solar tanks, and was assumed to have no thermal losses and the heat exchanger effectiveness was also detailed along with the plumbing details such as piping diameter, length and insulation; pump power and efficiency and the mechanical room air temperature. The solar storage tank geometry and heat loss coefficient were specified as well and hot water demand profiles were detailed in daily averages.

SAM's model output is dependent on the simulation parameters and variables that originate in the solar panel performance characteristics along with other model input parameters estimated by the user and the simulation engine. Solar panel performance characteristics in SAM were measured in rating and certification laboratories and these

estimates and their uncertainties contribute to the uncertainty in the model results. The expanded uncertainty of the solar thermal collector thermal efficiency has been reported to range from 1.6 to 5% (Mathioulakis et al. 1999, Kovacs 2012), while the calculated energy gain uncertainty exceeds 10% (Kovacs 2012). Additionally, utilizing a Monte-Carlo simulation technique, Mathioulakis et al. (2012) estimated an expected annual output uncertainty of 9% on a typical solar thermal system. Based on an estimate of the combined uncertainties of all the parameters in the simulation, the uncertainty was estimated to be ±5.46%. See the uncertainty and assumptions tabulated in Appendix A-43 for ore details.

Solar Energy Field Monitoring

Solar Photovoltaic System Field Monitoring

The photovoltaic system was monitored with the pre-existing PV monitoring system and the power production of the system was measured from 2012 to 2013 with intermittent outages. The accuracy of this system power measurement was stated to be ±5% by the manufacture (Enphase 2014).

Solar Hot Water System Field Monitoring

Solar collector output was measured by using 1-wire® digital thermometers that were installed and monitored as a part of the solar thermal system. The multi-drop, 1-wire® digital technology facilitated multiple temperature measurements with a cost-effective, and in addition it has a factory verified temperature accuracy of ± 0.5 °C (Adams 2012). These temperature probes were installed directly on the plumbing with thermal paste and tie-wraps, and then the exposed temperature sensors were insulated

with pipe insulation where necessary. Finally, the sensors were fed into an Internet-based data logger. Solar hot water system performance was estimated by using water temperature dynamics to evaluate the solar collector energy output to the solar hot water collector. Specifically, the heat energy gathered from the solar thermal system was estimated by measuring the heat acquired from the solar thermal collector as measured by the temperature difference of the solar collector along with manufacturer specifications on the gear pump, and the heat capacity of the fluid which was controlled with a differential temperature controller. Following Duffie and Beckman (2013) the following general equation was used to determine the estimated energy from the collector loop:

$$Q_{col} = m_j C_{p,fluid} (T_{co,j} - T_{ci,j})$$

where,

Q_{col} is the net energy output from the solar collector

m_j is the mass of the j^{th} increment of circulated antifreeze fluid

$C_{p,fluid}$ is the specific heat of antifreeze fluid

$T_{co,j}$ is the temperature of the collector outlet of the j^{th} increment of water

$T_{ci,j}$ is the temperature of the collector outlet,

+ indicates positive contributions are counted in the calculation.

A simplified method based on estimating the heat exchanger effectiveness and multiplying the effectiveness by the energy delivered by the collector alone was used to

estimate the fraction of energy delivered to the storage tank. The solar energy delivered from to the storage tank was estimated as:

$$Q_{stor} = \varepsilon\, Q_{col,\, i}$$

where,

Q_{stor} is the net energy delivered to the storage tank in i^{th} increment of water,

Q_{col} is the net energy of from the collector at i^{th} increment of water,

ε is the effectiveness of the heat transfer from the solar collector to the solar storage tank.

Solar Energy Analysis

The solar photovoltaic and hot water simulation models were simulated with parameters based on site conditions such as panel orientation and tilt and system components were modeled with SRCC and CEC datasets where available. Energy production was estimated based on field assessments and SAM simulations and is detailed in the following sections.

Solar Photovoltaic System

The energy production of the SPVS was modeled based on CEC PV module and inverter datasets. The PV system utilized micro-inverter technology that produced panel-level power production. Both the photovoltaic modules and micro-inverter were both rated at 175W. The characteristic curves of the photovoltaic module (volts vs. amperes) and micro-inverter (efficiency vs. output) are detailed in Appendix A-44 and A-45.

Temperatures correction was performed in the simulation with the nominal operating cell temperature method as documented in Duffie and Beckman (2013) and Neises (2011). Installation parameters included one-story height and rack-mounting with no shading modeled. The simulation utilized a titled surface radiation HDKR diffuse sky model with beam and diffuse irradiance components. According to Duffie and Beckman (2013), the HDKR model yields better results than either the isotropic or the Perez model in predicting utilizable radiation and model performance was closer to measured values. Simulations were run on TMY3 data for Hobby airport Houston, TX and were compared to field measured data. The energy production of the photovoltaic system was recorded utilizing existing equipment intermittently from February 2012 to November 2013. The data was aggregated and monthly outputs were computed and compared against the simulation monthly output. Figure 22 illustrates simulated vs. measured monthly energy for data obtained in 2012 and 2013. SAM PV predictions are generally regarded with an uncertainty of ± 8-15% (Freeman et al. 2013, 2014).

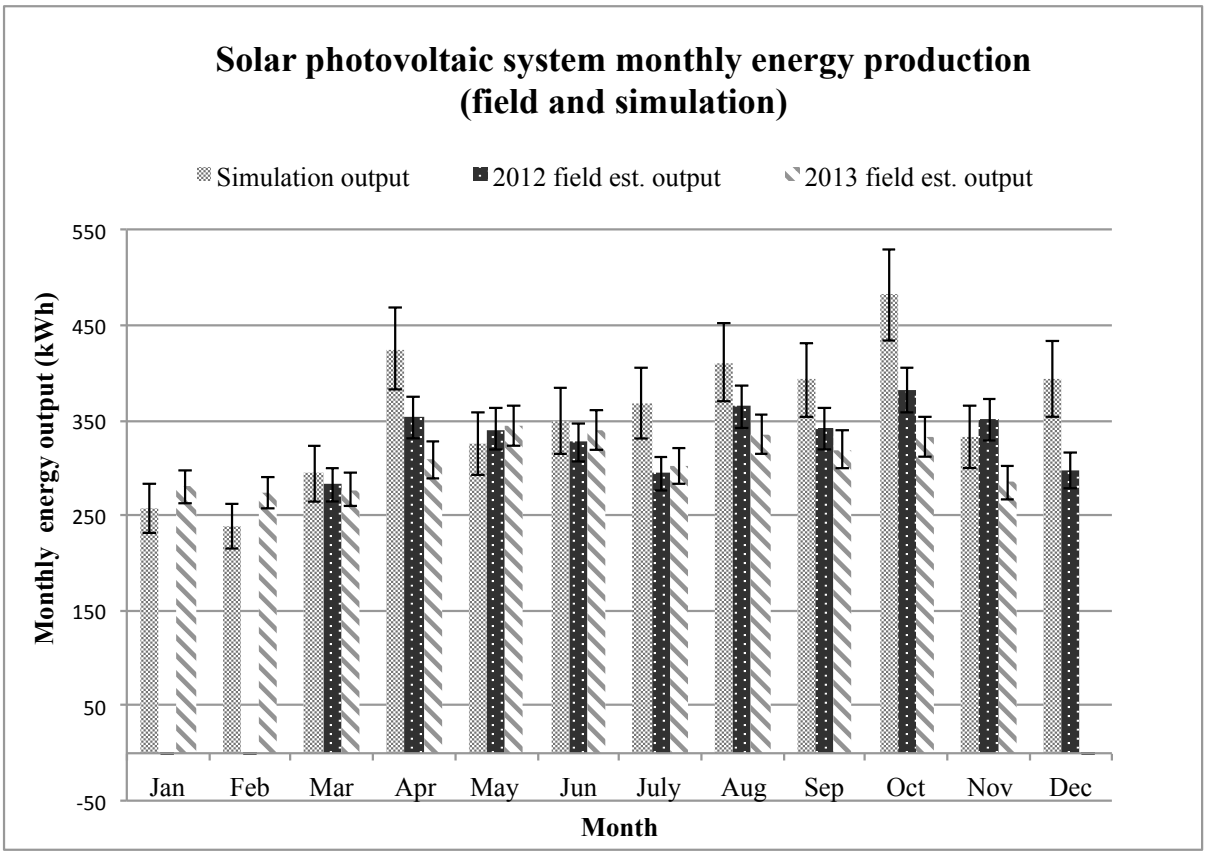

Figure 22. Solar photovoltaic system field and simulated and measured monthly energy with uncertainty bars

Measured data is based on instruments with reported accuracy of ± 5.46%. Annual field energy production was within 6% of predicted output for 2012 and 12% for 2013 with no degradation accounted for. Considering variations in weather in typical meteorological data and potential differences in associated derating and other loss factors (shading and soiling) the differences between simulated and measured data were considered acceptable for the life cycle evaluation.

Solar Photovoltaic System P50/P90 Analysis

P50/P90 analysis was performed to assess the annual energy exceedance probabilities calculated based on the 30-year NSRDB for Houston, Texas. SAM provides these capabilities in two types of probabilistic metrics, namely, P50 and P90. A P50 of 4,000 kWh a year is there is a 50% likelihood that the annual output will be greater the 4000 kWh. Similarly, a P90 value contains an annual output with a 90% likelihood of exceedance. The P50 and P90 values are obtained through the estimation of the cumulative distribution function (CDF). SAM achieves this through two types of estimation of the CDF, one that assumes the data fits a normally distribution (P50/P90-norm) and another that uses the radiation data to empirically generated the CDF (P50/P90-emp) as described in Dobos and Gilman (2012). Solar resource data are not known to fit a normal distribution well and the empirical-based CDF and values are considered a more reliable approach (Dobos and Gilman 2012). In this study both normal and empirical estimates were considered. Figure 23 illustrates the annual solar photovoltaic energy production of the P90/P50 and TMY3 simulation estimates.

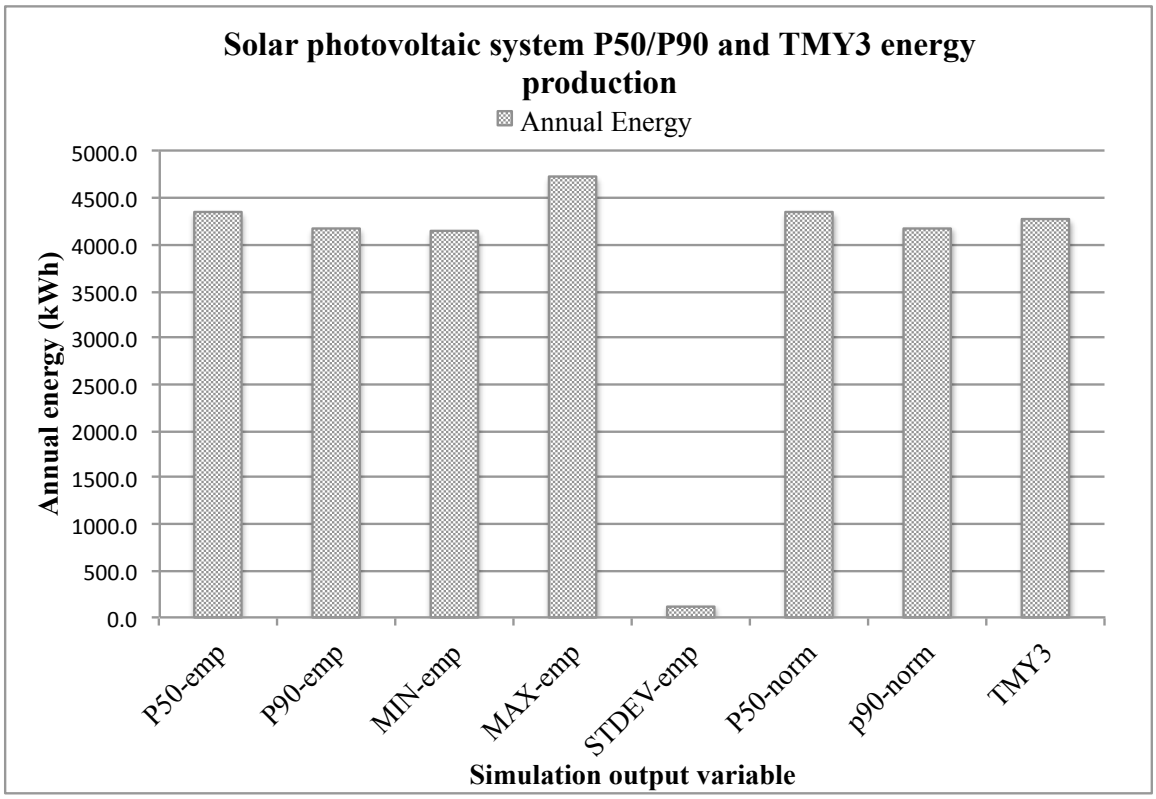

Figure 23. Annual solar photovoltaic energy production comparison of P50/P90 and TMY3 comparison

Normal and empirical methods of determining P50 and P90 annual energy production were within 15 kWh of each other. Normal and empirical estimation of P50 and P90 energy production were within 2.5% of the TMY3 estimate. These results indicate that the radiation dataset from the TMY3 closely resembles that of the 30-year NSRDB dataset suggesting that the TMY3 dataset is representative of the typical solar energy output. TMY3 simulation was utilized to estimate annual energy production of the SPVS at 4,268 kWh/yr at year one.

Solar Thermal Energy Production and Analysis

The simulation was setup with parameters from the installed solar hot water system installed and utilized a titled surface radiation HDKR diffuse sky model with beam and diffuse irradiance components. Annual availability was set at 99% with no shading and solar collector and site parameters were set based on Tables 13. Houston residential environments have been reported with an albedo ranging from 0.15 (Hitchcock 2004) and 0.2 (Rose et al. 2003). Albedo was set to 0.2 for the simulations run in this study. Hot water demand was not monitored directly and was estimated based on ASHRAE 90.2-2013 *Energy-Efficiency Design of Low-Rise Residential Buildings* (ASHRAE 2013b). The average gallons per day utilized for living units to be used in hot water energy consumption is based on the following equation:

AGPD = (CW+ SPA + B) (NP),

where:

AGPD = average gallons per day of hot water consumption,

CW = 2.0 gal/day per person if a clothes washer is present,

SPA = 1.25 gal/day per person additional hot water use if a “spa-tub” is present,

B = general “baseline” coefficient of 13.2 gal/day per person,

NP = number of people in the living unit.

For the case study, the number of persons living the dwelling is 4, however, guests do frequent the home and the number of persons was set to 4.5 to accomidate for

additional guest and higher than normal clothes-washing demand. The hot water demand was calculated and to an AGPD of 74.025 gal/day or 280.2 kg/day. Table 14 identifies the parameters necessary for the solar thermal simulation.

Table 14. Solar hot water collector, tank, heat exchanger and piping and plumbing simulation parameters

Solar hot water collector		
Tilt	22	°C
Azimuth	270	°
Total system flow rate	0.02	kg/s
Working fluid	Glycol	
Number of collectors	1	
Diffuse sky model	HDKR	
Irrandiance Inputs	Beam and Diffuse	
Albedo	0.2	
Collector area	2.87	m^2
System rated size	1.71253	kW

Solar tank and heat exchanger		
Tank volume	0.3	m^3
Solar tank height to diameter ratio	2.5	
Solar tank heat loss coefficient	0.55	$W/m^{2-}°C$
Solar tank max water temperature	99	°C
Heat exchanger effectiveness	0.75	
Outlet set temperature	54.44	°C
Mechanical room temperature	22.5	°C

Piping and plumbing		
Total pipiing length in system	10	m
Pipe diameter	0.0127	m
Pipe insulation conductivity	0.03	$W/m^{-}°C$
Pipe insulation thickness	0.006	m
Pump power	24	W
Pump efficiency	0.95	

Piping and plumbing characteristics are estimates from the field and piping length, and pipe insulation property estimates include the collector and heat exchnager loops. Solar tank, heat exchanger and piping heat losses were modeled within SAM.

The field estimates of the heat energy delivered by the solar hot water system were performed based on 2012 data. Monthly energy estimates were calculated using the average heat energy gained over the month. Missing data was estimated based on the average energy rate per hour for the month multiplied by the number of hours missing for the month.

The uncertainty of the solar thermal predictions in SAM is not well documented. However, surrogates for uncertainty can be assumed based on other findings for energy gain in defined conditions such as testing environments and Kovacs (2012) reports on that solar collector energy gain has an expected uncertainty that can be as much as 10% due to climatic data variability. Measured data is based on an estimated uncertainty of 5.46 %. Figure 24 illustrates a comparison chart of simulated vs. measured monthly delivered solar hot water energy. Annual field energy production was within 3.5% of predicted output.

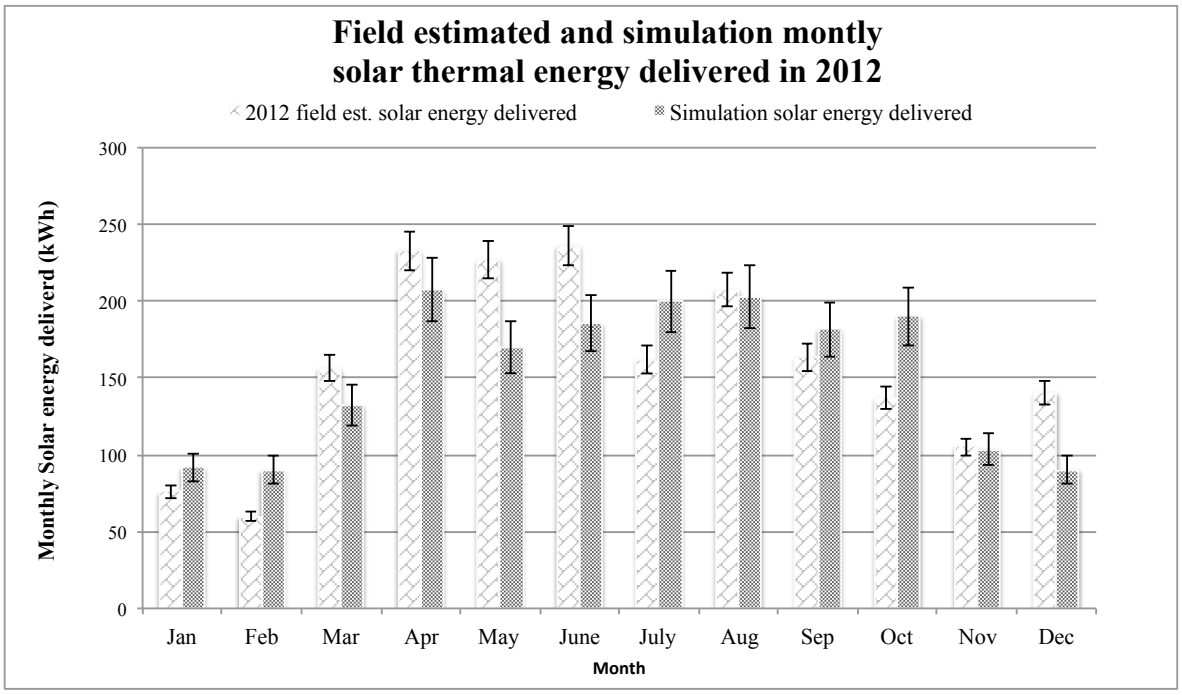

Figure 24. Solar hot water field and simulation monthly energy production with uncertainty bars

Error bars represent a ±5.46% and ±10% uncertainty for measured and simulated data respectively. Considering variations in meteorological data and other uncertainties the associated differences were considered minimal over a life cycle.

Solar Hot Water System P50/P90 Analysis

P50/P90 analysis was performed to assess the annual energy exceedance probabilities calculated based on the 30-yr NSRDB for Houston, Texas and the simulation estimates are illustrated in Figure 25. Normal and empirical methods of determining P50 and P90 were with in 8 kWh of each other. Normal and empirical estimation of P50 and P90 were within 6% of the TMY3 estimated output, with P90 results within 2% of the TMY3 results. These results indicate that the radiation dataset is

and that the TMY3 derived output closely resembles that of the majority of 30-year NSRDB dataset. TMY3 simulation was chosen to estimate annual energy production for an electric auxiliary SHWS at 1,846 kWh/year (first year).

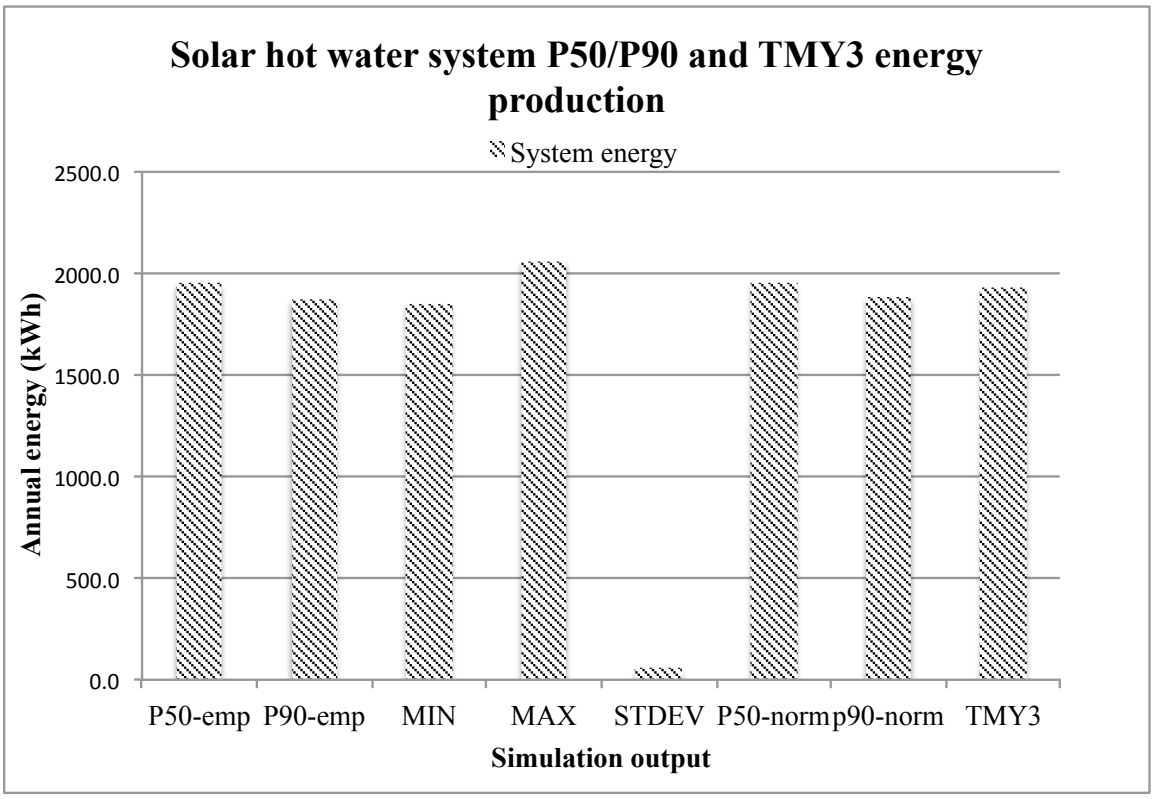

Figure 25. Solar hot water system P50/P90 and TMY3 comparison

Photovoltaic and Solar Thermal System Optimization

Azimuth and tilt adjustments were analyzed in SAM to investigate 'As-Built' design optimizations. Table 15 tabulates a series of model scenarios of panel tilt and azimuth with associated monthly and annual energy output and suggests the photovoltaic system could have been optimized to increase total annual output at a gain of 2%. However, the original design optimized the monthly output for winter months with a larger tilt angle, with only a slight sacrificed annual output. The design azimuth of the installation was properly established at 180° as indicated in Table 15.

Table 15. Solar energy systems annual energy production with various configurations

Solar photovoltaic system			Solar hot water system		
Azimuth (°)	Tilt (°)	Annual energy (kWh)	Azimuth (°)	Tilt (°)	Annual energy (kWh)
135	30	4126	180	22	2196
135	35	4074	180	32	2195
135	40	4003	180	40	2188
180	30	4314	225	22	2102
180	35	4282	225	32	2037
180	40	4226	225	40	2021
225	30	4124	270	22	1846
225	35	4073	270	32	1803
225	40	4001	270	40	1732

Table 15 also suggests that the solar hot water system was installed at a less than optimal azimuth of 270° and installing the system at 180° would have increased output by 19% at the design tilt of 22°, however, the system was installed at a location that

minimized piping losses and support structure. The simulated system output was more dependent on azimuth than tilt angle. In addition, the output of the solar hot water system could be increased dramatically with an additional solar collector module and the current system can readily accept an additional collector module with a marginal installation and material cost. The solar collector module would increase the energy annual output by 46% percent with an additional 41% increase in initial cost.

Life Cycle Energy Production and Costs

SAM annual simulations were developed over a 30-year life cycle to estimate life cycle production and economic performance for both the photovoltaic and solar thermal system. Solar photovoltaic and solar hot water systems are both known to function for over 20-25 years (Dunlop and Halton 2006, Hang et al. 2012, Realini et al. 2002, Skoczek et al. 2009). A thirty-year life cycle was determined to be a reasonable life cycle period for both systems and costs simulated included initial costs, operation and maintenance (O&M) costs, and lifetime replacement costs. Life cycle energy production is useful to determine the impact of renewable energy systems on a buildings operational energy usage and also for the determination of project economic indicators such as the net-present value (NPV), levelized cost of energy (LCOE) and monetary payback. NPV is a measure of a projects economic feasibility that includes both benefits and costs for the year, discounted and summed over a projects lifetime. LCOE is a combined performance and monetary ratio that is the total cost of installing and operating a system in dollars per kilowatt-hour of electricity generated by the system over its life.

In order to determine the LCOE and payback, other financial considerations such as loan terms, discount rate and Federal tax rates had to be considered. NPV, payback and LCOE are sensitive to inputs and parameters; therefore, a sensitivity analysis was performed on various costs and financial parameters.

System Initial Costs and Financial Considerations

Initial costs of solar electric and solar hot water include equipment, mounting hardware, installation, and interconnection fees (if applicable). Other additional expenses can include system design and engineering work, which are often bundled in the gross price. The prices used in this study were based on actual market prices in the last quarter of 2009 that were charged to the customer. The breakdowns of costs were developed with consultation from the renewable energy contractor and the cost breakdowns are listed in Table 16. The solar photovoltaic system initial cost was $26,500, and the solar hot water system was $6,350.

Table 16. Solar photovoltaic and solar hot water system initial costs

PHOTOVOLATIC SYSTEM COSTS		
Description	Percent of total	Cost
Module	30.1%	$ 7,968
Inverter	13.3%	$ 3,525
Balance of equipment	18.1%	$ 4,782
Installation labor	18.6%	$ 4,912
Overhead and profit	19.9%	$ 5,262
Price		$ 26,448

SOLAR HOT WATER SYSTEM COSTS		
Description	Percent of total	Cost
Appliance and collector	47.2%	$ 3,000
Storage Tank	11.0%	$ 700
Mounting hardware, piping, etc ..	4.7%	$ 300
Installion	15.7%	$ 1,000
Overhead and profit	21.3%	$ 1,350
Price		$ 6,350

The initial costs for both the SPVS and the SHWS were simulated with a 30-year mortgage loan arrangement at a 4.0% interest rate, with 100% debt fraction (no down payment). Additionally, a discount rate was applied at 4.4% with a Federal income tax rate of 33%. Sales tax was included at a rate of 8.25% of direct costs and a Federal tax credit incentive of 30% was applied. In addition to initial costs, recurring, lifetime costs must be estimated as well.

System Operation and Maintenance Costs

The systems have variety of costs and benefits that need to be accounted for in the estimation of the energy production and costs over the life cycle. Annual general maintenance for routine checks and collector washing was estimated based on the cost to clean the panels and routine maintenance. Both the SPVS and SHWS incurred a $40 cost every 3 years for the lifetime and lifetime replacement costs were estimated to be $1,200 and $600 for the SPVS and SHWS, respectively. SPVS and SHSW lifetime replacement costs assume three $400 and $200 payments every seven years and these costs were added at their respective time intervals to account for the timing of the costs. Table 17 is a summary of these parameters. Salvage value of the systems was estimated at 15% of total costs.

Table 17. Summary of solar energy system life cycle simulation parameters

Lifetime parameters	**Unit**	**Solar photovoltaic**	**Solar hot water**
Average lifetime	Years	30	30
Annual degradation	%	0.5	0.5
Annual maintenance	$/Year	$40	$40
Lifetime replacement costs	$/Avg Lifetime	$1,200	$600
Salvage value (% of original value)	%	15%	15%
Lifetime costs	$	$2,400	$1,800

Solar Energy System Life Cycle Performance

Solar energy systems are known to degrade in performance over the lifetime of the system, however, the amount of degradation occurring is controversial (Dunlop et al. 2005, Wohlgemuth et al. 2006). Many studies have been conducted on photovoltaic systems that have been in operation for over 20 years (Dunlop and Halt 2005, Realini et al. 2002, Skoczek et al. 2009) and the components of the electrical system are generally considered robust. However, gradual degradation of the polycrystalline silicon photovoltaic modules has being reported (Realini 2003, Dunlop et al. 2005, Dunlop and Halton 2006, Skoczek et al. 2009) with degradation reporting 0.5-1.0% per year over the lifetime. Solar hot water system life expectancy is not well reported on the in the literature, however there have been life cycle studies on this type system (Hang et al. 2012) and the typical life cycle was 20-25 years or more and for the purposes of estimating lifetime production and costs the model utilized an annual degradation factor of 0.5% per year for both the SPVS and the SHWS.

Life Cycle Energy Production

Life cycle energy production was estimated based on the aforementioned considerations and life cycle estimates of energy production of both the photovoltaic and solar hot water systems are presented in Table 18. Solar hot water energy output for both electric and natural gas heating auxiliary scenarios are presented. The annual energy saved for the solar with gas as auxiliary is higher than the auxiliary electric alternative due to the thermal efficiency differences. The electric heater in the electric as auxiliary

has a larger thermal conversion and as such uses less in energy, so the energy saved overall will be less than the gas auxiliary alternative.

Table 18. Solar energy systems life cycle energy production

Solar energy system type	Annual energy production (kWh)	30-year lifecycle energy production (kWh)
Solar photovoltaic system	4,226	117,994
Solar hot water system (natural gas heating)	2,393	66,820
Solar hot water system (electric heating)	1,846	51,555

Gas auxiliary simulations were performed with an estimated burning efficiency of 86% and tank losses at 20%. Lifetime energy saved from the photovoltaic system is about 1.76 to 2.28 times the solar hot water system with an average cost of 4.16 times higher.

Economic Performance Indicators

The net present value (NPV), levelized cost of energy and payback are well-established economic metrics of the projects ability to achieve an economic success (positive returns). The net present value is an accounting tool that is the sum, over the chosen planning lifetime, of all the net benefits (benefits minus costs) accruing to an action and discounted to current values terms (Griffin 2006).

$$NPV = \sum_{t=0}^{T} \frac{NBt}{(1+d)\,t}$$

where

t is the time period index (an individual year)

T is the life cycle (in years)

NB_t are the net benefits in period t, and

d is the discount rate.

The levelized cost of energy (LCOE) is the total cost of installing and operating a system in dollars per kilowatt-hour of electricity generated by the system over its life, which is defined as follows (Short et al. 1995)

$$\text{LCOE} = \frac{\sum_{n=0}^{N} \frac{C_n}{(1+d)^n}}{\sum_{n=1}^{N} \frac{Q_n}{(1+d)^n}}$$

where

C_n: annual project cost in year n,

Q_n: electricity generated by the system in year n,

d: discount rate, and

N: total analysis period in year.

For residential systems, LCOE is comparable to a $/kWh retail electricity rate and should be at or less than the local electricity retail rate for the project to be considered economically viable (NREL 2015). Real LCOE is a constant dollar, inflation-adjusted value and the nominal LCOE is the current dollar value. Many considerations are involved and because the LCOE takes into account the costs of the system over its

lifetime, the LCOE is very sensitive to the life cycle period of study, the discount rate, initial and recurring costs and the energy production performance and as previously discussed, energy production may vary at the location and degrade over time due to panel degradation.

The payback period is the time in years that it takes for the project savings in year two and later of the cash flow to equal the investment cost in year zero and SAM considers non-discounted cash flow values in the estimate (NREL 2015). Similar to LCOE, payback period is sensitive to energy production performance (energy cost savings), initial and recurring costs and tax savings and the energy performance of the system. Utilizing P50/P90 exceedance probability and TMY3 predictions of energy performance, NPV, LCOE and payback can be explored. Figure 26 illustrates the P90/P50 and TMY3 simulations impact on payback and LCOE for SPVS.

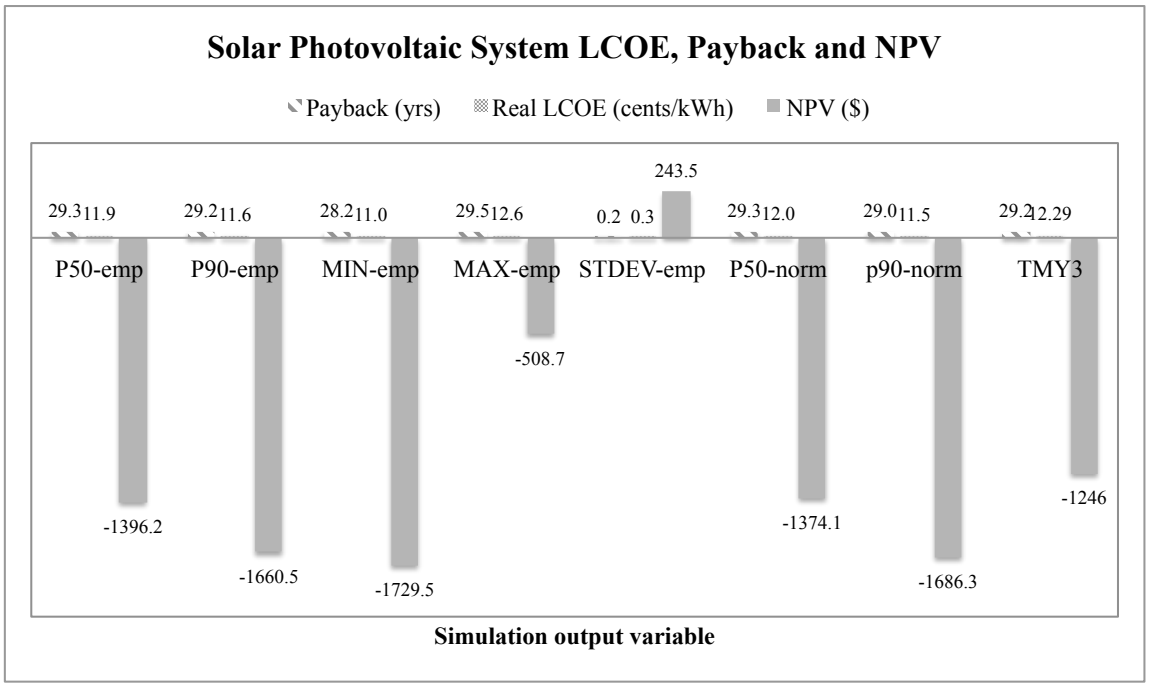

Figure 26. Solar photovoltaic system LCOE, payback and P50/P90 comparison with TMY3 predictions

Thirty year life cycle predictions of the photovolatic system payback is is mimnum of 28.2 and a maximum of 29.6 years and the LCOE is a minimum of 11.0 and and maximum of 12.6 ¢/kWh. The maximum LCOE in this analysis occurs in the TMY3 simulation at 12.29 ¢/kWh. The NPV is negative, indicating a less-than-optimal project in terms of achieving net benefits over the lifetime of the project. However, as indicated by the LCOE and the NPV the project is not far from achieving benefits. Similar trends can be seen in the solar hot water system, however, with more positive results. Figure 27 illustrates solar hot water system payback at a mimnum of 19.5 and a maximum of 21.8 years and the LCOE at a minimum of 7.3 ¢/kWh and a maximum of 8.1 ¢/kWh.

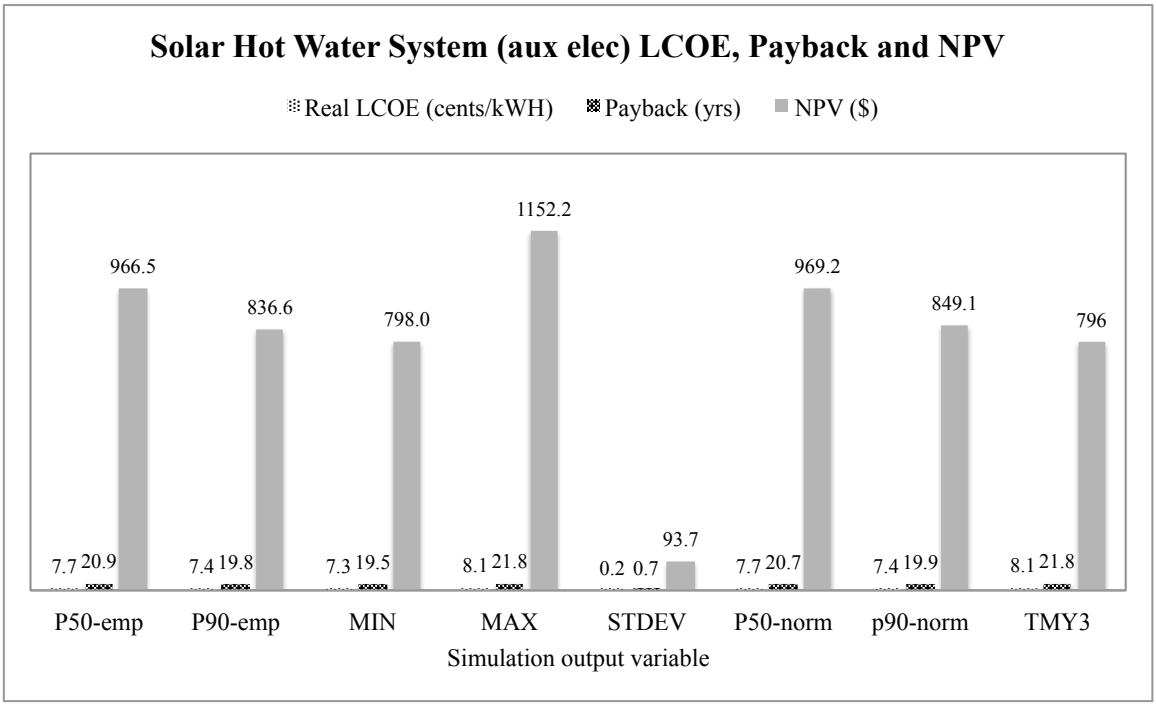

Figure 27. Solar hot water system LCOE, payback and P50/P90 comparison with TMY3 predictions

TMY3 results have a payback of 21.8 years and a LCOE of 8.1 ¢/kWh. The solar hot water system is operating below the local retail cost of the electricty. The net present value is greater than zero which indicates that the project achieves benefits within the lifecycle, indicating a successful project in economic terms. The net benefits are not extremely large but do indicate the system accures benefits over the life cycle.

Sensitivity Analysis

As previously mentioned, the cost estimation is based on many parameters that are unknown but can be generally assessed though sensitivity analysis and can illustrate the impact of certain variables on system outputs and conclusions. By adjusting the input variable by up and down, the relative impact of the parameters can be explored and as it

is a combined indicator of costs and benefits, LCOE is a good output variable to observe as a general indicator of energy and economic performance. As the LCOE approaches and drops below the price of retail electricity the more successful the project becomes.

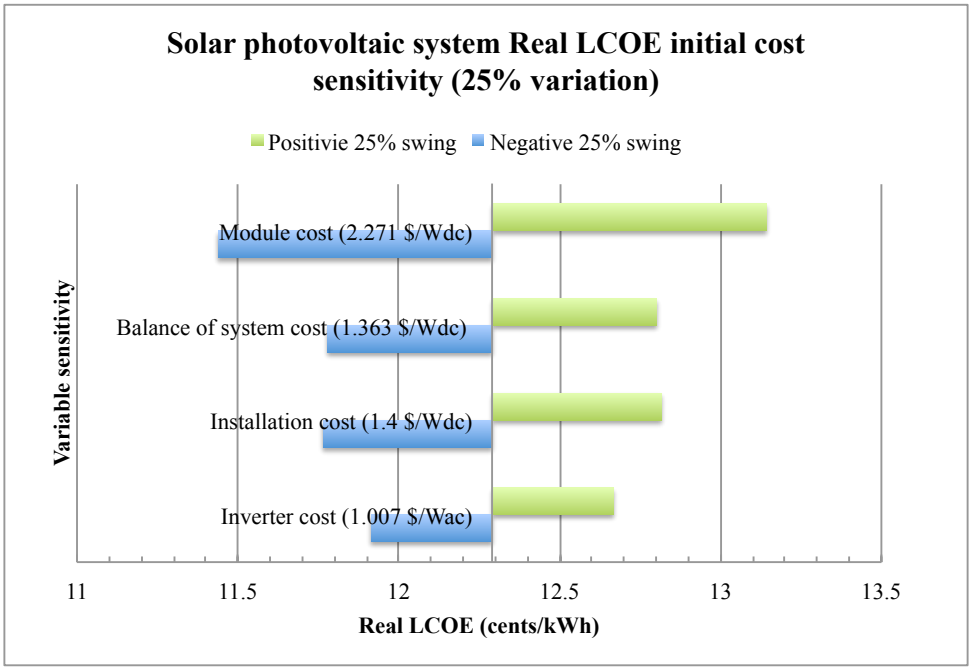

Figure 28. Sensitivity analysis of solar photovoltaic system initial costs vs. real LCOE

Figure 28 illustrates the impact of a twenty-five percent change may have on the real LCOE. The module cost had the most impact on the LCOE because it is the largest portion of the SPVS installed cost and further reducing all costs the project becomes more economically viable. The other initial costs have some impact but they are not as significant and in order to achieve a real LCOE of 10 ¢/kWh (estimated regional retail price of electricity) the module cost would have to be reduced 67% (0.75 $/Wdc)

Figure 29 illustrates the impact of financial parameters swing of twenty-five percent on the real LCOE. The loan rate of the mortgage has a significant impact on the LCOE. For SPVS, a twenty-five percent decrease the in loan rates drops the LCOE to the retail rate of electricity.

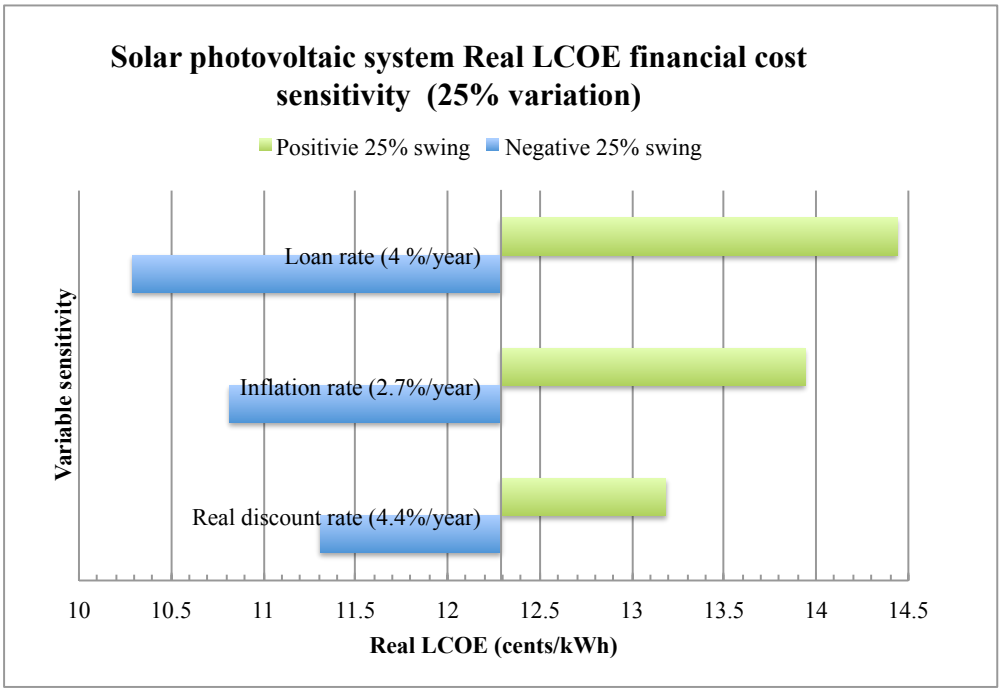

Figure 29. Sensitivity analysis of solar photovoltaic system financial parameters vs. real LCOE

Inflation and the real discount rate have a large impact on the LCOE, however, in the opposite direction of the loan rate and in general, decreases in the real discount rate or inflation will shift the LCOE to higher values. Figures 30 and 31 illustrate similar results for the solar hot water system. Figure 30 identifies the initial cost of the solar collector as having the largest impact on the LCOE and the LCOE decreases with

decreasing costs and Figure 31 indicates that the loan rate has the largest financial impact on the LCOE, slightly below 7 ¢/kWh with again, inflation rate and discount rate having negative (increasing) effect on the LCOE with decreasing rates.

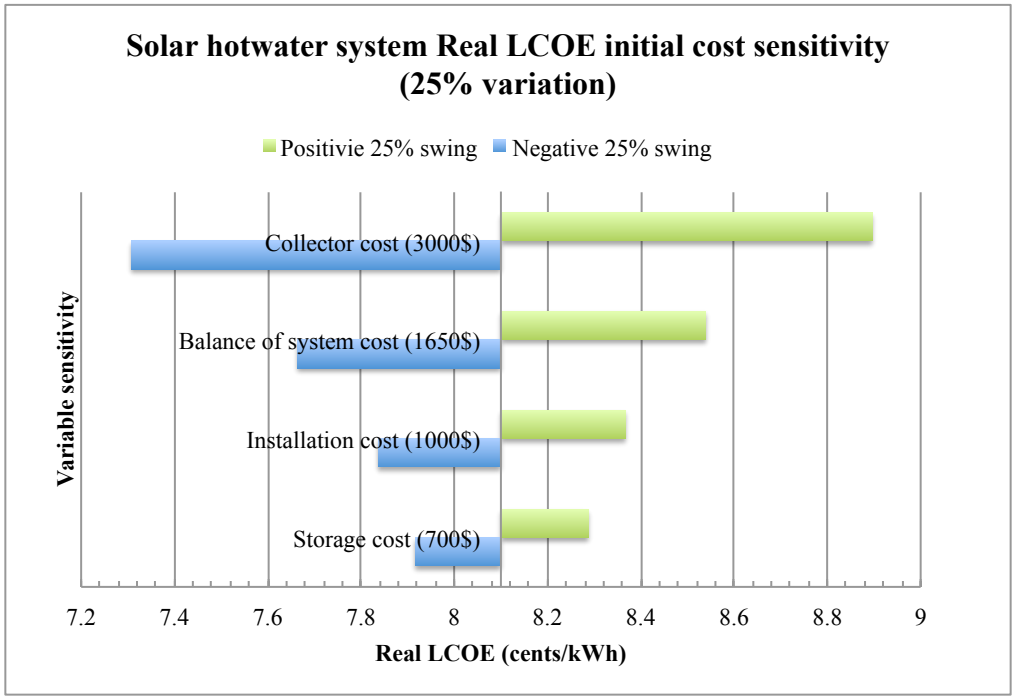

Figure 30. Sensitivity analysis of solar hot water system initial costs vs. real LCOE

Life Cycle and Loan Impacts On Economic Performance

Another significant aspect of evaluating the life cycle economic performance of a renewable energy project is establishing the temporal conditions with which the investment will exist. Two critical time periods need to be assessed when performing life cycle cost evaluations, namely the period of analysis (life cycle period) and the loan term (loan period).

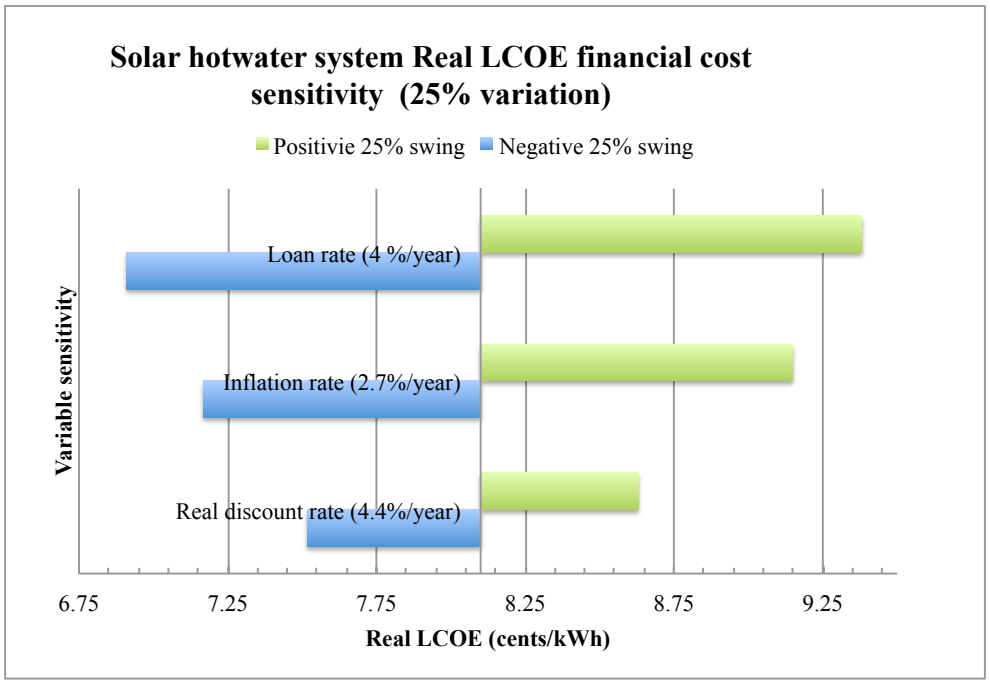

Figure 31. Sensitivity analysis of solar hot water system financial parameters vs. real LCOE

These items have a tremendous effect on the outcome and a series of simulations were run to investigate order loan terms and life cycle period combination effects on the economic indicators previously discussed. Figures 32 and 33 illustrates of various loan term and life cycle period effects on payback, NPV and LCOE for both the SHWS and SPVS.

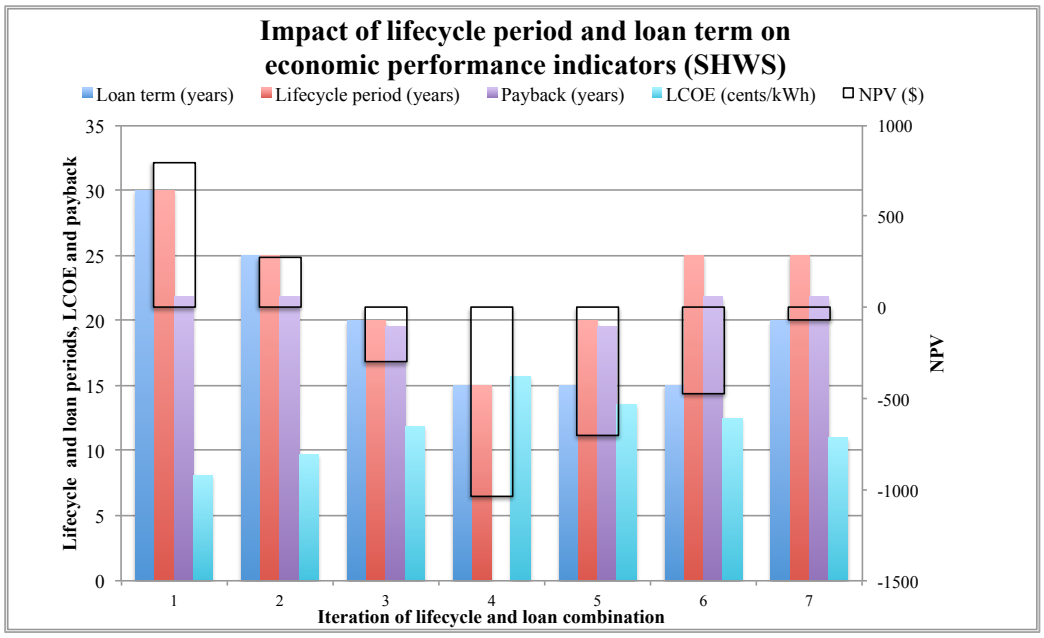

Figure 32. Life cycle period and loan term impact on economic performance of SHWS

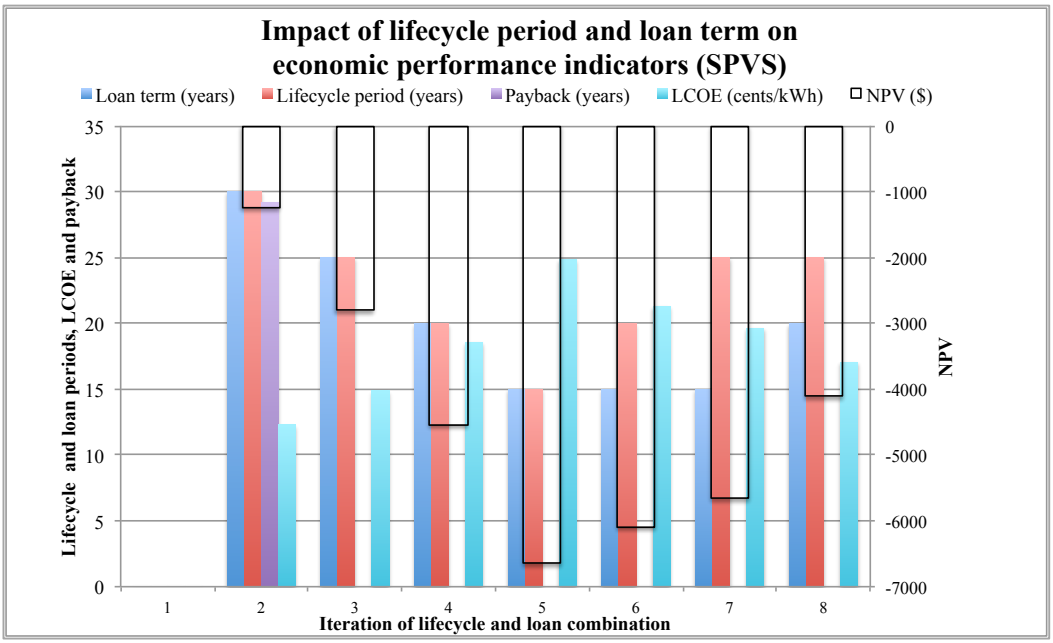

Figure 33. Life cycle period and loan term impact on economic performance of the SPVS

Not surprising, the results from Figures 32 and 33 both indicate more positive NPV and lower LCOE are produced with longer loan and life cycle analysis periods as benefits accrue and, in addition, with shorter loan and life cycle time horizons the investment has no payback and or very little economic incentive. A critical issue in determining life cycle costs is at what life cycle and loan terms are appropriate for the project being investigated. These general principles are important to consider in evaluating the life cycle costs of renewable energy investments. The production of the renewable energy system is all but one of the many parameters that need to be evaluated in the determination of the viability of renewable energy projects.

Summary and Conclusions

This research investigated the annual renewable production and costs of two residential solar-based systems installed in a LEED-Platinum home in humid, sub-tropical Houston, Texas, an IECC Zone 2. Field performance was estimated and compared to publicly available simulation, NREL's System Advisory Model, to estimate renewable energy life cycle energy production of the residence. Field results agreed with TMY3-based simulation estimates within the simulation and measurement system uncertainties. SAMs P90/P50 utility along with TMY3 and NSRDB weather data from the region provided estimates on the variation in radiation impacts on annual production. P50/P90 probabilities were within 3% and 6% of TMY3 predictions for both the SPVS and the SHWS respectively. Design optimization checks revealed the SPVS was installed in an optimized design, however the SHWS azimuth could have been better optimized at an azimuth of 180°.

SAM was furthered utilized to estimate life cycle production and life cycle costs and perform sensitivity analysis on critical parameters and economic indicators such as payback, NPV and LCOE. These economic indicators were explored for both systems and payback, NPV, and LCOE were considerably more favorable for the SHWS compared to SPVS due to high costs relative to output at the life cycle and loan periods evaluated. SHWS achieved a 21.8-year payback, NPV of $796 and an LCOE at 8.1 ¢/kWh, compared to 29.2-year payback, NPV -$1296 and an LCOE at 12 .29 ¢/kWh for SPVS. SPVS life cycle costs are very dependent on the PV module costs and were found to achieve a LCOE close to regional electricity prices at a module cost of 0.75 ¢/Wdc (67% reduction in module installed costs). SHWS life cycle costs are also dependent on capital costs; in particular, the solar hot water collector and pre-heat appliance are almost 50% o of the initial cost.

Additionally, loan, inflation, and discount rates were modeled with a 25% swing from the assumed case to determine the relative impact and the loan rate had the largest impact on the LCOE for both SPVS and SHWS at about 15-17% increase or decrease in the real LCOE. Additionally, life cycle period and loan term combinations were performed to illustrate the impact that various combinations of evaluation period and loan term may have on the economic indicators. Finally, the TMY3-based simulations of the SPVS achieved an annual and 30-yr energy production of 4,226 and 117,994 kWh, respectively, while the SHWS annual and 30-year energy production were 2,394 and 66,820 kWh with auxiliary gas and 1,846 and 51,555 kWh with auxiliary electrical.

Texas is a leader in residential energy consumption and carbon dioxide emissions in the United States, with the average annual electricity cost per household is $1,801 (US EIA 2009) among the highest in the nation and according to EIA's Residential Energy Consumption Survey, 656 million metric tons of carbon dioxide were emitted in 2011, 12% of the total for nation and twice that of California. Increases in residential renewable energy production in Texas has the potential to offset energy consumption and subsequent carbon dioxide production and further reduction in renewable energy system's capital and other initial costs, along with appropriate financial terms may help with market adoption and viability. However, as illustrated in this article, low regional fuel costs increase the constraints on the aforementioned initial costs. Finally, publicly available software tools such as NREL's System Advisory Model (SAM) facilitates a robust energy, economic and life cycle analytical platform to assist in renewable energy project design, analysis and decision support.

CHAPTER IV

RAINWATER HARVESTING SYSTEMS

Synopsis

Stressed water resources will lead to water price escalations and water rationing, making alternate water sources such as rainwater more attractive as options to handle increasing water demands and drought conditions. For example, rainfall in Houston, Texas, a humid, sub-tropical region, ranges from three to six inches per month, which affords an ample opportunity to catch and store water. Rainwater system performance and life cycle impacts are critical elements when reviewing the sustainability of a dwelling. However, the utility of rainwater collection systems is a balance of system design, rainfall inputs, water demand, and associated economic costs. The purpose of this research was to investigate the performance and economics of a rainwater collection system and underground cistern in an urban residential setting, focusing on rainfall, rainwater collection and life cycle costs. The project was part of a larger life cycle analysis of a durable, energy and water-efficient residential home. Field measurements and weather data were used in conjunction with analysis tools to analyze the performance of the installed rainwater collection system with a roof catchment area of 250 m^3 and a usable capacity of 22.6 m^3. Daily monthly water demand averages of 1.39 m^3/day for a four-person household were utilized in the simulation with a 30% variation imposed. Finally, a spreadsheet-based software tool was used to estimate hydraulic performance and economics over a 50-year life cycle. In this research, increasing the size of the rainwater cistern from 10 m^3 to 22.6 m^3 of usable capacity increased the payback in net-present

value terms from 21 to 43 years. Sensitivity and Monte Carlo analysis were also performed to analyze the life cycle scenarios with below average, average and above estimates of input parameters to assess relative contributions and to assess a probabilistic interpretation of the life cycle results. Using 30 year rainfall normal and Monte Carlo stochastic methods, there was a 45% - 48% probability of 73% of the annual demand being harvested and the annual water harvested in this interpretation was 370.3 m^3 (97,744 gallons).

Introduction

As competing demands and allocations of water rise, the management of water is of ever growing concern. Water scarcity in Texas is a concern in some locales (Griffin and Characklis 2011), with the state experiencing its worst drought in recorded history in 2011 (Texas Comptroller 2012). Onsite rainwater systems may provide clean water and water storage while offsetting costs and demand. Also, onsite rainwater system may offset centralized storm water systems. Managing water is part of sustainable building practice, and alternate water sources such as rainwater harvesting are becoming more attractive options to handle ever-increasing demands and costs of water supplies. According to Li et al. (2010), the motivating factors for these alternate water systems are: 1) consumer cost of water and wastewater rising, 2) climate change altering rainfall, 3) population growth and standard of living increases, 4) high quality water used for low quality purposes, and 5) runoff and wastewater handling reductions. Texas has a growing need for water and water conservation. As such, rainwater-harvesting technology has increased in Texas with an estimated 15,000 rainwater harvesting

systems deployed (Fewkes 2012), and in 2011, the Texas Legislature eliminated legal provisions that stipulated rainwater-harvesting systems being used only for non-potable purposes (Texas Comptroller 2012) which made rainwater available for human consumption and contact.

This research was part of a larger body of work to investigate and evaluate a United States Green Building Council's (USGBC) Leadership for Energy and Environmental Design (LEED) for Homes "Platinum" designated residential dwelling in Houston, Texas. In addition, the home achieved a "fortified" rating from the Institute for Building and Home Safety, and a "Zero-energy ready" home certification from the United States Department of Energy. This dwelling incorporated a durable and robust building envelope, as well as, efficient environmental controls and two renewable energy systems. This research investigated the hydraulic and economic performance of a rainwater harvesting system over 50 years by analyzing rainfall data, water demand, and life cycle cost performance projections.

A critical aspect in achieving a LEED-H Platinum rating is the management of water outside and inside the dwelling. Water reuse, rainwater collection, water-efficient plumbing systems, proper landscaping, and surface water management all contributed to the system. In addition to the rainwater collection system documented here, the dwelling used water-efficient fixtures, fittings and appliances throughout. An efficient irrigation system was also installed. Landscape and surface water management controls were also considered in the design. The turf was drought tolerant and was approximately 60% of the designed landscape. Finally, 75% of the installed plants were drought tolerant. The

USGBC issues LEED credits for buildings with water efficient and rainwater harvesting components (USGBC 2015).

Urban Water Management and Rainwater Systems

Rainwater harvesting (RWH) systems are an ancient technology that has been deployed globally for millennia (Antoniou et al. 2014), and they can be found around the world even to this day. Ancient cisterns were common in the Hellenic and Roman civilizations from the Minonan and Mycenaean period (1900 – 1100 BC) to the modern day (Antoniou et al. 2014, Crasta et al. 1982, Phoca and Valanis 1999). However, the use of rainwater systems has declined as water distribution technology has advanced (2012). Pressures of population growth and climate change have instilled renewed interest in RHW technology (Abdulla and Al-Shareef 2009, Villarreal and Dixon 2005). From 1990 to 2010, rain-based drinking water sustained a twofold increase worldwide (UNICEF and WHO 2012) and developed countries have seen a rise in RWH development in the past several decades.

Centralized water and wastewater systems have escalating environmental and economic costs that have refocused attention on decentralized approaches (rainwater collection, water reuse, etc.) and as water resources become more stressed, higher water pricing and regulations are being implemented, making alternate water sources, such as rainwater harvesting, more attractive options to handle ever-increasing demands and costs. Rainwater harvesting is an approach that can supply high quality water onsite; however, in temporary drought conditions, rainwater maybe less than optimal. Additionally, at any given time, onsite water demand may overwhelm collected rainfall,

thus yielding a less-optimum condition for a potentially costly solution. Therefore, competing costs and benefits of rainwater systems in an urban deployment require an analysis recognizing the uncertainty of rain and costs over a life cycle.

Life Cycle Costs and Benefits

A life cycle costing approach must be utilized to design and evaluate the utility of a rainwater system, and several authors have reported using this approach for specific situations and applications (Basupi 2013, Ghimire et al. 2014, Farreny et al. 2011, Roebuck and Ashley 2006, Ward et al. 2008). In particular, Roebuck and Ashley (2006) demonstrated verified life cycle software tools that will be used in the study reported herein. Using a macro-enabled spreadsheet, hydraulic simulation and life cycle analysis production and costs were performed on an urban rainwater system. Furthermore, this study analyzes the existing 'As-Built' system costs and benefits in the life cycle context for 50 years and will offer alternative redesigns for similar conditions in more competitive constraints.

System Characteristics

The system evaluated in the study utilized an underground cistern storage system constructed of a cement-rebar structure (underground tank) installed in the front lawn of the residence. The images in Figure 34 illustrate the pre and post landscape establishment at the residence as well as indicating the location of the cistern.

Figure 34. Pre-landscape with water collection cistern installed (left image) and landscape fully mature (right image)

The rainwater system is able to harvest water from approximately 75% of the roof (333 m^3), passing water through covered gutters to a macro-filtering system and then into an underground cistern with a usable capacity of 22.6 m^3 (5,970 gallons). Potable water can be accessed from the cistern or domestic water supply with all of the water being passed through an advanced water filtration system that utilizes reverse osmosis and ultraviolet radiation. Figure 35 is a schematic of the rainwater and domestic water components. The system is composed of collection, conveyance, storage and delivery components. Roof collection is delivered to an extensive system of covered and slotted gutters that minimize debris infiltration. A collection cistern was installed in the front lawn two feet below grade. The system is setup to operate with or without the cistern depending on the utility required.

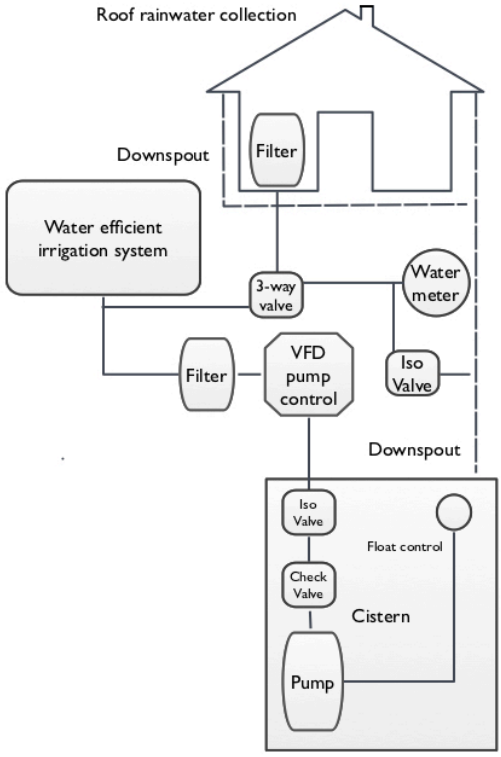

Rainwater system hydraulic diagram

Rainwater system debris controls

Rainwater system downspout

Figure 35. Rainwater system characteristics

All water utilized in the house is pre-filtered and further filtered by a micro-filter with activated carbon and ultraviolet light that filters water through a 0.2 micron high-capacity depth filter that traps particles, cysts and bacteria. Activated carbon removes chlorine, organics, and other chemicals that can affect taste, feel and the smell of the water. Finally, water is disinfected by an ultraviolet system that renders biological contaminants inactive.

Landscape Design

The landscape design incorporated a balanced integration of native plant species and material with colors and textures that maximize visual interest while maintaining sustainable conditions for plants. Zoysia grass with curving beds created the front yard landscape. Rock and gravel within the backyard landscape helped to create a natural balanced look while adding value visual appeal and drainage advantages. All vegetative beds incorporate a drip irrigation system that maximizes water efficient delivery. Irrigation occurs at 4-7 AM, three times a week and was established by the landscape company, resulting in an annual consumption of 32,200 gallons (121.9 m^3/yr) or 0.34 m^3/d.

Data and Methods

Using both regional and site specific hydraulic data in conjunction with economic data, a life cycle analysis was run to analyze the performance of the system in varying conditions over a lifetime. The tool is a spreadsheet-based system based on an Excel/VBA-based mass balance continuous simulation program using a yield-after-spill (YAS) algorithm with a hydraulic and whole life costing approach (Roebuck and Ashley, 2006, Ward 2008, 2010). The YAS model is as described by Jenkins et al. (1978) and it is a widely accepted and used methodology (Roebuck and Ashley 2006) that is based on a water mass balance around the storage volume, or

$V_t = V_{t-1} + Q_t - D_t$, Subject to $0 \leq V_t \leq S$

where:

V_t= Water in storage at time interval t

Q_t = Inflow during time interval, t

D_t = Demand during time interval, t

S = Storage capacity.

The yield is described by Fewkes (1999) ,

$$Y_t = min\begin{cases} D_t \\ V_{t-1} \end{cases} \qquad V_t = min\begin{cases} V_{t-1} + Q_t - Y_t \\ S - Y_t \end{cases}$$

where:

Y_t = Yield from storage during time interval, t.

The tool has been utilized in a number of rainwater system research contexts (Basupi 2013, Pinto 2010, Roebuck and Ashley 2006, Ward et al. 2008). Additionally, the model has been verified against previous models (Roebuck and Ashley 2006) by comparing the hydraulic outputs of the model against a methodology described by Fewkes and Warm (2001) and the model results were generally within 10%, with an average difference of 5.5%.

The spreadsheet-based macro optimizes a predicted tank size based on inputs such as rainfall and demand level in order to provide a balance between the estimated percentage of demand met and potential financial savings in relation to capital cost (Ward, 2012). Additionally, the system includes the facility to calculate the whole life cost, payback period and cost-benefit of a RWH system (with mains top-up) in comparison with an equivalent mains water supply (Ward 2012). Multiple hydraulic,

energetic and financial input parameters can be modeled in the program and the system can run lifecycle simulation for up to 100 years. The simulation offers sensitivity analysis to determine the impact of certain parameters when subjected to above average and below average conditions to input parameters. The simulations are constrained by input parameters based on-site water demand data, historical rainfall analysis and the other site specific information and financial inputs.

System Input Data Detail

A variety of inputs, both hydraulic and financial, are required to model the assessment: 1) rainfall data, 2) roof catchment area, 3) runoff coefficient, 4) first flush volume, (5) filter coefficient, 6) storage tank volume, 7) drain-down interval, 8) power rating of pump, 9) pumping capacity of pump and 10) water demand. Financial data are also required to do an assessment and Table 19 and 20 list a complete list of the required hydraulic and financial parameters.

Table 19. Hydraulic parameters used in the life cycle simulation

Hydraulic parameters	Model Input	Unit	Data source (s)
Rainfall	3.2 average	mm/day	NOAA 30 YR n ormals
Water demand	1.39 average	m^3/day	Avg. Texas per four-person household (TWDB,) and monitored data
Catchment area	333	m^2	Building roof plan
Runoff and filter coefficients	0.85, 0.92	Dimensionless	Heuristic
First flush volume	0.0	m^3	Case volume and optimized volume
Drain down interval	0.0	m^3	None present.
Pump power rating	0.7	kW	Pump specification sheet
Pumping capacity	56.77	L/min	Pump specification and measured water flow data

The necessary financial data are: 1) total capital cost, 2) maintenance and operational costs, 3) discount rate, 4) electricity costs, and utility water cost and are presented in Table 20.

Table 20. Financial parameters used in the life cycle simulation

Financial parameters	Model input	Unit	Data source
Total capital cost	Two scenarios	$USD	Estimated on components and labor polling
Maintenance operation costs	Scheduled maintenance, repairs and replacement of consumables.	$USD	Estimated on components and labor polling
Discount rate	4.4% average	%	Discount rates from TWDB and NRCS
Electricity costs	0.1$/kWhr	$USD/kWh	Regional electricity price
Mains water costs	$3.25/m^3	$USD/m^3	Regional composite water prices (water and wastewater and base price

Rainfall and Water Demand Detail

Local airport historical data from NOAA's NCDC (Arguez et al. 2012, NOAA 2014) were used to estimate incident rainfall. The supply-pump water flow was monitored and compared to average regional per-capita (0.325 m^3/day-person) water demand profiles from the Texas Water Development Board (TWDB 2014). TWDB regional averages were utilized and water demand variations in the simulation were set at ±30% of the demand average.

Catchment Surface and Filter Details

The catchment area of 333 m^2 was estimated from the roof area of the building that had gutter and conveyance systems. The effective runoff is defined as a fraction of water retained by the system that strikes the surface. Pitched roof tiles are typically around 0.75-0.9 (Roebuck and Ashley 2006), and they are generally more efficient at capturing intercepted rainfall than flat roofs, thus minimizing loss through pooling or absorption. The effective runoff captured in the storage tank was set to 0.85, with a variation of ± 0.05.

Rainwater Storage Detail

The underground cistern has a usable storage volume of 22.6 m^3 (5,970 gallons) for Scenario A, while Scenario B is modeled with 10 m^3 (2,600 gallons). In the simulation, water mains are used to top-up the storage tank to account for lack of rainfall and no maintenance flush losses are currently specified in the volume estimates.

Pump and UV Filtration Power Detail

The water pump has a nominal power rating of 1.1 kW with a variable speed drive (VSD) (0.72 KW) and a pumping capacity of 56.77 liters/min. The UV water filtration system has a power rating of 39.7 W and was considered operable 24 hours a day.

Financial Data Detail

The Nation Resource and Conservation Service discount rate statistics are a maximum of 5.625%, minimum of 3.5% and an average of 4.568% (NRCS 2014) for 2013 and 2014. Additionally, the Texas Water Development Board currently uses 4.4%

(TWDB 2014) for water construction projects. This value was used in the simulation for the average discount rate with a high of 5.0% and a low of 3.4%. Electricity costs were established at an average of 0.10 $/kWh, while maximum and minimum were set at 0.11 and 0.09$/kWh, respectively. Water pricing from Houston water bills (water, wastewater, and base charges averaged in) were set at an average of 3.25 $/m^3, with a maximum of 4 $/m^3 and a minimum of 3.1 $/m^3. Roebuck and Ashley (2006) recommend no more than 5-10% below expected values for minimum costs). Maximum water price was set at approximately 23% above the average.

Construction and Maintenance Costs

Tables 21 and 22 list the construction and maintenance costs that are used in the simulation and construction costs were estimated based on retail prices of equipment from various Internet resources. Gutter system was estimated at $48/meter and the cistern build-out costs were based on regional estimates on a volume basis and $264/m^3 was used as the price of the cistern cost. The costs were summed to a total cost of $19,000 and expected high and low estimates were based on the expected total cost ± 25%. Plumbing costs were estimated based on conversations with local plumbers and residential construction companies.

Table 21. Rainwater system construction costs

Rainwater construction costs	
Description	Cost
Advanced filter	$1,400
Pump and controls	$1,600
Gutter, downspouts, and debris filter (67.6 meter of roof line)	$3,300
Cistern ($264/$m^3$ (1$/gal) for cistern)	$7,700
Plumbing (including excavation)	$5,000
Expected Total Cost	$19,000
Expected High Cost	$23,750
Expected Low Cost	$14,250

Maintenance activity costs shown in Table 22 were estimated based on retail prices of equipment from various Internet resources and local labor rates from 2014 and maintenance frequency estimates were based on product replacement lifecycles.

Table 22. Maintenance activities and associated costs

Maintenance activities and associated costs				
Item	Frequency			Cost
Routine scheduled maintenance operations	Every	2	Years	$80.00
Repair/replace pump	Every	15	Years	$400.00
Replace UV lamp	Every	2	Years	$55.00
Clean filters/replace filter media	Every	1	Years	$30.00
Water quality treatment items	Every	1	Years	$20.00

Hydraulic Analysis

Rainfall and Sensitivity

National Oceanographic and Atmospheric Administration's (NOAA 2014) 30-year climate data was used for typical monthly rainfall with Hobby Airport in Houston, TX being the closet reliable weather station available. Climate normals are three-decade

averages of climatological variables such as temperature and precipitation, which are produced once every 10 years by NOAA's National Climatic Data Center (Arguez et al. 2012, NOAA 2014). Rainfall was characterized with an average and ±30% above and below average to characterize a range of values. Figure 36 depicts the 30-year normals at Hobby Airport illustrating average rainfall, the average temperature with average low and high temperatures in the error bars.

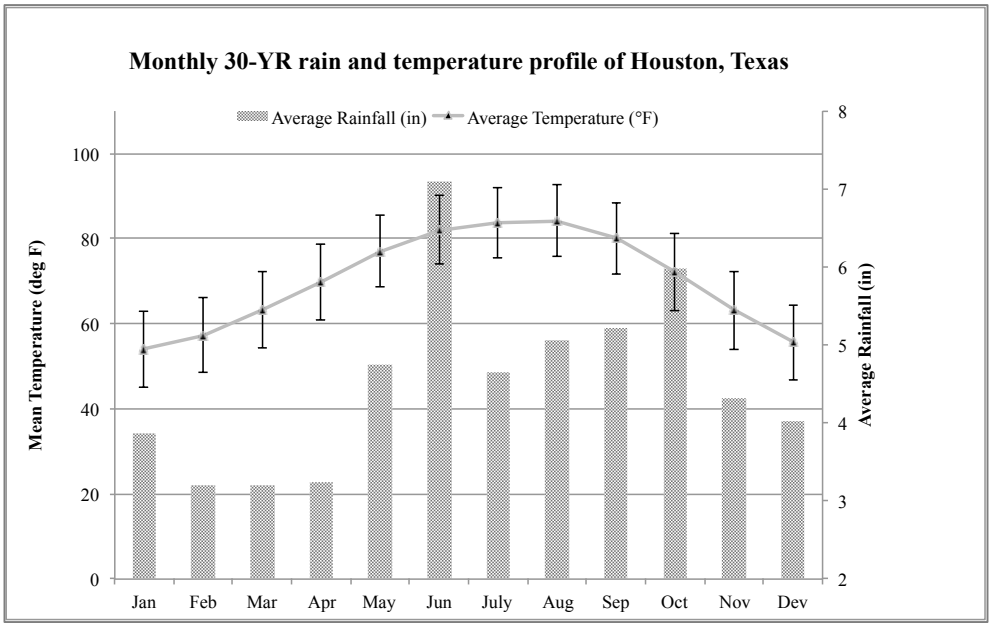

Figure 36. NOAA average, high and low average temperature and precipitation 30-YR normals at Hobby Airport, Houston, Texas for 1981-2010

Airport illustrating average rainfall, the average temperature with average low and high temperatures in the error bars.

Water Demand

Building water demand was based on regional per capita averages and local data recorded onsite with a water flow meter and logger provided data verification. This local data was compared to Texas regional per capita water use in order to determine the simulation input. Over 10-month period from October 2011 to July of 2012, the residence used an average of 1.29 m3/day for four persons. The average Texas regional use (TWDB 2014) for the years 2008-2012 is 0.347 m3/day per person or 1.39 m3/day (6% COV for the 5 years) for a four-person household, which was assumed to be a reasonable approximation of the average conditions over a year. Monthly variation in water demand exists and was approximated by a range of values utilizing a $\pm 30\%$ swing above and below the average.

Demand Analysis

Annual water demand was based on average-daily water demand and summed over the year producing an average of 508 m^3/yr of water demand. Table 23 illustrates hydraulic simulation results with 30-year rain normals, water demand, water harvested, and the annual shortfall estimated at 146 m^3/yr (38,569 gal/yr).

Table 23. Residential monthly and annual hydraulic results of water demand and rainwater harvesting analysis

Month	Rainfall (mm)	Measured demand (2011-2012) (m^3)	Demand simulated (m^3)	Harvested Water Supplied (m^3)	Shortfall (m^3)
Jan	98.3	16.66	43.09	25.60	17.49
Feb	81.53	15.35	38.92	21.23	17.69
Mar	81.28	NA	43.09	21.17	21.92
Apr	82.55	45.98	41.7	21.50	20.20
May	120.65	32.69	43.09	31.42	11.67
Jun	180.34	45.5	41.7	41.70	0.00
Jul	118.36	47.7	43.09	36.08	7.01
Aug	128.52	NA	43.09	33.47	9.62
Sep	132.33	NA	41.7	34.46	7.24
Oct	152.15	29.03	43.09	39.62	3.47
Nov	109.73	22.06	41.7	28.57	13.13
Dec	102.36	22.16	43.09	26.66	16.43
Annual total	1388.1	NA	507.35	361.47	145.88

Tank-optimization

The tank size optimization was performed in order to determine how the initial tank design performed based on an average payback period and an average savings, assuming the tank size can provide at least 70% of the water demand. Seventy percent of demand can be met with a tank volume of 2-5 m^3; however, rainfall is not consistent and this optimization provides little storage buffer. To provide a small buffer, one week of water demand was used to buffer against the probabilistic nature of rain and to provide extra water storage. For these reasons, a 10 m^3 tank size was considered as an alternate design. The original design provided a much larger buffering capacity of almost 2.5 weeks of water demand storage.

Life Cycle Performance

Two primary scenarios were modeled, consisting of Scenario A, the 'As-built' 22.6 m^3 system, and Scenario B, the more 'tank and storage optimized', lower-cost condition of 10 m^3. Rainfall and water demand were modeled with 30-year normals and Texas regional average daily water demand, respectively and with a ±30% span to model a range of possibilities. Table 24 illustrates Scenarios A and B as modeled, while Table 25 presents the 50-year life cycle results in a tabulated form.

Table 24. Life cycle simulation Scenarios A and B

Scenario	**Rainfall**	**Average water demand per day (m^3d)**	**Capital cost (USD)**	**Tank size (m^3)**
A	30 YR ± 30%	1.39 ± 30%	$20,000 ±25%	22.6
B	30 YR ± 30%	1.39 ± 30%	$14,000 ±25%	10

Table 25 illustrates the simulation estimated approximately 71% of the demand is met for either scenario with a payback of 43 years for Scenario A and 21 years for Scenario B. Total and annual savings for Scenario B are over seven times larger than Scenario A.

Table 25. 50-year life cycle performance of Scenarios A and B

Scenario	Long-Term Results			Average Per-Year Results		
	Demand Met (%)	Pay-Back Period (yrs)	Total Savings ($/50yrs)	RWH Cost ($/yr)	Mains Only Cost ($/yr)	Yearly Savings ($/yr)
A	71	43	932.24	675.64	694.28	18.6
B	71	21	6,932.24	555.64	694.28	138.6

Figure 37 illustrates average yearly cost breakdown and comparison of simulations Scenario A and B, and the mains-only (no rainwater component). All yearly maintenance costs are the same except capital costs. Decommissioning costs are set to zero.

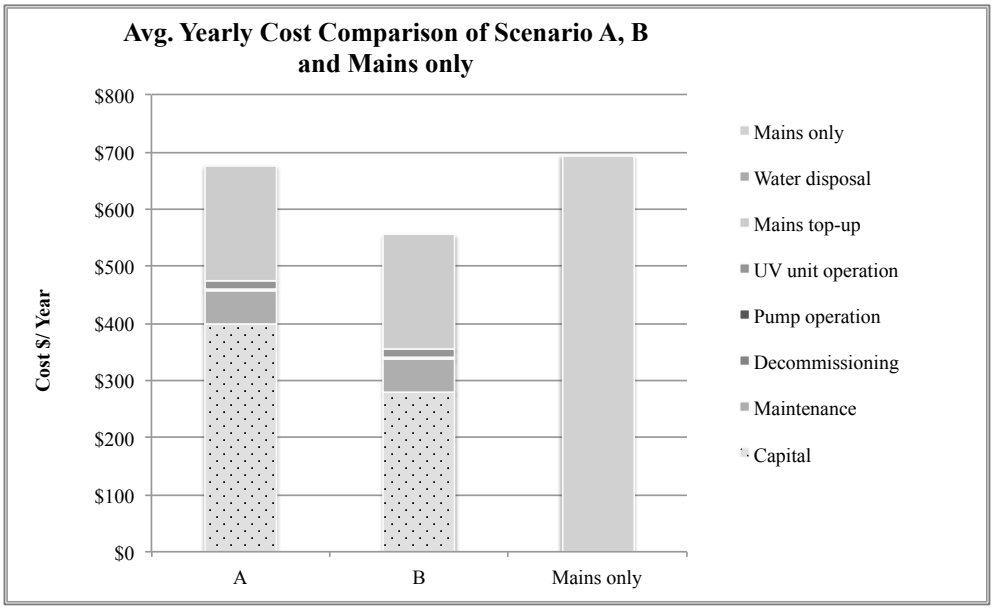

Figure 37. Average annual cost comparison of Scenarios A and B and mains only (no rainwater)

One hundred dollars a year in annual rainwater harvesting cost difference compound significantly over the life cycle. The average yearly costs comparison of the simulation scenarios and the main-only illustrate the implications of installing a larger system can have on yearly cost.

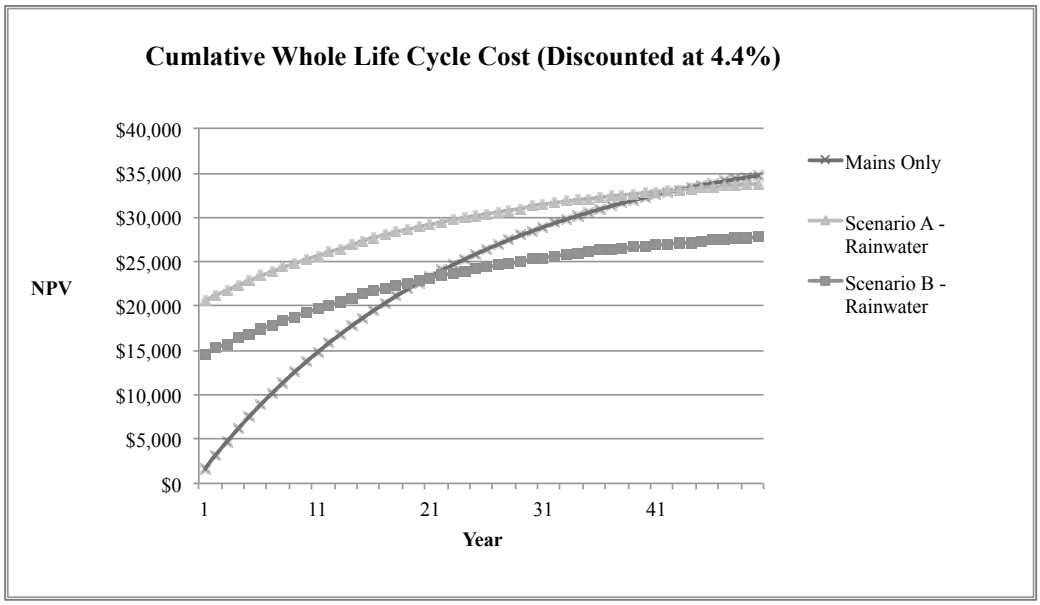

Figure 38. Net present value (NPV) over a 50-year life cycle of Scenarios A and B and mains only (no rainwater)

Figure 38 illustrates the estimated net-present value and payback (cross-over points) for Scenarios A and B compared to the mains-only system. Investing in a larger storage volume can have dramatic effects on the payback period for a rainwater system compared to smaller alternative. For example, the payback period is double the amount with a cistern volume 2.26 times larger.

Sensitivity Analysis

Figure 39 and Table 26 illustrate graphically and numerically the impact that the model parameter sensitivities have on the system savings for the 10 m^3 system. Low and high range analysis illustrate that certain parameters such as rainfall, mains water cost, the capital cost, discount rate, and the runoff and filter coefficients may affect the outcome.

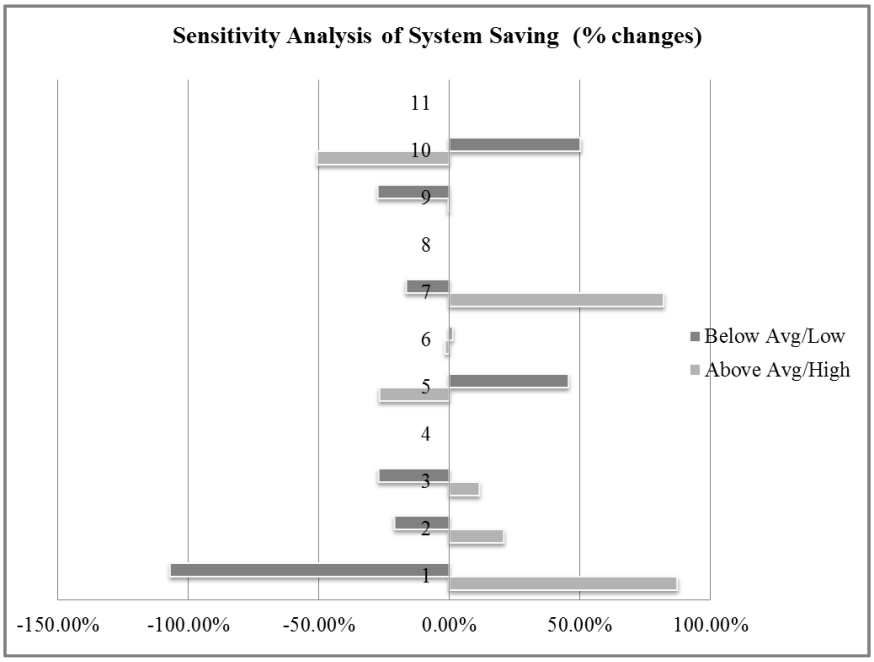

Figure 39. Sensitivity analysis of multiple input parameters on Scenario B (10 m^3) system payback

Rainfall and capital costs may affect the total change in savings by over 100% with the affects at 194 and 101%, respectively (Fig. 39 and Table 26). Mains water cost also has a large impact on the savings with a 98.8% swing in savings (Fig 8 and Table

7). The discount rate (72%), and the runoff (42%) and filter (38%) coefficients may also affect the outcome and other parameters such as the water demand (26.9%) and the electricity costs (2.8%) have a smaller impact on the results. Parameters that have impact on the payback can be categorized as controllable and non-controllable. Certain parameters such as rainfall, discount rate, and water pricing are not controllable.

Table 26. Input parameters impact on Scenario B system payback

RHW System Savings (% changes)				
Variable	Graph ID	Above Avg/High	Below Avg/Low	Total % Change
Rainfall profile	1	87.60%	-107.00%	194.70%
Catchment runoff coefficient	2	21.00%	-21.00%	42.00%
Rainwater filter coefficient	3	11.60%	-27.10%	38.80%
Additional inputs	4	0.00%	0.00%	0.00%
Discount rate	5	-26.80%	45.80%	72.50%
Electricity cost	6	-1.40%	1.40%	2.80%
Mains water cost	7	82.30%	-16.50%	98.80%
Disposal cost	8	0.00%	0.00%	0.00%
Water demand	9	-0.40%	-27.30%	26.90%
Capital cost	10	-50.50%	50.50%	101.00%
Decommissioning cost	11	0.00%	0.00%	0.00%

Other parameters such as the filter and runoff coefficients can be controlled through building roof design, filter design and proper maintenance. Capital costs are controllable to an extent however; regional wages and cost of materials vary. Additionally, the cost and complexity of the rainwater collection system can alter costs and the subsequent payback.

Uncertainty Analysis

In order to characterize the lifetime performance of the designs in this study, a consideration of uncertainty impacts on the simulated inputs is required. In this study, a probabilistic perspective of the system and parameters is achieved through a well-known analytical approach called a Monte Carlo simulation. This is performed through the introduction of randomness to the model inputs and the Monte Carlo simulation is a technique that uses random number generation and probability distributions to generate a distribution of input values for the input parameters; simulations are then run multiple times with individual input values from input distributions. The input distributions are often triangular or binomial, and in this study they are triangular and represent above-average, average and below-average values. The technique is useful in this case because of the possibility of many input parameter varying over the system lifetime and it offers a more realistic portrayal of likely (and not-so-likely occurrences).

The simulation was run seven hundred and fifty times to generate the results in Table 27; maximum (100%), average (73%) and minimum (43% and 45%) percentage of demand met for Scenario A and B are almost identical, due to adequate tank sizing. The probability of 73% of demand met for Scenario A and B was 45.8% and 48%, respectively and the probability of 100% of demand met was low for both scenarios, 2.4% and 0.2%, respectively (Table 27). The simulation results indicated that the payback is higher for the larger system (average 32.4 years compared to 25 years) and is due to larger capital costs. The probability of payback was considerable higher for the the 10 m^3 with (38.6% compared to 73.4%) (Table 27).

Table 27. Monte-Carlo simulation results of Scenarios A and B

SCENARIO	A (22.6 m^3)	B (10 m^3)
% of Demand Met		
Maximum % met	100%	100%
Mean (average) % met	73%	73%
Minimum % met	43%	45%
Standard deviation	15.1	14.3
Probability of 75% met	45.8%	48.0%
Probability of 100% met	2.4%	0.2%
Pay-Back Period (yrs)		
Shortest pay-back	14	10
Mean (average) pay-back	32	25
Longest pay-back	No payback	No payback
Standard deviation	9	9
Probability of pay-back	38.60%	73.4%

Summary and Conclusions

An installed rainwater collection system with a roof catchment area of 250 m^3 and a usable capacity of 22.6 m^3 was analyzed to determine the life cycle performance and economics in a residential urban setting. Field monthly demand measurements and regional weather patterns were utilized with modeling tools to determine hydraulic and life-cycle performance and life cycle comparisons with design optimizations were presented. Additionally, parameter sensitivity and stochastic analyses were also explored to determine the model's sensitivity to input below-average, average and above-average inputs.

Combined yield after spill and life cycle costing models provide valuable design and research tools for the study of rainwater harvesting systems in residential contexts.

An urban, residential, full-featured rainwater system was analyzed using regional water demand profiles and rainfall from NOAA 30-YR normal and other financial and cost assumptions. Average annual costs and NPV can be estimated to compare rainwater design against mains-only scenarios. On an annual, average basis, predictions with regional water demand and NOAA 30-year rainfall estimated 146 m^3/yr (38,569 gal/yr) to be collected for the installed system (22.6 m^2) and tank optimization indicated that a smaller system of 10 m^2 would suffice to provide 71% of demand.

Utilizing a life cycle analysis approach, oversizing rainwater collection systems may dramatically increase annualized costs and therefore increase payback time. In this research, more than doubling the size of the cistern from 10 m^3 to 22.6 m^3 of usable capacity increased payback in NPV terms from 21 to 43 years. Payback is highly dependent on the distribution of rainfall, mains water costs, discount rate, and capital costs.

A sensitivity analysis was run to evaluate the impact of the various input parameters. Rainfall may affect the total change in savings by largest amount (194% total swing) and capital and mains water cost also had a large impact on the savings swing (101 and 98% respectively). The discount rate (72%), runoff (42%) and filter (38%) coefficients may also affect the outcome and other parameters such as the water demand (26.9%) and the electricity costs (2.8%) have a much smaller impact on the results. Cistern capital costs can be moderately controlled through judicious optimization of tank volume. Capital costs are controllable to an extent; however, regional wages and cost of materials vary. Additionally, cost and complexity of the rainwater conveyance

and water treatment system can also impact costs and subsequent payback. Finally, using 30 YR rainfall patterns and Monte Carlo stochastic methods, there is a 45% or 48% probability (Scenario A, B respectively) of 73% of the annual demand being met and the annual water harvested in this interpretation is 370 m^3 (97,743 gallons).

The management of water of growing concern as resource demand increases in competitively constrained environments. The reduction of water consumption from utility mains may not only decrease demand of municipal water, but will decrease municipal electricity consumption associated with the reduction in water demand and, in large numbers, may mitigate costly infrastructure expansion through demand reduction.

CHAPTER V

SUMMARY AND CONCLUSIONS

Overview

The construction and occupation of buildings are substantial contributors to global emissions with almost a quarter of total CO_2 emissions being attributable to energy use in buildings (Metz et al. 2007). In addition, buildings play a dominant role in the consumption of energy as can be seen all over the world. The building sector has a significant influence on the total natural resource consumption and on the emissions released (Cabeza et al. 2014).

Although considerable advancements have been made to develop energy efficient residential building designs, there is ample potential for continued improvements. In this research, improvements identified and evaluated to control energy loads by utilizing a building envelope that has lower infiltration and better thermal resistance. Specifically, a life cycle study was performed on a LEED-Platinum rated home in Houston, Texas that incorporated an advanced and durable building envelope system. Comparisons were made to a more conventional, energy-efficient IECC 2012 code-based home, these operational energy comparisons of the individual homes were performed in Energy Plus, a robust building simulation software widely used and sponsored by US DOE. The HVAC portion of the model was validated with field-based data and then the 'As-Built' and 'Reference' models were compared. Space and water heating were modeled with both electric and gas heating systems. Additional portions of the model were based on Building America and PNNL reference code and assumption. Renewable energy and

rainwater systems were modeled for estimates of annual production, along with economic considerations and constraints. Both solar photovoltaic (electric) and solar hot water systems were modeled with NREL's System Advisory Model and annual predictions differences compared to field measurements and were within model uncertainties. A rainwater collection system was modeled with a yield-after-spill spreadsheet model, and water demand was based on average water consumed on site while rainfall inputs were derived from NOAA 30-year normal rainfall patterns. The annual outputs of these systems were compiled into a life cycle estimating tool for the purposes of estimating the life cycle environmental impacts of the buildings and relative impact by the associated subsystems.

Operational Energy Summary

The 'As-Built' model achieved a 31.2% and 28.9% reduction in total building energy when compared to the 'Reference' model for both gas and electrical supplemental heating, respectively. Ten percent of the total was found to be associated with the building envelope effect (infiltration held constant) alone. Comparing wood-framed IECC reference home to an ICF home, Marceau et al. (2006) reported a 7.7% reduction in total energy in Phoenix, AZ. Khahhat et al. (2009) also reported a reduction in total energy consumption of 4.7% for a wood-framed home compared to an ICF home. Total HVAC energy, as the average HVAC energy total, was 48.4% of the annual building energy for the 'As-Built' model and 60.2% of the annual energy for the 'Reference' model. The 'As-Built' models had 42% and 45.3% reductions, compared to the 'Reference' model for gas and electrical supplemental heating, respectively. The

lighting represented an average (electrical and gas models averaged) 5.4% and 3.8% while the appliances and plug-loads were an average of 35.1% and 24.6% of the annual energy for the 'As-Built' and 'Reference' model. Domestic hot water energy consumption was an average 11.2% and 7.8% of the annual energy for the 'As-Built' and 'Reference' model. Finally, the renewable energy systems contributed an annual average reduction of 15.5% and 12.5% for the 'As-Built' and 'Reference' operational energy, respectively.

Building EUIs and NEUIs are useful in comparing buildings to other buildings in a standardized way. In addition, they are useful to set performance goals and are currently being used by governmental agencies such as the US Energy Information Administration and building industry associations, such as ASHRAE (ASHRAE 2010 and US EIA 2015). In this study, the 'Reference' model achieved a EUI below the US EIA average and the 'As-Built' model is essentially at the 50% reduction target of EUI 19.4. Additionally, the EUI for the gas and electrical heating models achieved similar EUI and NEUI, with gas having a bit higher number due to extra energy usage resulting from process efficiency differences. The EUI for both the 'As-Built' model and the 'Reference' model were both strong achievers when compared with southern US regional averages. With renewable energy systems, the results were even stronger; however, the lowest NEUI attained, at 16.1, did not meet the 60% reduction target of the Architecture 2030 or the high achieving, Passivhaus standard. Finally, the annual energy use is a dominant portion of the life cycle use phase, and, as such, the EUI/NEUI, with the buildings associated square footage, yields a predictor of a large portion of the total

life cycle energy impact. As suggested previously, the literature reports 80-90% of the total life cycle energy of the building is from the use (and operational) phase of the building (Khakkat et al. 2009, Ortiz el al. 2009, Ramesh et al. 2010).

Renewable Energy Systems Summary

Renewable energy technologies can provide strategies to offset operational energy and are one of the key components in zero-energy-buildings (Li, D. et al. 2013, Wang et al. 2009). This research investigated the annual renewable energy production and costs of two residential solar-based systems installed in humid, sub-tropical environment (IECC Zone 2). Field performance was estimated and compared to a publicly available simulation tool, NREL's System Advisory Model for the purposes of estimating renewable energy life cycle energy production of the residence. Field results agreed with TMY3-based simulation estimates within the simulation and measurement system uncertainties. SAMs P90/P50 probabilistic utility along with TMY3 and NSRDB weather data from the region provided estimates on the variation in radiation impacts on annual production. P50/P90 probabilities were within 3% and 6% of TMY3 predictions for both the SPVS and the SHWS, respectively. Design optimization checks revealed the that SPVS was installed in an optimized design; however, the SHWS azimuth could have been better optimized at an azimuth of 180°, but, a complicated, multi-angled roof proved to challenge the optimal position.

SAM was further utilized to estimate life cycle production and life cycle costs and to perform sensitivity analysis on critical parameters and economic indicators such as payback, NPV and LCOE. These economic indicators were explored for both

systems, and payback, NPV, and LCOE were considerably more favorable for the SHWS compared to SPVS due to high costs relative to output at the life cycle and loan periods evaluated. SHWS achieved a 21.8-year payback, a NPV of $796 and an LCOE of 8.1 ¢/kWh, compared to a 29.2-year payback, a NPV -$1296 and an LCOE of 12 .29 ¢/kWh for SPVS. The SPVS life cycle costs are dependent on the PV module costs and were found to achieve a LCOE close to the regional electricity prices at a module cost of 0.75 ¢/Wdc, representing a 67% reduction in module installed costs. Feldman et al. (2014) report from NREL's Sun Shot initiative, that the United States is at an all time historically low module median price of 67¢/Wdc, further stating that the market trends have been decreasing 6-7 percent year from 1998 to 2013. This holds incredible promise for not only offsetting operational energy impacts, but also renewable energy market penetration. SHWS life cycle costs are also dependent on capital costs and the solar hot water collector and pre-heat appliance are almost 50% of the initial cost.

Additionally, loan, inflation, and discount rates were modeled with a 25% swing from the assumed case to in order determine the relative impact while the loan rate had the largest impact on the LCOE for both SPVS and SHWS at about 15-17% increase or decrease in the real LCOE. Additionally, the life cycle period and loan term combinations were performed to illustrate the impact that various combinations of the evaluation period and loan term may have on the economic indicators. Finally, the TMY3-based simulations of the SPVS achieved an annual and 30-yr energy production of 4,226 and 117,994 kWh, respectively, while the SHWS annual and 30-yr energy

production were 2,394 and 66,820 kWh with auxiliary gas and 1,846 and 51,555 kWh with auxiliary electrical.

Texas is a leader in residential energy consumption and carbon dioxide emissions in the United States, with the average annual electricity cost per household being $1,801 (US EIA 2009). Increases in residential renewable energy production in Texas have the potential to offset energy consumption and subsequent carbon dioxide production. Therefore, further reduction in renewable energy system's capital and other initial costs, along with appropriate financial, terms may help with market adoption and viability. However, low regional fuel costs increase the constraints on the aforementioned initial costs. This research has provided field-validated casework of renewable energy system performance in humid, subtropical Texas with publicly available software tools such as NREL's System Advisory Model, which facilitates a multifactor energy, economic and life cycle analytical platform to assist in renewable energy project design, analysis and decision support.

Rainwater Harvesting System Summary

Many studies have demonstrated the effectiveness of rainwater harvesting systems to offset main water demand and to alter diurnal water pattern flow in the distribution networks (Fewkes and Wam 2001, Lucas et al. 2010), and rainwater harvesting systems in Texas have experienced growth in the use of RWH over the past ten to fifteen years (Fewkes 2012), with this growth being spurred by available water resource and population pressures (Fewkes 2012, TWDB 2014). Additionally, green building programs, such as LEED, acknowledge rainwater harvesting collection systems

as a contributor to the over-arching environmental quality of a building design, as evidence by inclusion in their rating systems. To meet the need for regional rainwater system studies and their impact on buildings, an evaluation of the installed rainwater collection system was performed. The system had a roof catchment area of 250 m^3 and a usable storage capacity of 22.6 m^3. Monthly water demand measurements and regional weather patterns were utilized with modeling tools to determine hydraulic and life-cycle performance, and life cycle comparisons with design optimizations were also presented. Additionally, parameter sensitivity and stochastic analyses were explored to determine the model's sensitivity to below average, average and above average inputs.

Utilizing a life cycle analysis approach, oversizing rainwater collection systems may dramatically increase annualized costs, thus increasing the payback time. In this research, more than doubling the size of the cistern from 10 m^3 to 22.6 m^3 of usable capacity increased the payback in NPV terms from 21 to 43 years. Payback is highly dependent on the distribution of rainfall, water costs, discount rate, and capital costs. A sensitivity analysis was run to evaluate the impact of the various input parameters. Rainfall may affect the total change in savings by the largest amount (194% total swing) while capital and water cost also had a large impact on the savings swing (101 and 98% respectively). The discount rate (72%), runoff (42%) and filter (38%) coefficients may also affect the outcome while other parameters such as the water demand (26.9%) and the electricity costs (2.8%), have a much smaller impact on the results. Cistern capital costs can be moderately controlled through judicious optimization of tank volume. Furthermore, capital costs are controllable to an extent; however, regional wages and

cost of materials vary. Additionally, the cost and complexity of the rainwater conveyance and water treatment system can also impact costs and subsequent payback. Finally, using 30-year rainfall patterns and Monte Carlo stochastic methods, there is a 45% or 48% probability (Scenario A, B respectively) of 73% of the annual demand being satisfied and the annual water harvested in this interpretation is 370 m^3 (97,743 gallons).

A combination of the yield after spill and the life cycle costing models provide valuable design and research tools for the study of rainwater harvesting systems in residential contexts. An urban, residential, full-featured rainwater system was analyzed by using regional water demand profiles and rainfall from NOAA 30-year normal along with other financial and cost assumptions based on regional information. Average annual costs and NPV can be estimated to compare rainwater designs against mains-only scenarios. On an annual, average basis, predictions with regional water demand and NOAA 30-YR rainfall estimated that 146 m^3/yr (38,569 gal/yr) can to be collected for the installed system (22.6 m^3) while tank optimization indicated that a smaller system of 10 m^3 would suffice to provide 71% of demand.

The management of water is a growing concern as resource demand increases in competitively constrained environments. The reduction of water consumption from utility mains may not only decrease the demand of municipal water, but it will also decrease municipal electricity consumption associated with the reduction in water demand; however, in large numbers, it may mitigate costly infrastructure expansion through demand reduction.

Life Cycle Analysis Summary

Building energy estimations and environmental impacts were performed with the Impact Estimator, a publicly available LCA software from the Athena Sustainable Materials Institute. The model development and the results are presented herein. The annual operational energy was reduced 31.2% and 28.9% for the gas and electrical space and water heating models, respectively while the reductions due to the decrease in HVAC energy and reductions in HVAC loads were determined to be largely from infiltration and building envelope differences in the 'Reference' and 'As-Built' models. For the gas space and water heating models, the embodied energy phase (product production, construction, transportation) was 6% and 12% of the total energy while the use phase (operational and maintenance) lifetime energy was 93% and 87% for the 'Reference' and 'As-Built' models. The electrical space and water heating models followed similar trends with slightly more (1-2%) energy being utilized in the operational phase. The relative fraction of the embodied and use phase was consistent with the literature (Khahhat et al. 2009, Ortiz et a. 2009, Ramesh et al. 2010). Ramesh et al. (2010) performed a literature review of 73 cases, across 13 countries, and found a use phase fraction of 80-90% of the life cycle energy.

The embodied energy in the 'Reference' model was almost half (48%) of embodied energy in the 'As-Built', but the 'As-Built' model achieved an overall reduction of total primary energy over the building's life cycle of 23-24% compared to the 'Reference' model, which was due to the larger amount of concrete and steel material found in the 'As-Built' design. However, over 50-year life cycle, the 'As-Built'

design achieved a reduction of 6,314 GJ (1.75 E06 kWh) and 402 metric tons of primary energy and GWP, respectively (gas and electric space and water heating models averaged and compared to the 'Reference' case). These trends are also consistent with building envelope life cycle energy literature (Khahhat et al. 2009, Marceau et al. 2006). For the gas space and water heating, the embodied energy was 1,608 GJ and 2,376 GJ over the 50-year period for the 'Reference' and 'As-Built' models, respectively. Embodied energy intensities (GJ/m^2) were 2.7 and 4.0, respectively for the 'Reference' and 'As-Built' cases. Monahan and Powell (2011) reported on 14 homes in the UK that has 1.3- 7.3 GJ/m^2 of embodied energy intensity while other studies reported at 5.3 GJ/m^2, all consistent with estimates presented herein. Operational energy was 24,483 and 17,226 GJ, with energy intensities of 41.4 and 29.5 GJ/m^2 over the 50-year period for the 'Reference' and 'As-Built' models. Total primary energy over the life cycle was 26,216 and 19,983 GJ, with energy intensities of 44.4 and 33.8 GJ/m^2 for the 'Reference' and 'As-Built' models.

Embodied global warming potentials followed distribution patterns similar to that of the primary energy. For example, GWP intensities (kg CO_2-eq/m^2) for the gas space and water heating models were 193 and 286, respectively for the 'Reference' and 'As-Built' cases. Citherlet ad Defaux (2007) reported about 4 kg CO_2-eq/m^2-yr while Monahan and Power (2011) reported 405 kg CO_2-eq/m^2, all of which are consistent with other reported estimates. Use phase GWP intensities were 2,626 and 1861 kg CO_2-eq/m^2 over the 50-year period for the 'Reference' and 'As-Built' models, respectively.

Total life cycle GWP intensities of 2,835 and 2,166 kg CO_2-eq/m^2 were found for the 'Reference' and 'As-Built' models. The GWP intensities for this study were consistent with Ortiz et al. (2010), who reported 2,340 kg CO_2-eq/m^2 over a 50-year period. Citherlet and Defaux (2007) reported standard, efficient and very efficient homes in Switzerland and found 50-year GWP densities varying from 500-1,250 kg CO_2-eq/m^2, lower GWP densities and overall variations that were attributed to energy mix differences and to large contributions in hydropower (60%) and nuclear (40%). The embodied phase was 7% and 13% and the use phase 93% and 86% of the total primary energy for the 'Reference' and 'As-Built' model, respectively. Again, electrical space and water heating models followed similar trends as the gas models with the operational energy and total energy slightly higher.

As summarized previously, renewable energy systems decreased the annual operating energy 12.5% - 15.5% for the 'Reference' and 'As-Built' models, respectively. Over the life cycle at a 0.5% annual degradation factor, reductions the total life cycle primary energy of 9.4% and 13.4% were found for the 'Reference' and 'As-Built' models. This corresponded to an average reduction of 2,570 GJ of total primary energy, which is the equivalent of offsetting the embodied phase portion of the 'As-Built' model.

With no rainwater harvesting considered, total water consumption was 29.68 (24.06 acre-foot) and 31.78 mega-liters (ML) (29.76 acre-foot) for the 'Reference' and 'As-Built' models, respectively, additionally the 'As-Built' model contained 49% more water consumption in the product phase and 46% more in the construction phase and 7% more overall compared to the 'Reference' model while the end-of-life phase had no

water consumption. The use phase dominates both models with 85 and 80% of the use phase for the 'Reference' and 'As-Built' model, respectively. Although stochastic in nature and difficult to predict, rainwater harvesting systems may dramatically offset the life cycle use phase. The studies presented herein, based on a Monte-Carlo simulation, yielded a 73% demand reduction with 48% probability. This reduction in demand was approximately equivalent to the corresponding embodied water in the 'As Built' alone.

Future Research and Closing Remarks

The results from the life cycle analysis and impact assessment compared one life-cycle stage with the other (or one assembly to another) and helped in identifying those building design components that have the largest energy and environmental impact. LCA is a quantitative, but approximate, approach for integrated building design, and it evaluates building systems along with overall impacts and tradeoffs. The techniques employed herein are useful to help understand and guide designs and decision-making in the building sciences and construction process. Building use energy analysis, through operational energy simulation, determines those building phases and components that have the highest energy demand, allowing them to be identified and targeted for improvements. Primary energy can give a useful indication of the greenhouse gas emissions attributable to buildings and their impact on the environment. Additionally, renewable energy systems can have a substantial impact not only on reducing building energy demand, but also in the reduction of environmental emissions to air and water. As of 2013, median PV module costs yield a LCOE that is competitive with local electricity prices and suggest future SPVS investments to be more likely. Finally,

rainwater collection systems and their output, although highly dependent on rainfall, may have a significant impact on life cycle mains water consumption. The cost of the rainwater harvesting system is a critical factor for the widespread use of the technology, and, as illustrated in this study, proper sizing of the storage volume is a critical element in analysis of the system.

Future Research

This work focused on an actual large urban home in Houston, Texas with specific systems under evaluation. This study did not look at the performance of the building and renewable energy systems in different climates to ascertain the building envelope and infiltration impact on operational energy; this will be the subject of future work. Building operational energy use projections are based on static assumptions from the annual estimates, meaning that model sensitivities have not been rigorously explored. Infiltration, lifestyle factors and climate variability may increase their associated loads.

The size of the home in this study is more than double the average size home in the United States, and future work will utilize smaller footprint models such as PNNL IECC code-testing models (223 m^2, 2400 ft^2). Utilizing common and more robust building envelope structures, such as ICF, the embodied energy contained in these models can be determined and Energy Plus derived operational energy can be used to calculate a complete life cycle performance of the PNNL models. To date, it is not clear that this approach has been reported in the literature.

Finally, mains water demand reduction due to the rainwater collection system production did not include energy or associated environmental impacts that may arise

from reductions in water distribution energy requirements at the utility. Additionally, the reduction of the water use associated with the energy reductions in the model comparisons (building operational energy or renewable energy offsets) were not accounted for either. These "water and energy nexus" issues are items of future research.

Closing Remarks

Texas has one of the largest economies in the United States, and as of 2014, it has the second highest gross state product of $1.68 trillion dollars (Chantrill 2015). As such, Texas is a leader in residential energy consumption and carbon dioxide emissions in the United States. Furthermore, Texas average annual electricity cost per household is $1,801 (US EIA 2009), among the highest in the nation and according to US EIA's Residential Energy Consumption Survey six, hundred and fifty-six million metric tons of carbon dioxide were emitted in 2011, which is 12% of the total for the nation and twice that of California (US EIA 2009). Reducing residential energy and water demand through improved methods of building envelope construction along with implementing energy and water offsetting subsystems, such as renewable energy and rainwater collection systems, reduces total primary energy, water consumption, other resource burdens and environmental impacts such as global warming potential. Finally, these improvements reduce energy and water requirements from stressed utilities and their distribution networks. The promotion of building codes that stress building envelope design that promotes thermal resistance and minimizes infiltration is critical to reduce the environmental burden of buildings. Furthermore, the retention of tax incentives for renewable energy system is important for their continued market penetration. However,

rainwater systems, although free of sales tax currently in Texas, do not have large incentives, and as Fewkes (2012) states, they may remain largely uneconomic.

REFERENCES

Abdulla, F. A. and Al-Shareef, A. W. 2009. Roof rainwater harvesting systems for household water supply in Jordan. *Desalination*, *243*(1):195-207.

Adams, P. A., Calibration of DS18S20, Email. Personal correspondence, Director of Quality and Reliability Assurance, Maxim, Inc. January 2012.

Adalberth, K., Almgren, A. and Holleris Petersen, E. 2001. Life-cycle assessment of four multi-family buildings. *International Journal of Low Energy and Sustainable Buildings 2*:1-21.

Antoniou, G., Kathijotes, N., Spyridakis, D.S. and Angelakis, A.N. 2014. Historical development of technologies for water resources management and rainwater harvesting in the Hellenic civilizations. *International Journal of Water Resources Development* 30(4):680-693, DOI: 10.1080/07900627.2014.900401.

Antonopoulos, K. A. and Koronaki, E. 1999. Envelope and indoor thermal capacitance of buildings. *Applied Thermal Engineering* 19(7):743–756.

Architecture 2030. 2015. 2030 Challenge Targets: US Residential Regional Averages, 2006-2010, Data source: US Environmental Protection Agency, US Energy Information, Administration, Santa Fe, New Mexico, http://architecture2030.org/files/2030_Challenge_Targets_Res_Regional.pdf. Visited August 2015. Architecture 2030 Inc.

Arguez, A., Durre, I., Applequist, S., Vose, R. S., Squires, M. F., Yin, X., Heim, Jr., R. R. and Owen, T. W. 2012. NOAA's 1981-2010 US climate normals: An overview. *Bulletin of the American Meteorological Society* 93(11):1687-1697.

Aratesh, D., Kohler C., Griffith, B. 2009. *Modeling Windows in Energy Plus with Simple Performance Indices*. Report LBNL-2804E. Golden, CO: National Renewable Energy Laboratory.

ASHRAE. 2011. ANSI/ASHRAE Standard 140-2011, *Standard Method of Test for the Evaluation of Building Energy Analysis Computer Programs*. Atlanta, GA: ASHRAE.

ASHRAE. 2013a. ANSI/ASHRAE Standard 55-2013, *Thermal Environmental Conditions for Human Occupancy*. Atlanta, GA: ASHRAE.

ASHRAE. 2013b. ANSI/ASHRAE Standard 90.2-2007, *Energy-Efficient Design of Low-Rise Residential Buildings*. Atlanta, GA: ASHRAE.

ASHRAE. 2014a. *ASHRAE Guideline 14-2014 for Measurement of Energy and Demand Savings*. Atlanta, GA: ASHRAE.

ASHRAE. 2014b. ASHRAE Standard 105-2014*, Standard Methods of Measuring, Expressing and Comparing Building Energy Performance*. Atlanta, GA: ASHRAE.

ASHRAE Technical Committee 7.6. 2010. *Report from ASHRAE Performance Measurement Protocols for Commercial Buildings the Technology Council Ad Hoc Committee on Energy Targets*. Atlanta, GA: ASHRAE.

ASMI. 2014. *User Manual and Transparency Document, Impact Estimator for Buildings v.5*. September 2014. IE4B v.5.0.0105. Ottawa, Ontario: Athena Sustainable Material Institute.

Basupi, I. 2013. *Adaptive Water Distribution System Design under Future Uncertainty.* Ph.D. dissertation, University of Exeter, Exeter, Devon EX4, UK.

Bayer, C., Gamble, M. and Entry, R. 2010. AIA Guide to Building Life Cycle Assessment in Practice, Washington, DC: The American Institute of Architects.

Blair, N., Dobos, A. and Sather, N. 2012. *Case Studies Comparing System Advisor Model (SAM) Results to Real Performance Data,* NREL/CP-6A20-54676. Golden, CO: National Renewable Energy Laboratory.

Blair, N., Dobos, A., Freeman, J., Neises, T., Wagner, M., Ferguson, T., Gilman, P. and Janzou, S. 2014. *System Advisor Model*, SAM 2014.1.14, General Description. NREL No. TP-6A20-61019. Golden, CO: National Renewable Energy Laboratory.

Brown, M. T. and Herendeen, R. A. 1996. Embodied energy analysis and EMERGY analysis: a comparative view. *Ecological Economics* 19(3):219–235.

Brown, M. T, and Ulgiati, S. 1997. Emergy-based indices and ratios to evaluate sustainability: monitoring economies and technology toward environmentally sound innovation. *Ecological Engineering* 9(1-2):51–69.

Burch and Christensen. 2007. *Towards Development of an Algorithm for Mains Water Temperature.* Golden, CO: National Renewable Energy Laboratory.

Bushi, L. and Meli, J. 2014. *An Environmental Life Cycle Assessment of Portland Limestone and Ordinary Portland Cements in Concrete*. Prepared for the Cement Association of Canada, Ottawa, Canada, Athena Sustainable Material Institute.

Buyle, M., Braet, J. and Audenaert, A. 2013. Life cycle assessment in the construction sector: A review. *Renewable and sustainable energy reviews 26*:379-388.

Cabeza, L. F., Rincón, L., Vilariño, V., Pérez, G. and Castell, A. 2014. Life cycle assessment (LCA) and life cycle energy analysis (LCEA) of buildings and the building sector: A review. *Renewable and sustainable energy reviews 29*:394-416.

Chantrill, C. 2014. State Growth and Debt Rank for 2014. http://www.usgovernmentspending.com/compare_state_spending_2014bZ0a. Visited 2015.

Chasar, D., Center, F. S. E., Moyer, N., Parker, D. and Chandra, S. 2002. Measured and Simulated Cooling Performance Comparison; Insulated Concrete Form Versus Frame Construction. *ACEEE Summer Study on Energy Efficiency in Buildings* 43.

Chen, T. Y., Burnett, J. and Chau, C. K. 2001. Analysis of embodied energy use in the residential building of Hong Kong. *Energy* 26(4):323–340.

Ciambrone, D. F. 1997. *Environmental life cycle analysis*. CRC Press.

Citherlet, S. and Defaux, T. 2007. Energy and environmental comparison of three variants of a family house during its whole life span. *Building and Environment* 42(2):591-598.

Crasta, F.M., Fasso, C.A., Patta, F. and Putzu, G. 1982. Carthaginian – Roman cisterns in Sardina, *Proceedings of the International Conference on Rainwater Cistern Systems,* University of Hawaii, Honolulu.

De Meester, B., Dewulf, J., Verbeke, S., Janssens, A. and Van Langenhove, H. 2009. Exergetic life-cycle assessment (ELCA) for resource consumption evaluation in the built environment. *Building and Environment*, *44*(1):11-17.

Dobos, A. and Gilman, P. 2012. P50/P90 Analysis for Solar Energy Systems Using the Systems Advisor Model, 2012 *World Renewable Energy Forum*, Denver, Colorado, May 13-17 2012.

Duffie, J. A. and Beckman, W. A. 2013, *Solar Engineering for Thermal Processes*, 4th Edition. Hoboken, NJ: John Wiley & Sons, Inc.

Dunlop, E. D. and Halton, D. 2006. The performance of crystalline silicon photovoltaic solar modules after 22 years of continuous outdoor exposure. *Progress Photovoltaics: Research and Applications* 14(1):53–64.

Elcock, D. 2007. *Lifecycle Thinking within the Oil and Gas Exploration and Production Industry*. Report ANL/EVS/R-07/5. Argonne, IL: Argonne National Laboratory.

Enphase Energy Inc. 2014. *Envoy Installation and Operation*, 141099911 Rev 05, http://enphase.com/global/files/Envoy_Installation_and_Operation_NA.pdf.

EPRI. 2002. Water and Sustainability (Vol 4): US Electricity consumption for water supply and treatment - the next half century; No. 1006787. *Electric Power Research Institute*.

Farreny, R., Gabarrell, X. and Rierdevall, J. 2011. Cost-efficiency of rainwater harvesting strategies in dense Mediterranean neighborhoods. *Resources, Conservations and Recycling* 55:686-694.

Feldman, D., Barbose, G., Margolis, R., Darghouth, N., James, T., Weaver, S., ... & Wiser, R. 2014. Photovoltaic System Pricing Trends: Historical, Recent, and Near-Term Projections–2014 Edition. *Golden, CO: National Renewable Energy Laboratory, PR-6A20-62588.*

Fewkes, A. 1999. Modeling the performance of rainwater collection systems: Towards a generalized approach. *Urban Water* 1:323-333.

Fewkes, A. and Wam, P. 2001. A method of modeling the performance of rainwater collection systems in the *UK. Proc. of 1st Nat. Conf. on Sustainable Drainage.* Coventry University, UK, 232-242.

Fewkes, A. 2012. A review of rainwater harvesting in the UK. *Structural Survey*, *30*(2): 174-194.

Finlayson, G. 2015. Athena Sustainable Material Institute, Ottawa Ontario, Email correspondence with the author, August 21.

Freeman, J., Whitmore, J., Kaffine, L., Blair, N. and Dobos, A. P. 2013. *System Advisor Model: Flat Plate Photovoltaic Performance Modeling Validation Report*. http://www.osti.gov/scitech/servlets/purl/1115788.

Freeman, J., Whitmore, J., Kaffine, L., Blair, N., Dobos, A. 2014. *Validation of Multiple Tools for Flat Plate Photovoltaic Modeling Against Measured Data*, NREL/TP-6A20-61497. Golden, CO: National Renewable Energy Laboratory.

Ghimire, S. R, Johnson, J. M., Ingwersen, W. W., Hawkins, T. R. 2014. Life cycle assessment of domestic and agricultural rainwater harvesting systems. *Environmental Science and Technology* 48:4069-4077.

Gilman, P. 2014. *SAM Photovoltaic Model (pvsamv1) Technical Reference,* https://sam.nrel.gov/sites/sam.nrel.gov/files/SAM%20DRAFT%20Photovoltaic%20Reference%20Manual%20May%2014%202014.pdf.

Griffin, R.C. 2006, *Water Resource Economics, the Analysis of Scarcity, Policies and Projects,* MIT Press, Massachusetts Institute of Technology.

Griffin, R. C. and Characklis, G. W. 2011. Issues and trends in Texas water marketing. *Journal of Contemporary Water Research and Education* 121(1):5.

Google Maps. 2014. 3703 Drummond St. Houston, Texas Street Map. Retrieved from https://www.google.com/maps/place/3703+Drummond+St,+Houston,+TX+77025/@29.6960509,-95.4340621,41m/data=!3m1!1e3!4m2!3m1!1s0x8640c03491c645a5:0x123f59a226f3bd9

Haapio, A. and Viitaniemi, P. 2008. A critical review of building environmental assessment tools. *Environmental impact assessment review* 28(7):469-482.

Hang, Y., Qu, M. and Zhao, F. 2012. Economic and environmental life cycle analysis of solar hot water systems in the United States, *Energy and Buildings* 45:181-188.

Hendron, R. and Engebrecht, C. 2009. *National Renewable Energy Laboratory. Building America Research Benchmark Definition*. NREL/TP-550-47246. Golden, Colorado: National Renewable Energy Laboratory.

Hendron, R. and Engebrecht, C. 2010. *National Renewable Energy Laboratory. Building America House Simulation Protocols*. Golden, CO: National Renewable Energy Laboratory.

Henze, G. P. 2005. Energy and cost minimal approach of active and passive building thermal storage inventory. *Solar Energy Engineering* 127:343-351.

Hitchcock, D. 2004. *Cool Houston! A Plan for Cooling the Region.* Houston Advanced Research Center.

http://files.harc.edu/Projects/CoolHouston/CoolHoustonPlan.pdf. Visited Feburary 2015.

Hobbi, A. and Siddiqui, K, 2009. Optimal design of a forced circulation solar water heating system for a residential unit in cold climate using TRNSYS, *Solar Energy* 83(5):700–714. http://www.twdb.state.tx.us/waterplanning/waterusesurvey/estimates/data/Texas%20Statewide%20Media%20Report.pdf. Visited July 2014.

Horvath, A. 2004. Construction materials and the environment. *Annual Reviews of Environment and Resources 29*:181-204.

Huijbregts, M. A., Rombouts, L. J., Hellweg, S., Frischknecht, R., Hendriks, A. J., van de Meent, D. and Struijs, J. 2006. Is cumulative fossil energy demand a useful indicator for the environmental performance of products?. *Environmental Science and Technology*, *40*(3), 641-648.

Huijbregts, M. A., Hellweg, S., Frischknecht, R., Hendriks, H. W., Hungerbühler, K. and Hendriks, A. J. 2010. Cumulative energy demand as predictor for the environmental burden of commodity production. *Environmental science and technology 44*(6):2189-2196.

ISO, ISO 14040-2006. *Environmental Management – Life Cycle Assessment – Principles and Framework.* Geneva, Switzerland: International Organization for Standardization.

Jenkins D. and Pearson, F. 1978. *Feasibility of rainwater collection system in California.* Contribution No. 173, California Water Resource Center, University of California, US.

Joshi, S. 2000. Product environmental life-cycle assessment using input-output techniques. *Journal of Industrial Ecology 3*(2-3):95-120.

Kahhat, R., Crittenden, J., Sharif, F., Fonseca, E., Li, K., Sawhney, A. and Zhang, P. 2009. Environmental impacts over the life cycle of residential buildings using different exterior wall systems. *Journal of Infrastructure Systems* 15(3):211-221.

Kalogirou, S. 2009. Thermal performance, economic and environmental life cycle analysis of thermosiphon solar water heaters. *Solar Energy* 83(1):39–48.

Keoleian, G. A., Blanchard, S. and Reppe, P. 2000. Life-Cycle Energy, Costs, and Strategies for Improving a Single-Family House. *Journal of Industrial Ecology* 4(2):135–156.

Kosny, J., Christian, J.E., Desjarlais, A.O., Kosseka, E. and Berrenberg, L. 1998. Performance Check between Whole Building Thermal Performance Criteria and Exterior Wall Measured Clear Wall R-Value, Thermal Bridging, Thermal Mass, and Airtightness / Discussion. *ASHRAE Transactions* 104:1379.

Kossecka, E. and Kosny, J. 2002. Influence of insulation configuration on heating and cooling loads in a continuously used building. *Energy and Buildings* 34(4):321-331.

Kovacs, P. 2012. *Quality Assurance in solar thermal heating and cooling technology – keeping track with recent and upcoming developments – A guide to the standard EN* 12975. Boras, Sweden: Technical Research Institute of Sweden (TRIS).

Langston, Y. L. and Langston, C. A. 2008. Reliability of building embodied energy modeling: an analysis of 30 Melbourne case studies. *Construction Management and Economics* 26(2):147-160.

Li, D. H., Yang, L. and Lam, J. C. 2013. Zero energy buildings and sustainable development implications–a review, *Energy* 54:1-10.

Li, K., Zhang, P., Crittenden, J. C., Guhathakurta, S., Chen, Y., Fernando, H. and Torrens, P. M. 2007. Development of a framework for quantifying the environmental impacts of urban development and construction practices. *Environmental science and technology 41*(14):5130-5136.

Li, Z., Boyle, F. and Reynolds, A. 2010. Rainwater harvesting and greywater treatment systems for domestic application in Ireland. *Desalination* 260(1-3):1–8.

Lucas, S., Coombes, P., & Sharma, A. 2010. The impact of diurnal water use patterns, demand management and rainwater tanks on water supply network design. *Water Science and Technology: Water Supply* 10(1):69-80.

Marceau, M.L. and VanGeem, M. G. 2006. Comparison of the life cycle assessments of an insulating concrete form house and a wood frame house. *Journal of ASTM International* 3(9):1-11.

Marszal, A. J., Heiselberg, P., Bourrelle, J. S., Musall, E., Voss, K., Sartori, I. and Napolitano, A. 2011, Zero Energy Building–A review of definitions and calculation methodologies, *Energy and Buildings* 43(4):971-979.

Mathioulakis, E., Panaras, G. and Belessiotis, V. 2012. Uncertainty in estimating the performance of solar thermal systems, *Solar Energy* 86:3450-3459.

Mathioulakis, E., Voropoulos, K. and Belessiotis, V. 1999. Assessment of Uncertainty in Solar Collector Modeling and Testing. *Solar Energy* 66(5):337-347.

Mendon, V., Lucas, R. and Goel, S. 2013. *Cost-Effectiveness Analysis of the 2009 and 2012 IECC Residential Provisions-Technical Support Document.* PNNL-22068. Richland, WA: Pacific Northwest National Laboratory.

Metz, O.R. Davidson, P.R. Bosh, R. Dave, L.A. Meyer, (Eds). 2007. Construction and occupation of buildings is substantial contributor go global Co2 emissions with almost a quarter of total CO2 emissions attributable to energy use in buildings — . Climate Change 2007: Mitigation of Climate Change. *Contribution of Working Group III to the Fourth Assessment Report of the Intergovernmetnal Panel on Climate Change,.IPCC Fourth Assessment Report (AR4)*, Cambridge, UK: Cambridge University Press.

Monahan, J. and Powell, J. C. 2011. An embodied carbon and energy analysis of modern methods of construction in housing: A case study using a lifecycle assessment framework. *Energy and Buildings 43*(1):179-188.

National Ocean and Atmospheric Administration (NOAA), National Climatic Data Center (NCDC). 2014. 1981-2010 *US Climate Normals.* http://www.ncdc.noaa.gov/data-access/land-based-station-data/land-based-datasets/climate-normals/1981-2010-normals-data. Visited July 2014.

National Resources and Conservation Service (NRCS). 2014. *Price Indexes and Discount Rates.* http://www.nrcs.usda.gov/wps/portal/nrcs/detailfull/national/cntsc/?cid=nrcs143_009709. Visited August 2014.

Neises, T. 2011. *Development and Validation of a Model to Predict the Temperature of a Photovoltaic Cell*. Masters of Science. University of Wisconsin-Madison.

Neymark, J. and Jodkoff, R. 1995. *International Energy Agency Building Energy Simulation Test (BESTEST) and Diagnostic Method*. NREL TP-472-6231. Golden, CO: National Renewable Energy Laboratory.

Neymark, J.and Jodkoff, R. 2002. *International Energy Agency Building Energy Simulation Test and Diagnostic Method for Heating, Ventilating, and Air-Conditioning Equipment Models (HVAC BESTEST).* Vol 1: Cases E100-E200. NREL TP-550-30152. Golden, CO: National Renewable Energy Laboratory.

NREL. 2014. *System Advisor Model (SAM), About,* Golden, CO: National Renewable Energy Laboratory. https://sam.nrel.gov/about.

NREL. 2015. *System Advisor Model (SAM),* Version 2015.1.30. Golden, CO: National Renewable Energy Laboratory. https://sam.nrel.gov/content/downloads.

Olgyay, V. and Herdt, J. 2004. The application of ecosystems services criteria for green building assessment. *Solar Energy 77*(4):389-398.

Ortiz, O., Castells, F. and Sonnemann, G. 2009. Sustainability in the construction industry: A review of recent developments based on LCA. *Construction and Building Materials 23*(1):28-39.

Pehnt, M. 2006. Dynamic life cycle assessment (LCA) of renewable energy technologies. *Renewable energy* 31(1):55-71.

Perez-Garcia, J., Lippke, B., Briggs, D., Wilson, J. B., Bowyer, J. and Meil, J. 2005. The environmental performance of renewable building materials in the context of residential construction. *Wood and Fiber Science* 37(12):3-17.

Phoca, I. and Valananis, P. 1999. *Rediscovering Ancient Greece: Architecture and City Planning,* Kedros Books, Athens.

Pinto, E. J. C. 2010. *Rainwater Harvesting Systems Implementation Inside Karunya University*, Ph.D. dissertation, University of Porto, Faculty of Engineering. Porto, Portugal.

Pulselli, R. M., Simoncini, E., Pulselli, F. M. and Bastianoni, S. 2007. Energy analysis of building manufacturing, maintenance and use: Em-building indices to evaluate housing sustainability. *Energy and Buildings* 39(5):620–628.

Ramesh, T., Prakash, R. and Shukla, K. K. 2010. Life cycle energy analysis of buildings: An overview. *Energy and Buildings* 42(10):1592-1600.

Rasouli, M., Simonson, C. J. and Besant, R. W. 2010. Applicability and optimum control strategy of energy recovery ventilators in different climatic conditions. *Energy and Buildings* 42(9):1376-1385.

Realini, A., Burà, E., Cereghetti, N., Chianese, D. and Rezzonico, S. 2002. *Mean time before failure of photovoltaic modules (MTBF-PVm) Annual Report 2002*. Project number BBW 99.0579. Stuttgart, Switzerland: Swiss Federal Office of Energy (SFOE).

Reddy, G. B. 2000. An experimental investigation of subsurface ground temperature in Texas: a complete study. *International Journal of Ambient Energy* 21(4).

Richman, R., Pasqualini, P. and Kirsh, A. 2009. Life-cycle analysis of roofing insulation levels for cold storage buildings. *Journal of Architectural Engineering* 15(2):55-61.

Roebuck, R.M. and Ashley, R.M. 2006. Predicting the hydraulic and life-cycle cost performance of rainwater harvesting systems using a computer based modeling tool. *7th International Conference on Urban Drainage Modeling*, April 2006, Melbourne, Australia.

Rose, L.S., Akbar, H. and Taha, H. 2003. *Characterizing the fabric of the urban environment: A case study of Greater Houston, Texas*. Berkeley, CA: Lawrence Berkeley National Laboratory.

Rudie, E., Thornton, A., Rajendra, N. and Kerrigan. S. *System Advisor Model Performance Modeling Validation Report: Analysis of 100 sites*, 2014. http://locusenergy.com/WhitePapers/sam-modeling-accuracy/, Visited March 9th, 2015.

Sadineni, S. B., Madala, S., Boehm, R. F. 2011. Passive building energy savings: A review of building envelope components. *Renewable and Sustainable Energy Reviews* 15(8):3617-3631.

Sartori, I. and Hestnes, A. G. 2007. Energy use in the life cycle of conventional and low-energy buildings: A review article. *Energy and buildings* 39(3):249-257.

Sharma, A., Saxena, A, Sethi, M., and Shree, V. 2011. Life cycle assessment of buildings: a review. *Renewable and Sustainable Energy Reviews* 15(1):871-875.

Short, W., Packey, D.J. and Holt, T. 1995. *A Manual for the Economic Evaluation of Energy Efficiency and Renewable Energy Technologies*. NREL/TP-462-5173. Golden, CO: National Renewable Energy Laboratory.

Shu-hua, L., Yuan, C. and Xue, Z. 2010, July. Notice of Retraction Life-cycle energy assessment of urban residential buildings in China. *Advanced Management Science (ICAMS), 2010 IEEE International Conference 1*:186-190.

Siddiqui, O. and Fung, A. 2009. Utilization of Thermal Mass in the Toronto Net Zero Energy House for Thermal Comfort and Energy Savings. *Eleventh International IBPSA Conference, Glasgow, Scotland.*

Singh, A., Berghorn, G., Joshi, S. and Syal, M. 2010. Review of life-cycle assessment applications in building construction. *Journal of Architectural Engineering*.

Skoczek, A., Sample, T. and Dunlop, E. D. 2009, The results of performance measurements of field-aged crystalline silicon photovoltaic modules *Prog. Photovolt: Res. Appl., 17*: 227–240.

Solomon, S., Qin, D., Manning, M., Chen, Z., Marquis, M., Averyt, K., Tignor, M., and Miller, H. 2007. *Intergovernmental Panel on Climate Change, 4th Assessment Report, Climate Changer 2007 The Physical Science Basis*. New York and Cambridge. UK: Cambridge University Press.

SRCC 06-160 *Testing method and minimum standard for certify solar collectors-referenced ISO Standard* 980 6-1 Section 9.

Stek, E., DeLong, D., McDonnell, T. and Rodriguez, J. 2011. Life cycle assessment using ATHENA impact estimator for buildings: A case study. *Proceedings of the 2011 Structures Congress, Las Vegas, Nevada*.

Stern, N. 2007. *The Economics of Climate Change: The Stern Review*. New York and Cambridge. UK: Cambridge University Press.

Straube, J. 2009. The Passive House (Passivhaus) Standard: A Comparison to Other Cold Climate Low-energy Houses. *Insight* 1-7.

Sustainable Building Industry Council (SBIC). 2012. *High Performance and Sustainability Topics*, http://www.sbicouncil.org/high-performance-buildings. Accessed June 20th, 2012.

System Advisor Model Version 2014.1.14 (SAM 2014.1.14) User Documentation. *Sizing the Flat Plate PV System.* Golden, CO: National Renewable Energy Laboratory.

System Advisor Model Version 2014.1.14 (SAM 2014.1.14). Golden, CO: National Renewable Energy Laboratory. https://sam.nrel.gov/content/downloads. Visited October 16, 2013.

Texas Comptroller of Public Accounts. 2012. The Impact of the 2001 Drought and Beyond. http://www.window.state.tx.us/specialrpt/drought/96-1704-Drought.pdf. Visited Sep 2014.

Texas Water Development Board (TWDB). 2014. *Annual Statewide Water Use*. http://www.twdb.state.tx.us/waterplanning/waterusesurvey/estimates/data/Texas%20Statewide%20Media%20Report.pdf. Visited July 2014.

Thevenard, D. and Pelland, S. 2011. Estimating the uncertainty in long-term photovoltaic predictions, *Solar Energy 191*:432-445.

Theis, T. 2005. *Summary: Materials Use: Science, Engineering and Society (MUSES)*. http://www.nsf.org/geo/ere/ereweb/beconf/muses2004/muses_ws_oct2005.pdf.

Thompson, G. L. 1995. *Airtightness tests for American Polysteel form houses*, Contract # SW1547AF. Southwest Infrared Inc.

Thompson, H. K. 2010. A fortified, LEED home of the US gulf coast: The How's and Why's of a Building System That Makes Sense, *Journal of Green Building* 5(1): 19-35.

Thormark, C. 2002. A low energy building in a life cycle—its embodied energy, energy need for operation and recycling potential. *Building and environment* 37(4):429-435.

Torio, H., Angelotti, A. and Schmidt, D. 2009. Exergy analysis of renewable energy-based climatisation systems for buildings: A critical view. *Energy and Buildings* 41(3):248–271.

Treloar, G., Fay, R., Ilozor, B. and Love, P. 2001. Building materials selection: greenhouse strategies for built facilities. *Facilities* 19(3/4):139-150.

Trusty, W. B. and Meil, J. K.1999. Building life cycle assessment: residential case study. *Proceedings: Mainstreaming Green: Sustainable Design for Buildings and Communities. Chattanooga, TN*.

U. S. Department of Energy (US DOE), Energy Efficiency and Renewable Energy, Building Technologies Program. 2011. *Building Energy Databook*.

US DOE, Energy Efficiency and Renewable Energy. 2014a. *EnergyPlus Energy Simulation Software – Testing and Validation.* http://apps1.eere.energy.gov/buildings/energyplus/energyplus_testing.cfm. Visited July 2015.

US DOE, Office of Energy Efficiency and Renewable Energy. 2014b. *Zero Energy Ready Home*, http://www.energy.gov/eere/buildings/zero-energy-ready-home. Visited November 2014.

US Energy Information Administration (US EIA). 2004-2009. *Residential sector energy intensities, Total square feet of housing units (US and Census Region).* http://www.eia.gov/emeu/efficiency/recs_tables_list.htm. Visited August 2015.

US EIA. 2009. *Household energy use in Texas.* http://www.eia.gov/consumption/residential/reports/2009/state_briefs/pdf/tx.pdf. Visited June 2015.

US EIA. 2013. *Heating and cooling no longer majority of US home energy use*. March 7, 2013. http://www.eia.gov/todayinenergy/detail.cfm?id=10271. Visited August 2015.

US EIA. 2015. *Drivers of US Household Energy Consumption,* 1980-2009. http://www.eia.gov/analysis/studies/buildings/households/pdf/drivers_hhec.pdf. Visited July 2015.

US Environmental Protection Agency (US EPA). 2011. *Life Cycle Assessment (LCA),* http://www.epa.gov/nrmrl/lcaccess/. Visited March 2011.

UNICEF and WHO 2012. *Progress on drinking water and sanitation. 2012 Update WHO/UNICEF Joint Monitoring Program for Water Supply and Sanitation*, WHO Library Cataloging-in-Publication Data.

United States Green Building Council (USGBC). 2015. *LEED Homes credits and points*, http://www.usgbc.org/articles/leed-homes-credits-and-points. Visited June 2015.

Vignola, F., Grover, C., Lemon, N. and McMahan, A. 2012. Building a Bankable Solar Radiation Dataset. *Solar Energy* 86(8):2218-2229.

Villarreal, E. L. and Dixon, A. 2005. Analysis of a rainwater collection system for domestic water supply in Ringdansen, Norrköping, Sweden. *Building and Environment* 40(9): 1174-1184.

Wang, L., Gwilliam, J., & Jones, P. 2009. Case study of zero energy house design in UK. *Energy and buildings* 41(11):1215-1222.

Ward, S. L. 2012. *Rainwater harvesting in the UK: a strategic framework to enable transition from novel to mainstream*, PhD in Engineering, University of Exeter, Exeter, Devon EX4, UK.

Ward, S., Memon, F. A. and Butler, D. 2008. Rainwater harvesting: model-based design evaluation, *11th International Conference on Urban Drainage, Edinburgh, Scotland, UK, Scotland, UK*, 2008.

Wilcox, S. and Marion, W. 2008. *Users Manual for TMY3 Data Sets, NREL Technical Report,* NREL/TP-581-43156. Golden, CO: National Renewable Energy Laboratory

Wohlgemuth, J. H., Cunningham, D. W., Monus, P., Miller, J., and Nguyen, A. 2006. Long term reliability of photovoltaic modules. *Photovoltaic Energy Conversion, Conference Record of the 2006 IEEE 4th World Conference* 2:2050-2053.

Zargarzadeh, M., Karimi, I. A. and Alfadala, H. E. 2007. Olexan: a tool for online exergy analysis. *17th European symposium on computer-aided process engineering Bucharest, Romania, computer-aided chemical engineering* 24.

Zhang, Y., Singh, S. and Bakshi, B. R. 2010. Accounting for ecosystem services in life cycle assessment, Part I: a critical review. *Environmental science and technology* 44(7):2232-2242.

Zhou, Y. P., Wu, J. Y. and Wang, R. Z. 2007. Performance of energy recovery ventilator with various weathers and temperature set-points. *Energy and Buildings* 39(12): 1202-1210.

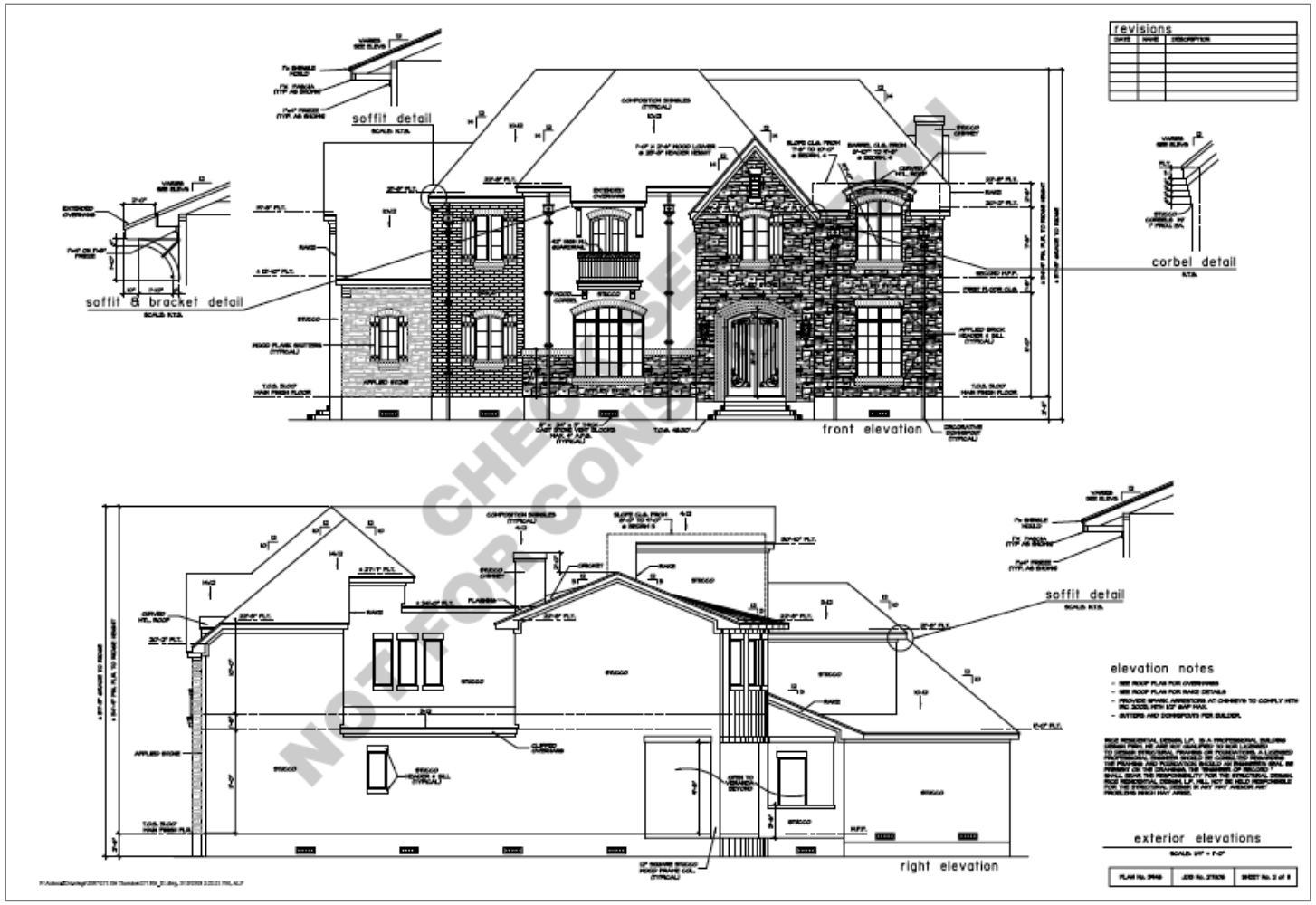

Appendix A-1. North and south elevations

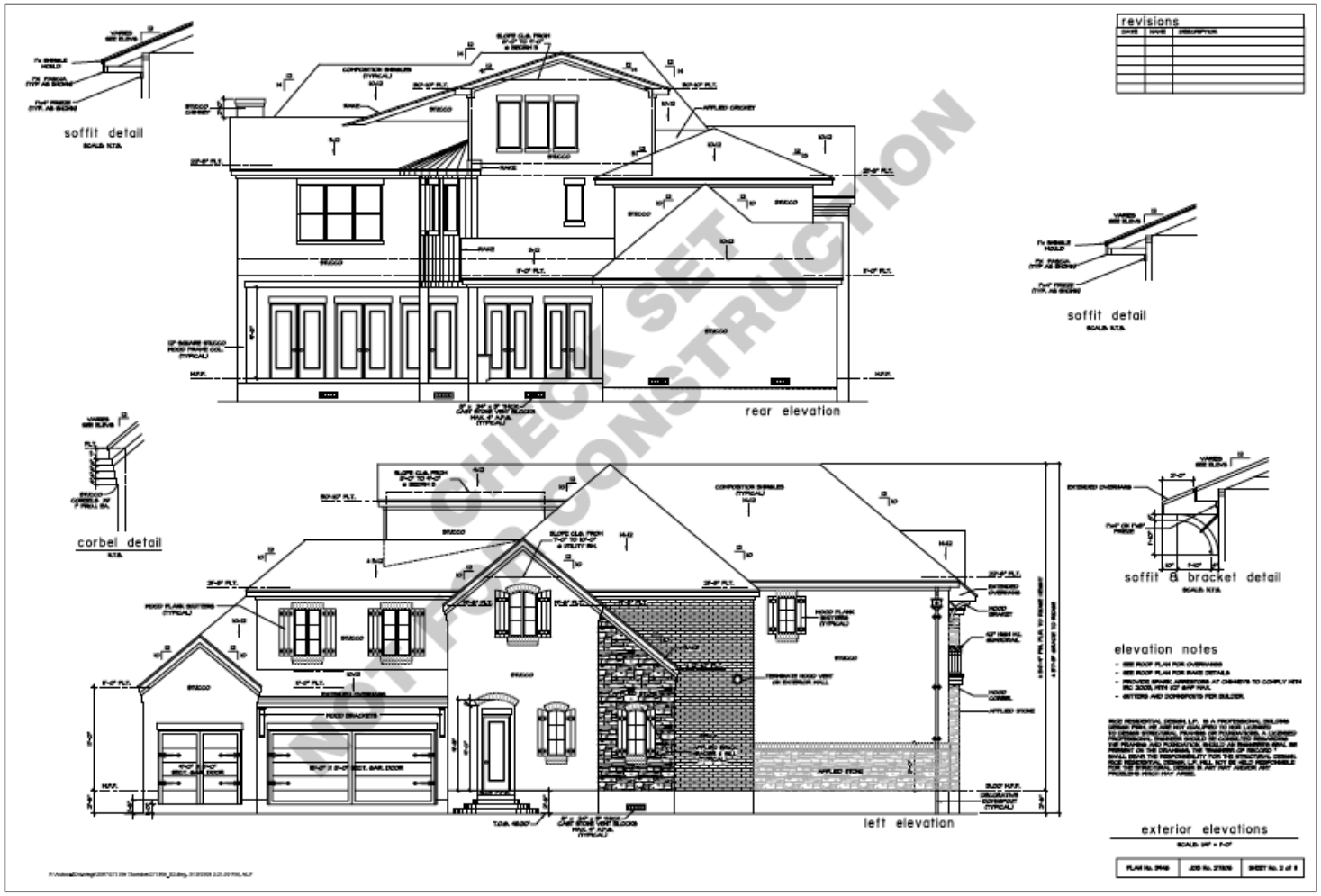

Appendix A-2. South and east elevations

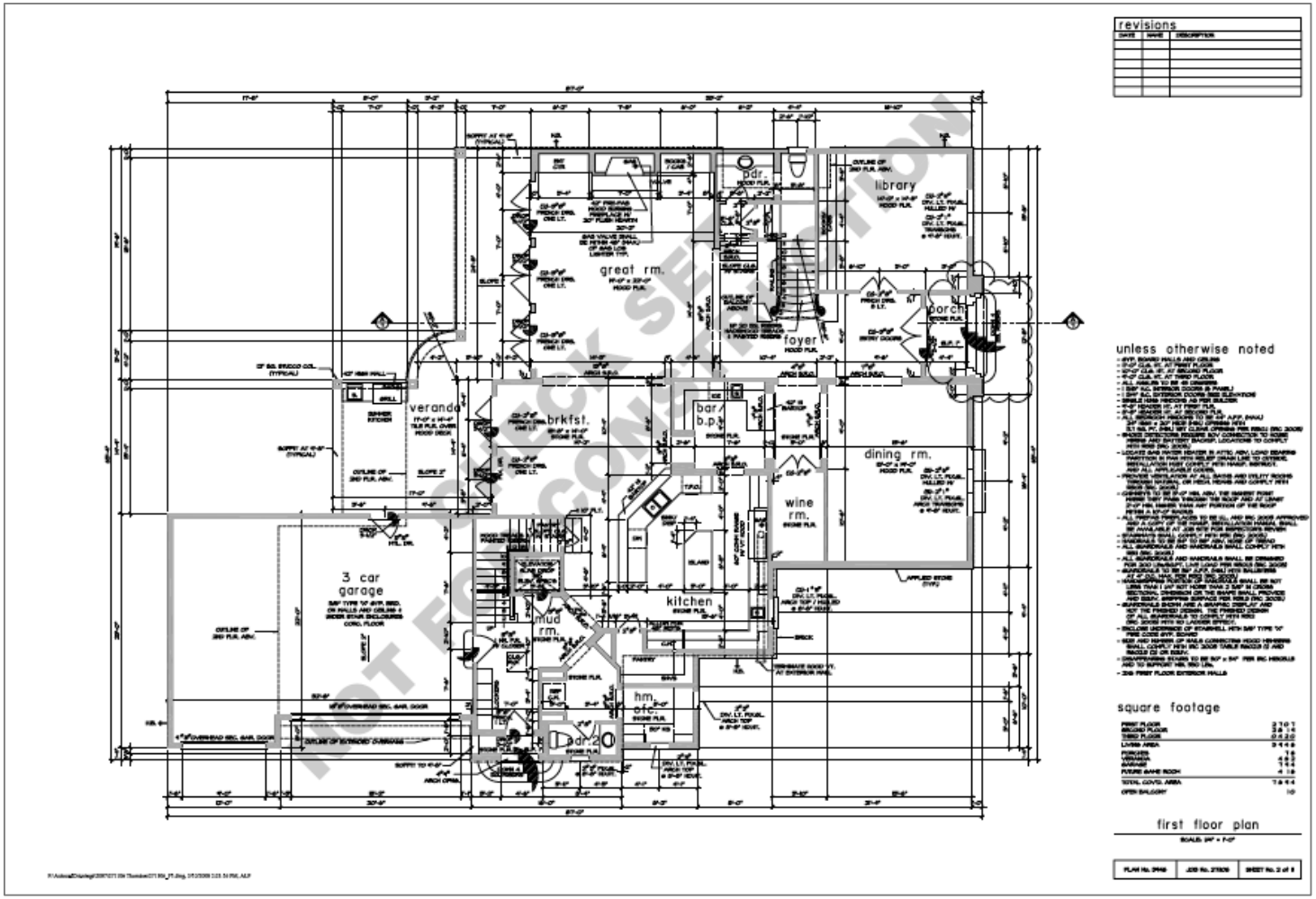

Appendix A-3. First floor plan

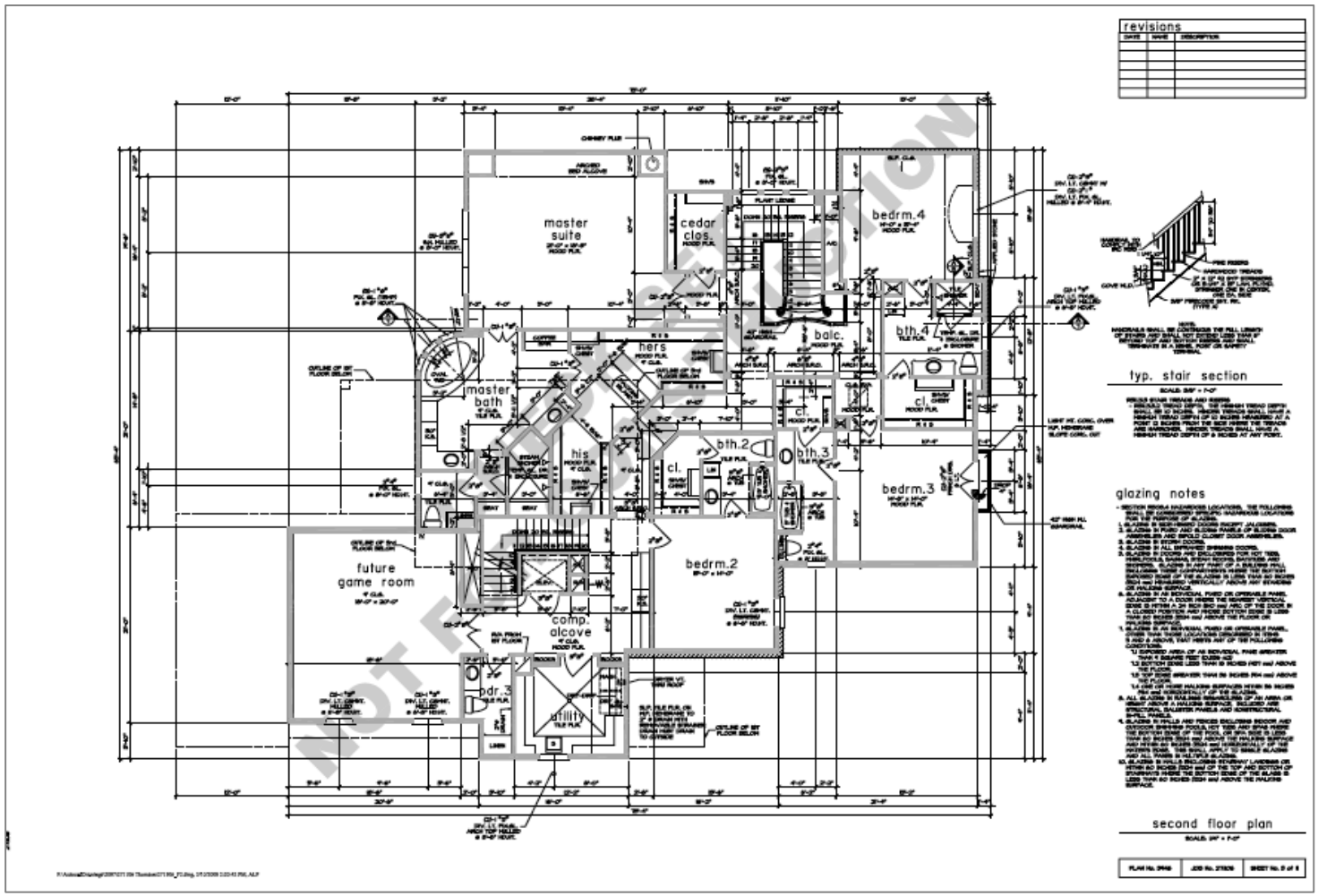

Appendix A-4. Second floor plan

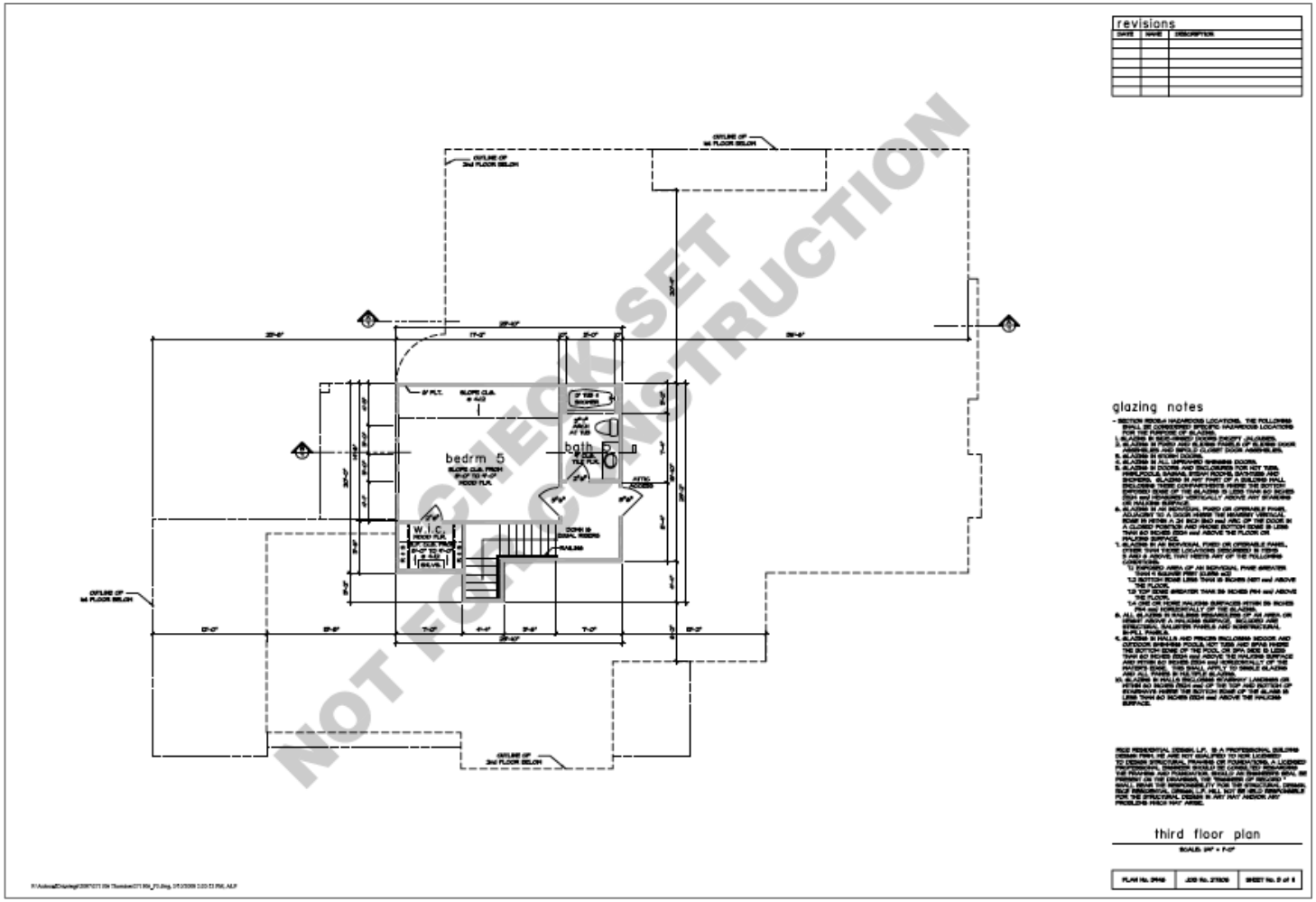

Appendix A-5. Third floor plan

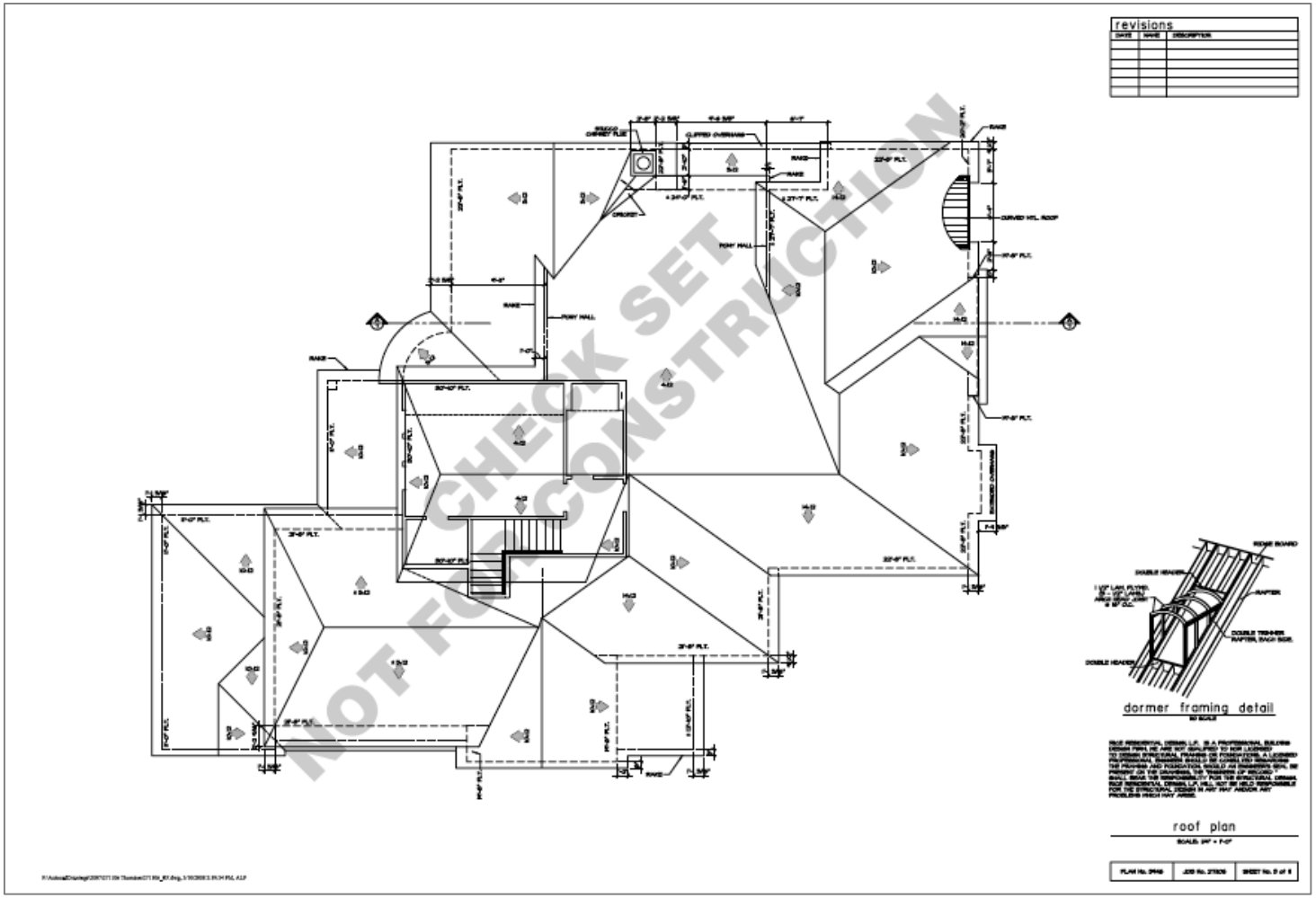

Appendix A-6. Roof plan

Month	Temperature (°F)
Jan	67.83
Feb	68.84
Mar	71.34
April	77.91
May	82.99
June	84.52
July	86.1
August	88.58
September	87.11
October	82.14
November	73.76
December	68.22

Appendix A-7. Monthly ground temperatures at 1 ft below grade (Reddy 2000)

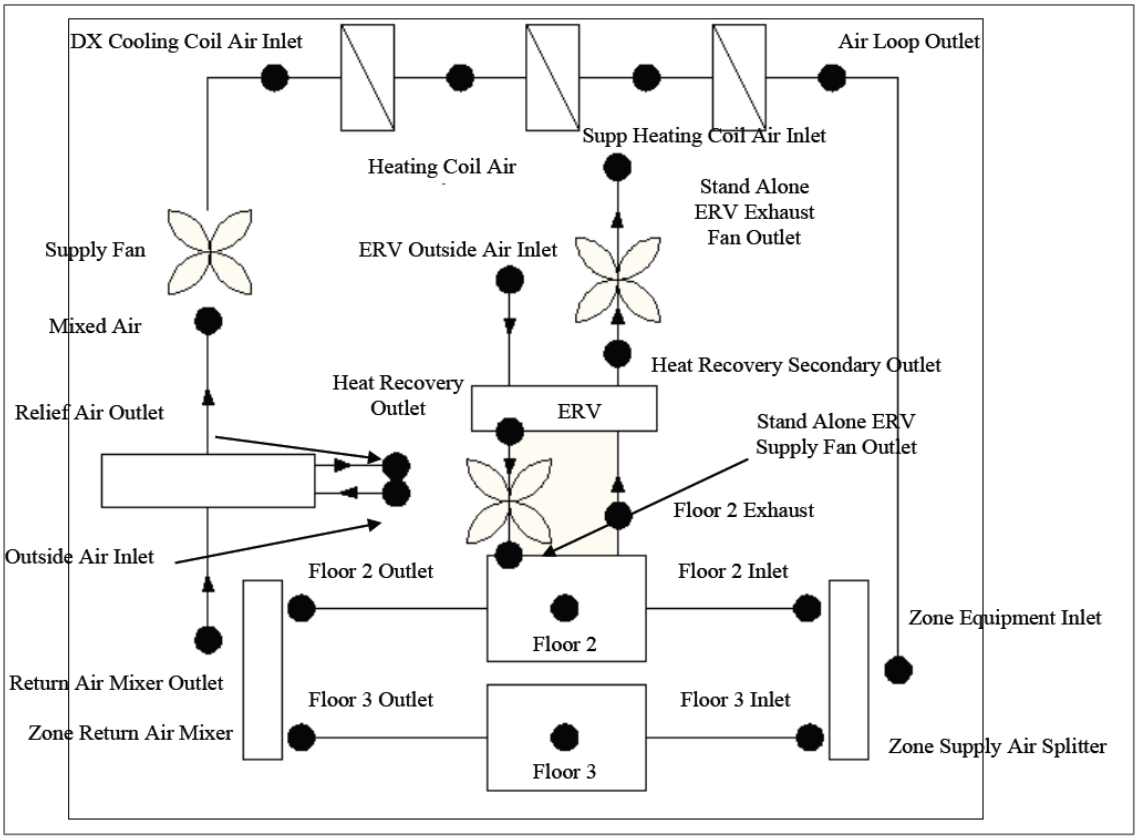

Appendix A-8. Simulation idealized airflow model

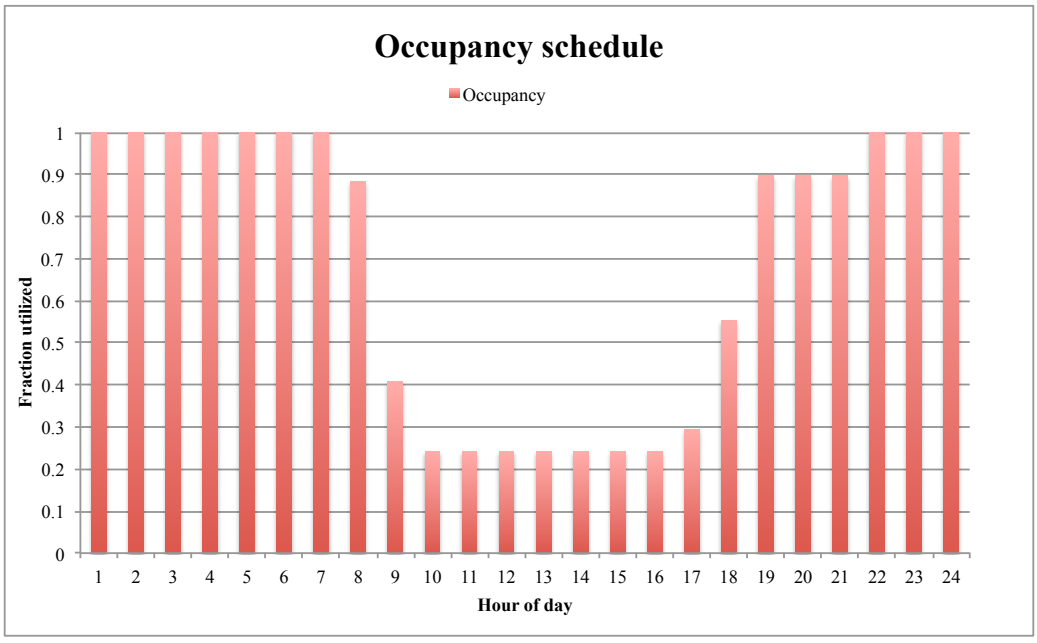

Appendix A-9. Occupancy 24-hour fractional schedule

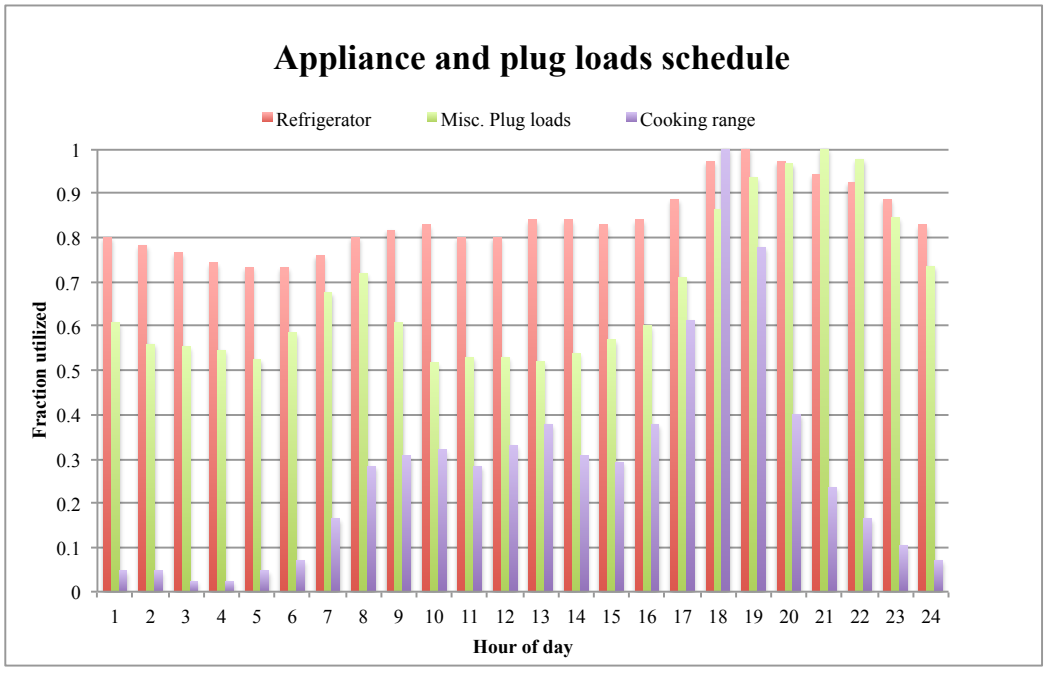

Appendix A-10. Appliance and plug load 24-hour fractional schedule

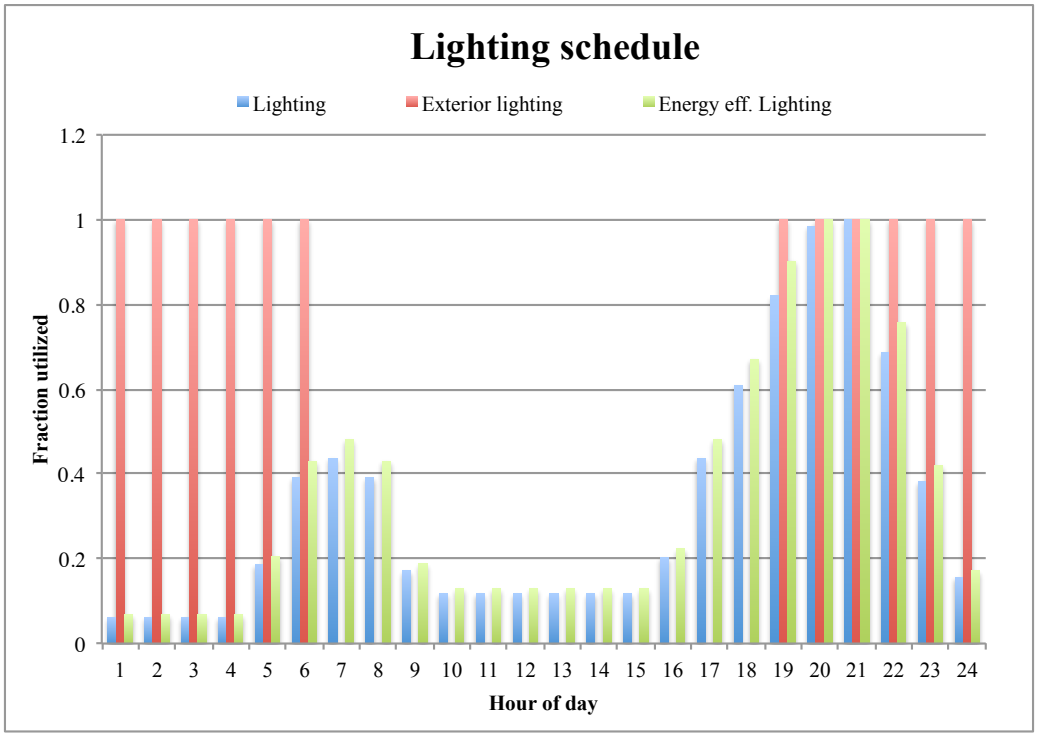

Appendix A-11. Lighting 24-hour fractional schedule

Appliance	Power	Total Electricity (kWh/yr)	Fraction Sensible	Fraction Latent	Fraction Lost	Internal heat gains (kWh/yr) IECC 2012
Refrigerator	91.09 W	668.9	1	0	0	669
Clothes Washer	29.6 W	109.216	0.8	0	0.2	87
Clothes Dryer	222.11 W	868.15	0.15	0.05	0.8	174
Dishwasher	68.33 W	214.16	0.6	0.15	0.25	161
Range (ele/gas)	248.97 W	604.9	0.4	0.3	0.3	423
Misc plug loads	0.228 W/ft^2	8585.1	0.69	0.06	0.25	6439
Misc ele loads	182.5 W	1598	0.69	0.06	0.25	1199
IECC adjustment factor	0.275 W/ft^2	1035.47	0.69	0.06	0.25	777
Lighting		1580.5	1	0	0	1580.5
Occupants						2831

Appendix A-12. Model annual internal gains and electrical loads

Type	Energy Use
Interior hardwired	0.8 × CFA × 0.542 +334 kwh/yr
Interior plug-in lighting	0.2 × CFA × 0.542 +334 kwh/yr
Garage lighting	Garage area × 0.08 +8 kwh/yr
Exterior lighting	CFA × 0.145 kwh/yr

Appendix A-13. Baseline lighting energy use for the IECC PNNL estimates based Mendon et al. 2013. CFA = conditioned floor area

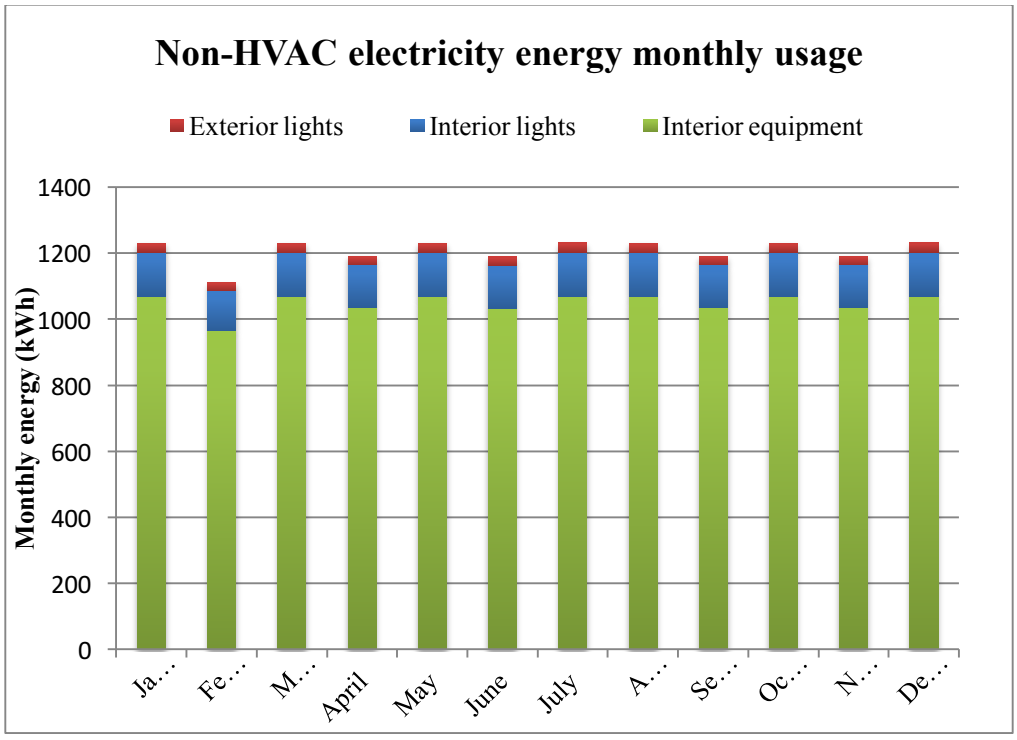

Appendix A-14. Non-HVAC monthly electricity of interior equipment, interior and exterior lighting

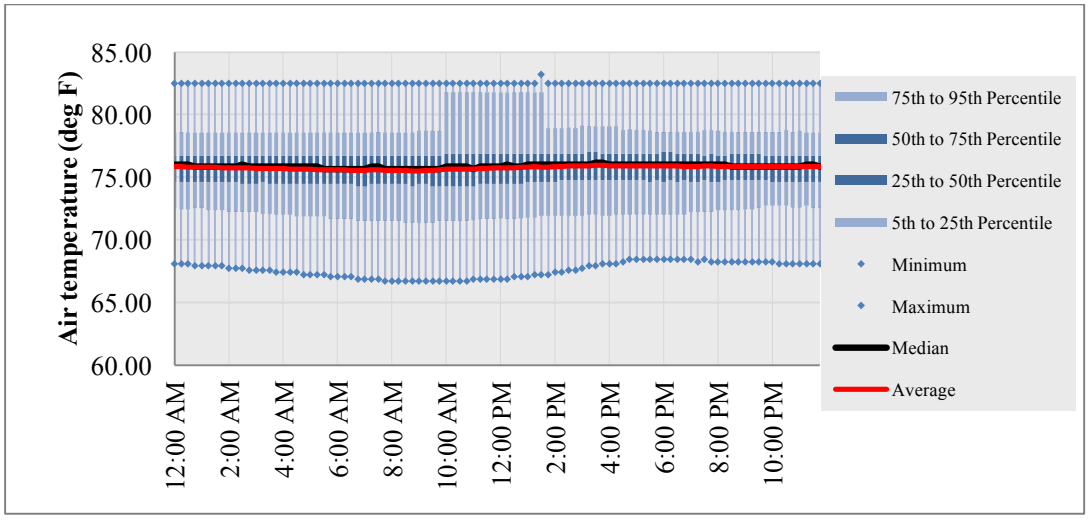

Appendix A-15. First floor air temperature daily profile at the thermostat

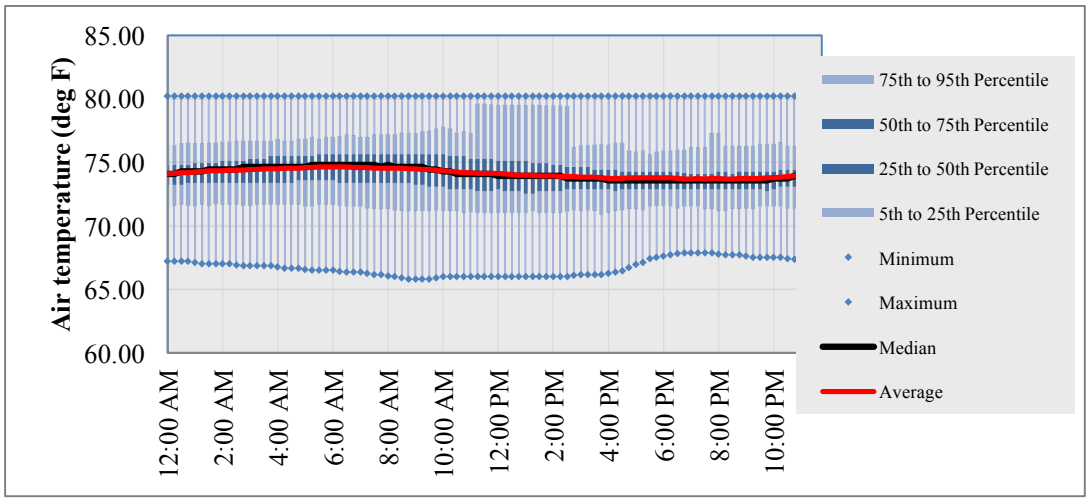

Appendix A-16. Second floor air temperature daily profile at thermostat

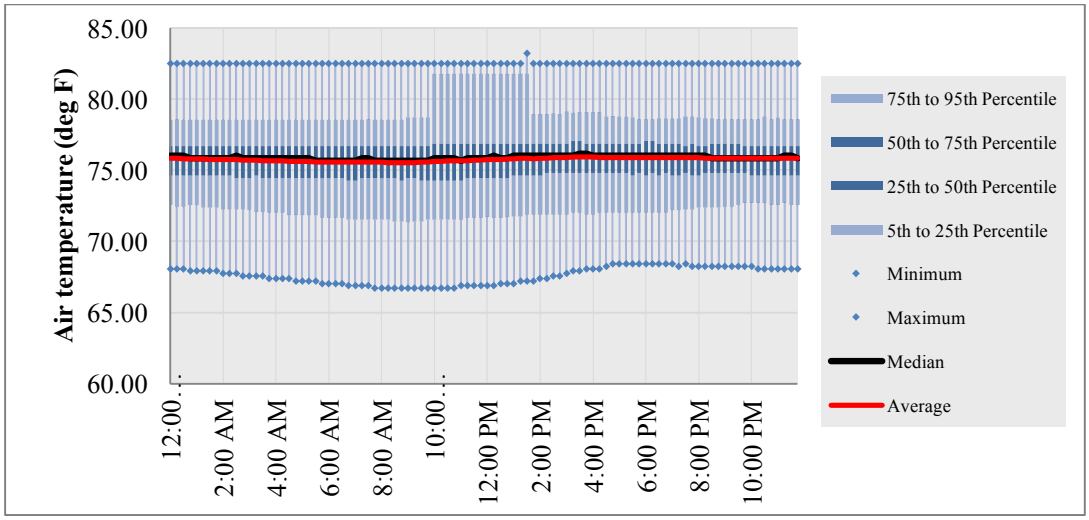

Appendix A-17. Third floor air temperature daily profile at the thermostat

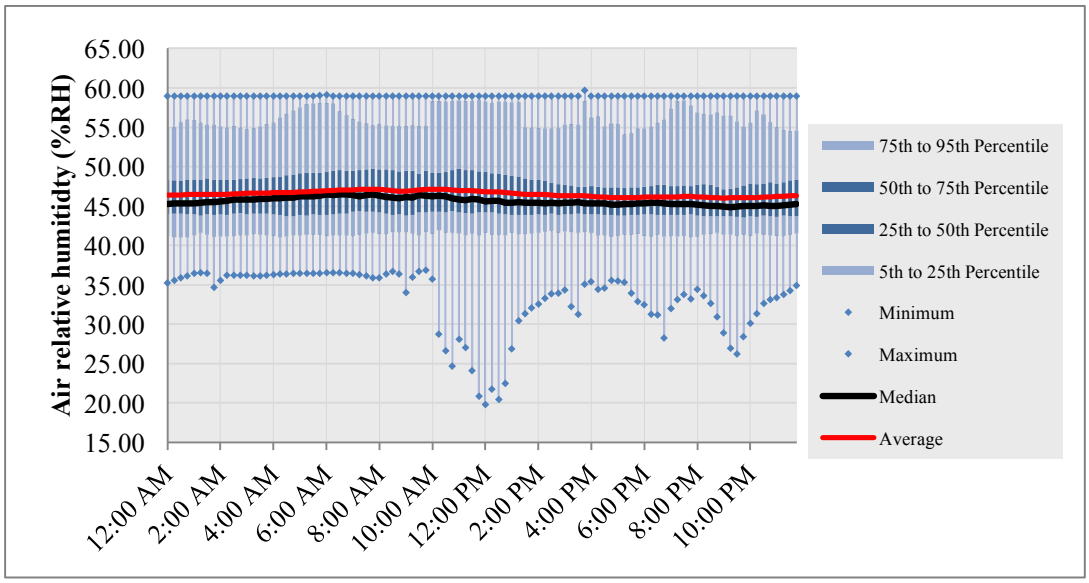

Appendix A-18. First floor air relative humidity at thermostat

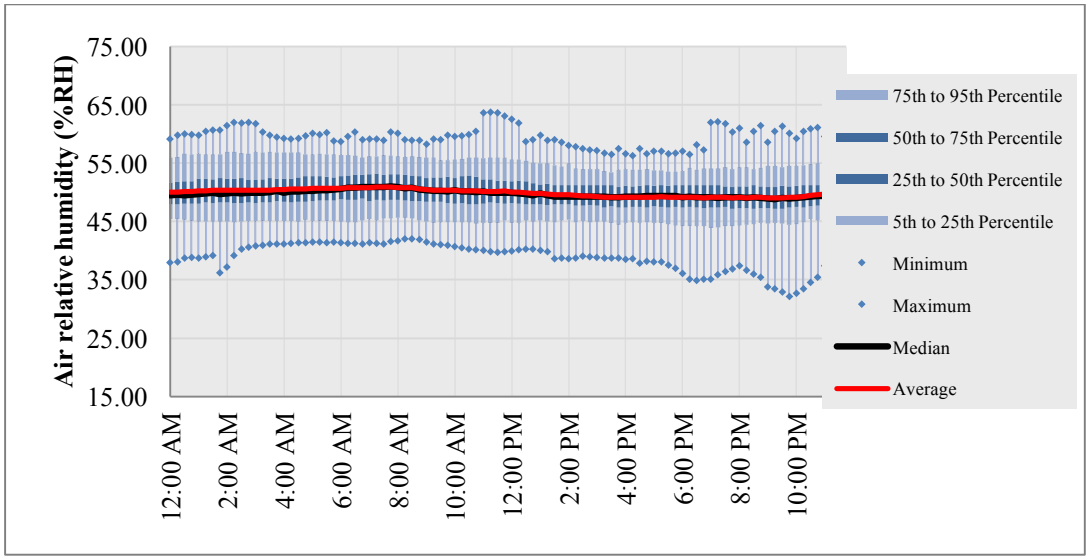

Appendix A-19. Second floor air relative humidity at thermostat

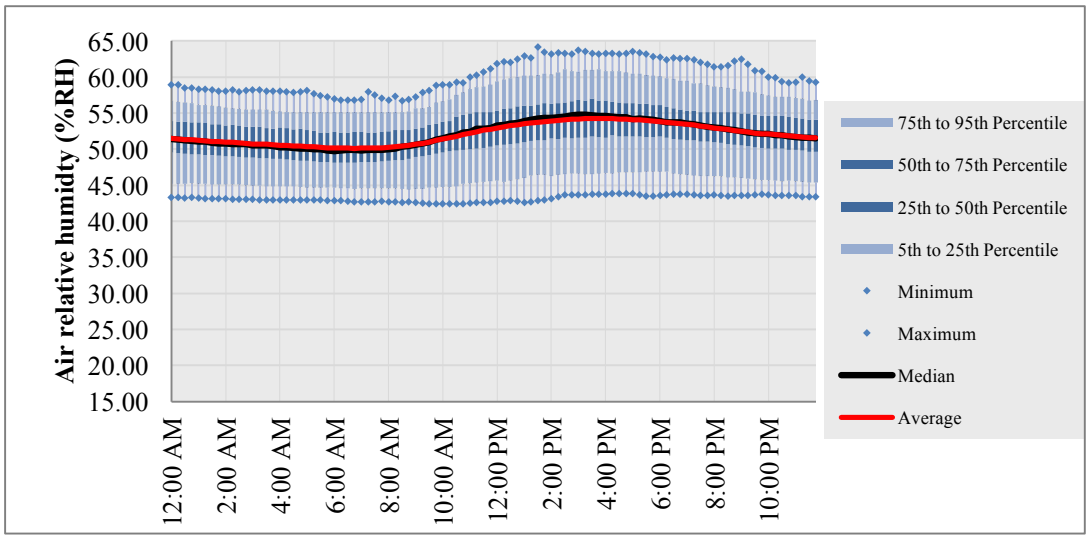

Appendix A-20. Third floor air relative humidity at thermostat

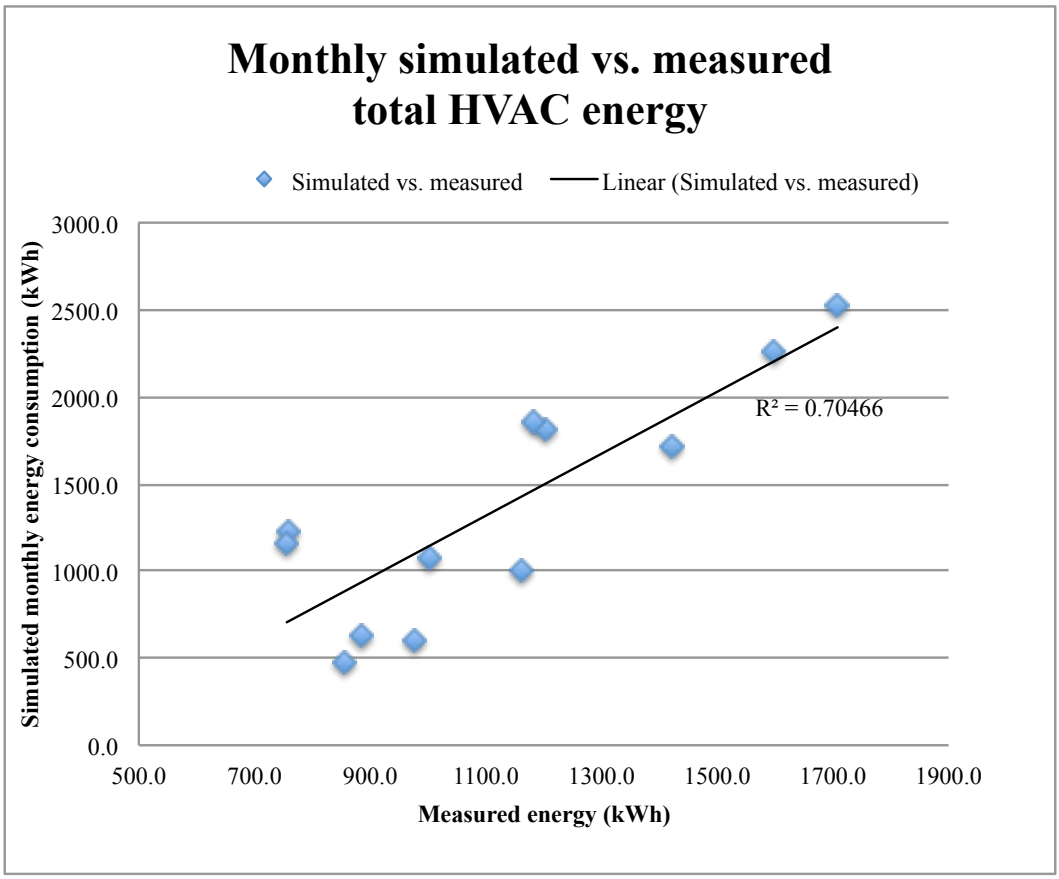

Appendix A-21. Monthly simulated vs. measured HVAC energy

Life Cycle Analysis Environmental Indicators Overview

LCA environmental impact indicators are mappings from quantities of emissions to the environmental impacts that these emissions cause and these impact categories have been established from nationally recognized standards established by agencies such as the Environmental Protection Agency, Occupational Safety and Health Administration, and National Institutes of Health (Bayer et al. 2010). These impacts are usually given as a ratio of the quantity of the impact per functional unit of product produced. Each category is an indicator of the contribution of a product to a specific environmental problem (Bayer et al. 2010). A group of impact indicators common in many LCA methods are provided on the following page.

Indicator	Description	Unit
Global Warming Potential (GWP)	Global Warming Potential, or GWP, has been developed to characterize the change in the greenhouse effect due to emissions and absorptions attributable to humans. The unit for measurement is grams equivalent of CO2 per unit of product (note that other greenhouse gases, such as methane, are included in this category, thus the term "CO" is an impact and not an emission).	CO_2 equiv mass
Acidification Potential (AP)	Acidifying compounds emitted in a gaseous state either dissolve in atmospheric water or fixed on solid particles. They reach ecosystems through dissolution in rain. The two compounds principally involved in acidification are sulfur and nitrogen compounds. The unit of measurement is grams of hydrogen ions per functional unit of product.	H+ equiv. mass
Eutrophication Potential (EP)	Eutrophication is the addition of mineral nutrients to the soil or water. In both media, the addition of large quantities of mineral nutrients such as nitrogen and phosphorous results in generally undesirable shiftsinthenumberofspeciesinecosystemsandareductioninecologicaldiversity. In waterways, excess nutrient leads to increase biological oxygen demand (BOD) from the dramatic increase in flora that feed on these nutrients, a subsequent reduction in dissolved oxygen levels, and the collapse of fish and other aquatic species. The unit of measurement is grams of nitrogen per functional unit of product.	N equiv. mass
Fossil Fuel Depletion	This impact addresses only the depletion aspect of fossil fuel extraction, not the fact that the extraction itself may generate impacts. The unit for measurement is mega joules (MJ) of fossil-based energy per functional unit of the product. This category helps demonstrate positive environmental goals, such as reducing the energy needed to produce a product, or such as producing a product with renewable, non- fossil-based energy.	MJ
Smog Formation Potential	Under certain climatic conditions, air emissions from industry and fossil-fueled transportation can be trapped at ground level, where they react with sunlight to produce photochemical smog. The contribution of a product or system to smog formation is quantified by this category. The unit of measurement is grams of nitrogen oxide per functional unit of product. This highlights an area where a regional approach to LCA may be appropriate, as certain regions of the world are climatically more susceptible to smog.	O_3 equiv. mass
Ozone Depletion Potential	Emissions from some processes may result in the thinning of the ozone layer, which protects the earth from certain parts of the solar radiation spectrum. Ozone depletion potential measures the extent of this impact for a product or system. The unit of measurement is CFC-11 per functional unit of the product.	CFC-11 equiv. mass

Appendix A-22. Life cycle analysis environmental impact indicators (Adapted from Bayer et al. 2010)

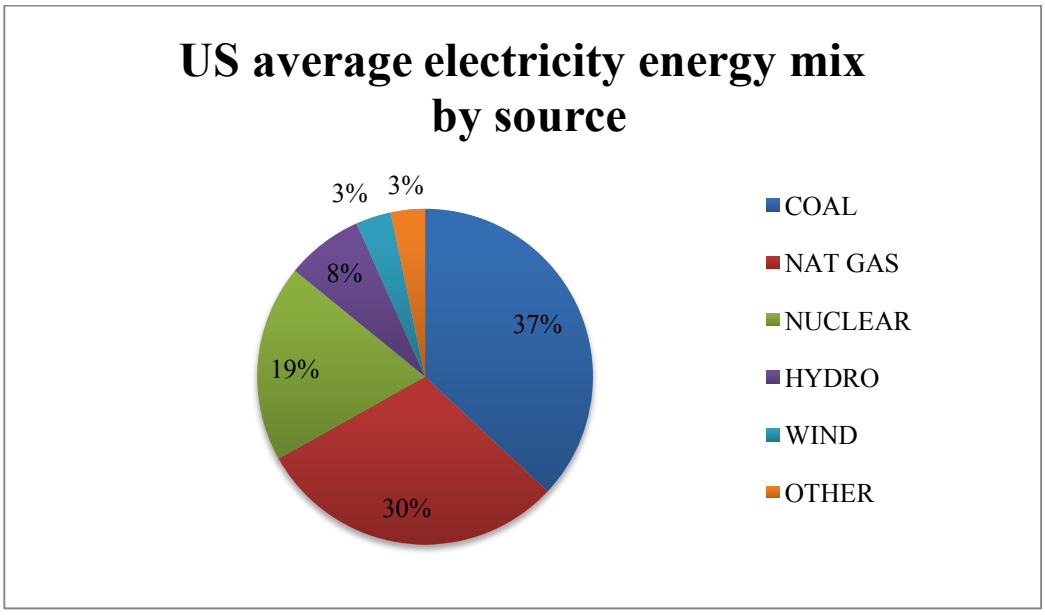

Appendix A-23. Average US energy mix utilized in Impact Estimator based on average 2012 US energy mix data from the US DOE (Finlayson 2015)

ENVIRONMENTAL INDICATOR		REFERENCE MODEL					AS-BUILT MODEL					REFERNCE	AS-BUILT
Summary Measure	Unit	FOUNDATION	WALLS	ROOF	FLOORS	EXTRA MAT.	FOUNDATION	WALLS	ROOF	FLOORS	EXTRA MAT.	TOTAL	TOTAL
Global Warming Potential	(kg CO2 eq)	8.99E+04	8.18E+03	-3.17E+03	-1.33E+04	-3.61E+03	9.14E+04	4.96E+04	1.35E+04	-1.39E+04	-4.53E+03	7.80E+04	1.36E+05
Acidification Potential	(kg SO2 eq)	5.04E+02	1.97E+02	5.65E+01	1.02E+02	1.19E+01	5.25E+02	4.04E+02	1.44E+02	1.00E+02	1.39E+01	8.71E+02	1.19E+03
HH Particulate	(kg PM2.5 eq)	2.15E+02	6.12E+01	1.93E+01	4.17E+01	8.05E+00	2.17E+02	1.25E+02	3.96E+01	4.11E+01	9.42E+00	3.45E+02	4.32E+02
Eutrophication Potential	(kg N eq)	2.08E+01	1.16E+01	3.48E+00	9.39E+00	1.28E+00	2.24E+01	1.91E+01	7.65E+00	9.03E+00	1.54E+00	4.65E+01	5.97E+01
Ozone Depletion Potential	(kg CFC-11 eq)	5.17E-04	2.22E-04	2.47E-06	6.46E-05	2.56E-05	5.19E-04	4.93E-04	1.94E-04	5.62E-06	2.56E-05	8.31E-04	1.24E-03
Smog Potential	(kg O3 eq)	1.03E+04	2.70E+03	9.50E+02	1.91E+03	2.64E+02	1.11E+04	6.67E+03	2.12E+03	1.83E+03	3.13E+02	1.61E+04	2.20E+04
Total Primary Energy	(MJ)	9.35E+05	4.55E+05	2.61E+05	2.78E+05	3.82E+04	9.53E+05	8.92E+05	7.32E+05	2.65E+05	4.46E+04	1.97E+06	2.89E+06
Non-Renewable Energy	(MJ)	9.30E+05	3.83E+05	2.25E+05	1.81E+05	2.15E+04	9.48E+05	8.25E+05	6.91E+05	1.69E+05	2.42E+04	1.74E+06	2.66E+06
Fossil Fuel Consumption	(MJ)	8.38E+05	3.61E+05	2.16E+05	1.62E+05	1.88E+04	8.62E+05	7.92E+05	6.32E+05	1.52E+05	2.14E+04	1.60E+06	2.46E+06

Appendix A-24. Life cycle environmental impact indicator by building assembly

ENVIROMENTAL INDICATOR		REFERENCE MODEL LIFE CYCLE STAGE				AS-BUILT MODEL LIFE CYCLE STAGE				REFERENCE	AS-BUILT
Summary Measure	Unit	PRODUCT	CONSTRUCTION	USE	END OF LIFE	PRODUCT	CONSTRUCTION	USE	END OF LIFE	TOTAL	TOTAL
Global Warming Potential	(kg CO2 eq)	9.67E+04	1.76E+04	1.55E+06	8.96E+03	1.45E+05	2.37E+04	1.10E+06	1.15E+04	1.68E+06	1.28E+06
Acidification Potential	(kg SO2 eq)	5.50E+02	1.53E+02	1.20E+04	1.03E+02	7.72E+02	2.06E+02	8.47E+03	1.32E+02	1.28E+04	9.58E+03
HH Particulate	(kg PM2.5 eq)	2.88E+02	1.94E+01	1.34E+03	5.16E+00	3.70E+02	2.52E+01	9.62E+02	6.35E+00	1.65E+03	1.36E+03
Eutrophication Potential	(kg N eq)	2.81E+01	9.31E+00	1.02E+02	6.74E+00	3.58E+01	1.26E+01	7.30E+01	8.70E+00	1.46E+02	1.30E+02
Ozone Depletion Potential	(kg CFC-11 eq)	7.34E-04	3.25E-05	6.58E-05	3.52E-07	1.11E-03	4.95E-05	7.43E-05	4.54E-07	8.33E-04	1.24E-03
Smog Potential	(kg O3 eq)	7.44E+03	4.38E+03	4.18E+04	3.54E+03	1.07E+04	6.08E+03	2.99E+04	4.56E+03	5.72E+04	5.12E+04
Total Primary Energy	(MJ)	1.37E+06	2.36E+05	2.45E+07	1.25E+05	2.06E+06	3.15E+05	1.74E+07	1.60E+05	2.62E+07	2.00E+07
Non-Renewable Energy	(MJ)	1.17E+06	2.23E+05	2.34E+07	1.25E+05	1.85E+06	3.01E+05	1.67E+07	1.60E+05	2.49E+07	1.90E+07
Fossil Fuel Consumption	(MJ)	1.01E+06	2.16E+05	2.03E+07	1.24E+05	1.66E+06	2.94E+05	1.44E+07	1.59E+05	2.17E+07	1.66E+07

Appendix A-25. Life cycle environmental impact indicator by life cycle stage (gas space and water heating)

ENVIROMENTAL INDICATOR		REFERENCE MODEL LIFE CYCLE STAGE				AS-BUILT MODEL LIFE CYCLE STAGE				REFERENCE	AS-BUILT
Summary Measure	Unit	PRODUCT	CONSTRUCTION	USE	END OF LIFE	PRODUCT	CONSTRUCTION	USE	END OF LIFE	TOTAL	TOTAL
Global Warming Potential	(kg CO2 eq)	9.67E+04	1.76E+04	1.63E+06	8.96E+03	1.45E+05	2.37E+04	1.17E+06	1.15E+04	1.76E+06	1.35E+06
Acidification Potential	(kg SO2 eq)	5.50E+02	1.53E+02	1.25E+04	1.03E+02	7.72E+02	2.06E+02	8.93E+03	1.32E+02	1.33E+04	1.00E+04
HH Particulate	(kg PM2.5 eq)	2.88E+02	1.94E+01	1.45E+03	5.16E+00	3.70E+02	2.52E+01	1.04E+03	6.35E+00	1.76E+03	1.44E+03
Eutrophication Potential	(kg N eq)	2.81E+01	9.31E+00	1.06E+02	6.74E+00	3.58E+01	1.26E+01	7.62E+01	8.70E+00	1.50E+02	1.33E+02
Ozone Depletion Potential	(kg CFC-11 eq)	7.34E-04	3.25E-05	6.59E-05	3.52E-07	1.11E-03	4.95E-05	7.44E-05	4.54E-07	8.33E-04	1.24E-03
Smog Potential	(kg O3 eq)	7.44E+03	4.38E+03	4.46E+04	3.54E+03	1.07E+04	6.08E+03	3.20E+04	4.56E+03	5.99E+04	5.32E+04
Total Primary Energy	(MJ)	1.37E+06	2.36E+05	2.56E+07	1.25E+05	2.06E+06	3.15E+05	1.84E+07	1.60E+05	2.73E+07	2.09E+07
Non-Renewable Energy	(MJ)	1.17E+06	2.23E+05	2.44E+07	1.25E+05	1.85E+06	3.01E+05	1.75E+07	1.60E+05	2.59E+07	1.99E+07
Fossil Fuel Consumption	(MJ)	1.01E+06	2.16E+05	2.09E+07	1.24E+05	1.66E+06	2.94E+05	1.51E+07	1.59E+05	2.23E+07	1.72E+07

Appendix A-26. Life cycle environmental impact indicators by life cycle stage (electrical gas and water heating)

ENVIROMENTAL INDICATOR		REFERENCE MODEL		AS-BUILT MODEL	
Summary Measure	Unit	USE STAGE	USE STAGE WITH RE	USE STAGE	USE STAGE WITH RE
Global Warming Potential	(kg CO2 eq)	1.55E+06	1.41E+06	1.10E+06	9.55E+05
Acidification Potential	(kg SO2 eq)	1.20E+04	1.08E+04	8.47E+03	7.34E+03
HH Particulate	(kg PM2.5 eq)	1.34E+03	1.22E+03	9.62E+02	8.44E+02
Eutrophication Potential	(kg N eq)	1.02E+02	9.26E+01	7.30E+01	6.32E+01
Ozone Depletion Potential	(kg CFC-11 eq)	6.58E-05	6.57E-05	7.43E-05	7.41E-05
Smog Potential	(kg O3 eq)	4.18E+04	3.80E+04	2.99E+04	2.61E+04
Total Primary Energy	(MJ)	2.45E+07	2.22E+07	1.74E+07	1.51E+07
Non-Renewable Energy	(MJ)	2.34E+07	2.12E+07	1.67E+07	1.45E+07
Fossil Fuel Consumption	(MJ)	2.03E+07	1.83E+07	1.44E+07	1.25E+07

Appendix A-27. Use phase environmental impact indicators comparison of 'Reference' and 'As-Built' models with and without renewable energy (RE)

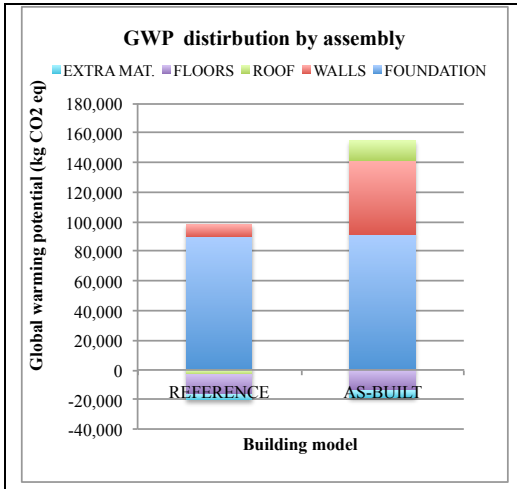

Appendix A-28. Global warming potential by building assembly

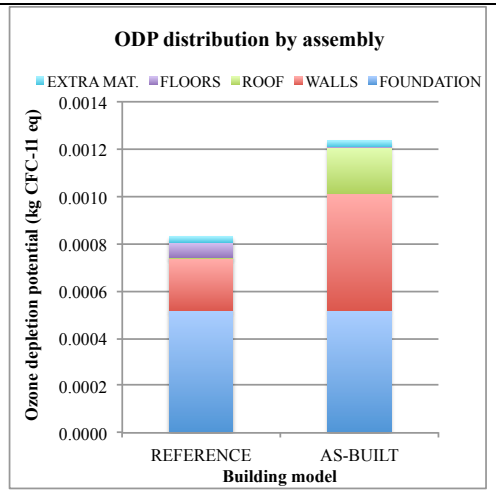

Appendix A-29. Ozone depletion potential by building assembly

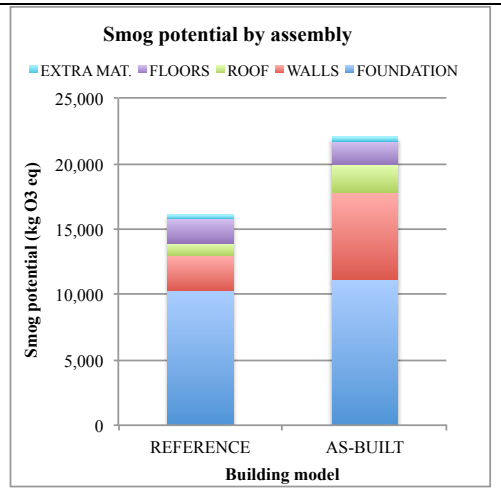

Appendix A-30. Smog potential by building assembly

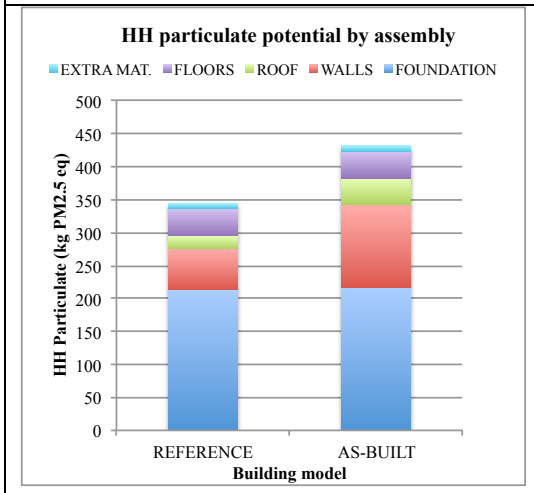

Appendix A-31. Human health potential by building assembly

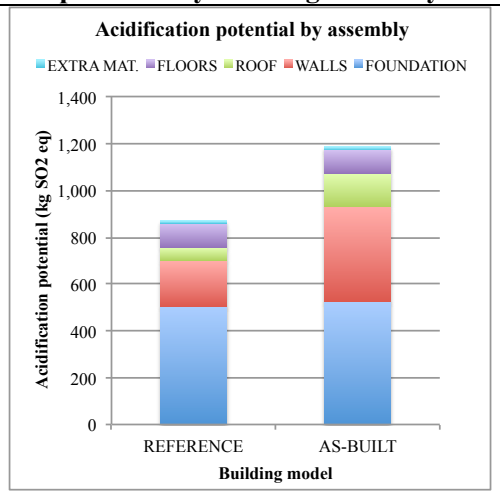

Appendix A-32. Acidification potential by building assembly

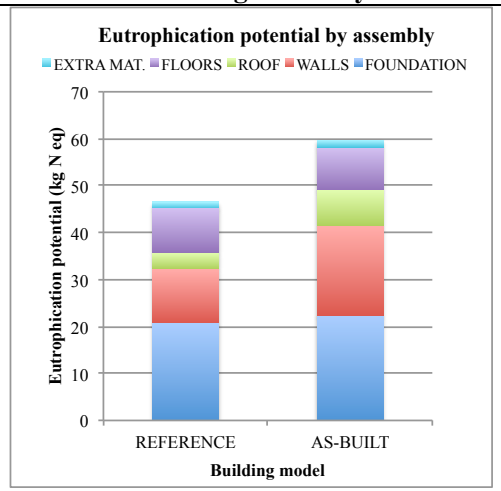

Appendix A-33. Eutrophication potential by building assembly

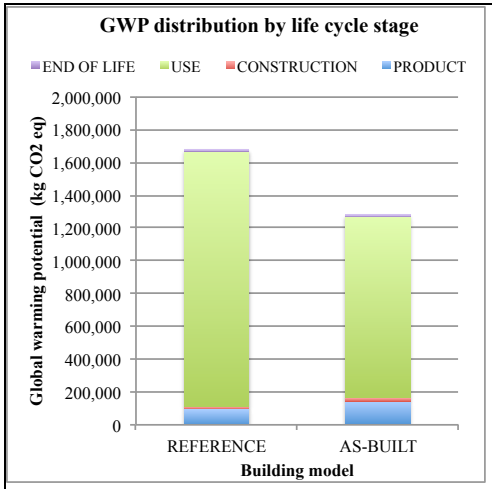

Appendix A-34. GWP distribution by life cycle stage

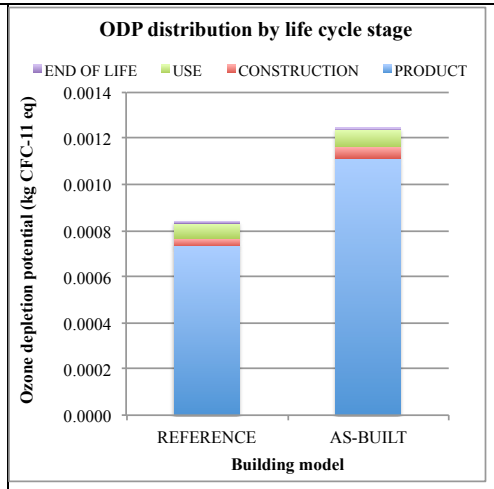

Appendix A-35. ODP distribution by life cycle stage

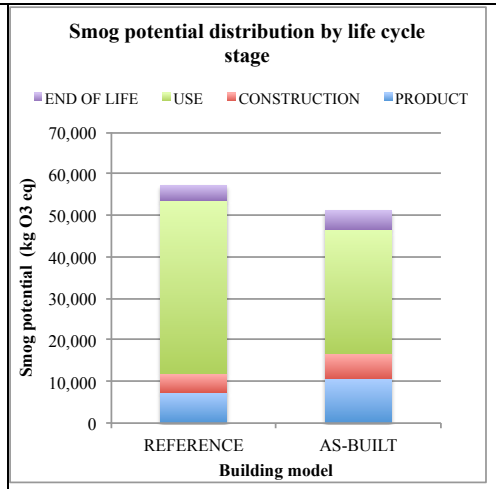

Appendix A-36. Smog potential distribution by life cycle stage

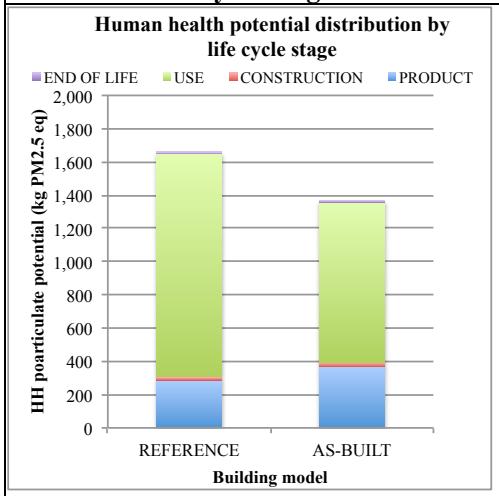

Appendix A-37. Human health potential distribution by life cycle

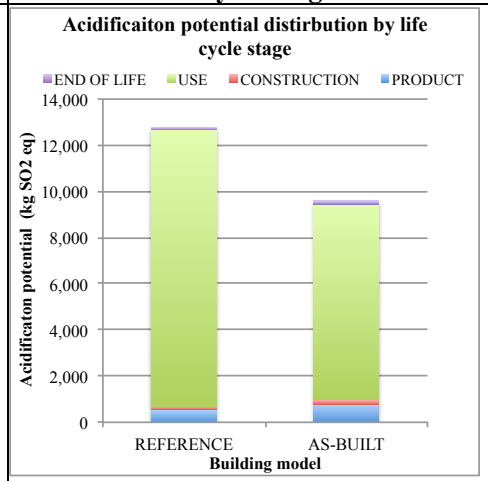

Appendix A-38. Acidification potential distribution by life cycle

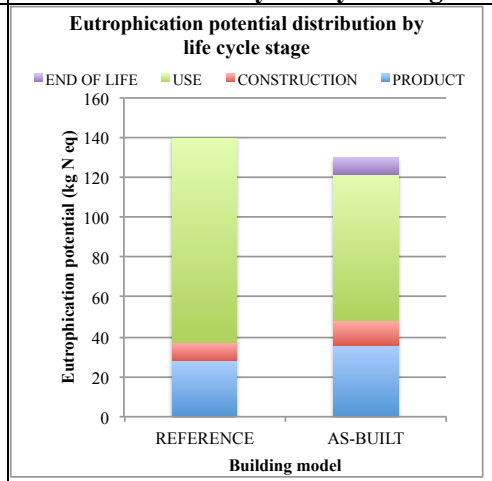

Appendix A-39. Eutrophication potential distribution by life cycle stage

GAS SPACE AND WATER HEATING MODELS							
ENVIRONMENTAL INDICATOR	REFERENCE MODEL	AS-BUILT MODEL	RELATIVE CHANGE	ENVIRONMENTAL INDICATOR	REFERENCE MODEL	AS-BUILT MODEL	RELATIVE CHANGE
EMBODIED ENERGY (GJ)	1,608.2	2,376.2	-48%	EMBODIED GWP (kg CO2-eq)	114,280	168,772	-48%
EMBODIED ENERGY INTENSITY (GJ/m^2)	2.7	4.0	-48%	EMBODIED GWP INTENSITY (kg CO2-	193.37	286	-48%
USE ENERGY (GJ)	24,483.3	17,446.5	29%	USE GWP (kg CO2-eq)	1,552,017	1,099,910	29%
USE ENERGY INTENSITY (GJ/m^2)	41.4	29.5	29%	USE GWP INTENSITY (kg CO2-eq/m^2)	2626	1861	29%
TOTAL PRIMARY ENERGY (GJ)	26,216.8	19,983.0	24%	TOTAL GWP (kg CO2-eq)	1,675,252	1,280,176	24%
TOTAL PRIMARY ENERGY (GJ/m^2)	44.4	33.8	24%	TOTAL GWP INTENSITY (kg CO2-eq/m	2835	2166	24%
EMBODIED ENERGY QUOTIENT (%)	6%	12%		EMBODIED GWP QUOTIENT (%)	7%	13%	
USE ENERGY QUOTIENT (%)	93%	87%		USE GWP QUOTIENT (%)	93%	86%	

Appendix A-40. Environmental indicator summary primary energy and global warming potential totals and intensities for the 'Reference' and 'As-Built' gas space and water heating models

ELECTRICAL SPACE AND WATER HEATING MODELS							
ENVIRONMENTAL INDICATOR	REFERENCE MODEL	AS-BUILT MODEL	RELATIVE CHANGE	ENVIRONMENTAL INDICATOR	REFERENCE MODEL	AS-BUILT MODEL	RELATIVE CHANGE
EMBODIED ENERGY (GJ)	1,608	2,376	-48%	EMBODIED GWP (kg CO2-eq)	114,280	168,772	-48%
EMBODIED ENERGY INTENSITY (GJ/m2)	2.7	4.0	-48%	EMBODIED GWP INTENSITY (kg CO2-eq/m2)	193.37	285.57	-48%
USE ENERGY (GJ)	25,597	18,401	28%	USE GWP (kg CO2-eq)	1,632,951	1,166,140	29%
USE ENERGY INTENSITY (GJ/m2)	43.31	31	28%	USE GWP INTENSITY (kg CO2-eq/m2)	2763	1973	29%
TOTAL PRIMARY ENERGY (GJ)	27,331	20,937	23%	TOTAL GWP (kg CO2-eq)	1,756,187	1,346,406	23%
TOTAL PRIMARY ENERGY (GJ/m2)	46	35	23%	TOTAL GWP INTENSITY (kg CO2-eq/m2)	2972	2278	23%
EMBODIED ENERGY QUOTIENT (%)	6%	11%		EMBODIED GWP QUOTIENT (%)	7%	13%	
OPERATIONAL ENERGY QUOTIENT (%)	94%	88%		OPERATIONAL GWP QUOTIENT (%)	93%	87%	

Appendix A-41. Environmental indicator summary primary energy and global warming potential totals and intensities for the 'Reference' and 'As-Built' electric space and water heating models

Classification	Coefficients	Unit	Mean, m (preset)	Uncertainty, u (%)	u^2	Remamrks	Cited From
System	Inverter Module Efficiency	%	97	3	9.00		PV1
	Subarrary AC Wiring Loss	%	2	1.5	2.25	Total AC loss 4.45%, u=1.5%	own
	Subarray DC Wiring Loss	%	1	1.5	2.25	total DC loss 6.89%, u=1.5%	own
	Nameplate Loss	%	5	1.5	2.25	u=1.5%	own
	Soiling Loss	%	0.5	1.5	2.25	Not applicable to SAM Stochastics	own, PV1
	Albedo	-	0.2	2.9	8.33	Not applicable to SAM Stochastics	own, PV1
	Temperature Coeff pow	%/°C	-0.453	0	0.00	u=±0.05%	MFG
	Temperature Coeff Isc	%/°C	0.065	0	0.00	u=±0.015%	MFG
	Temperature Coeff Voc	mV/°C	-160	0	0.00	u=±20mV/°C	MFG
	NOCT	°C	46	0	0.00	u=±2°C	MFG
Resource	Solar (ir)Radiation	%		3.59	12.85	see 'Solar Resource Statistics'	NREL
	COMBINED UNCERTAINTY (%)			6.26			

Appendix A-42. Solar photovoltaic system uncertainty

Classification	Coefficients	Unit	Mean (preset)	Uncertainty, u (%)	u^2	Remamrks	Cited From
System	Total System Flow Rate	kg/s	0.02	0.8	0.64	0.80%	ST1
	Albedo	-	0.2	2.9	8.33		own
	Collector- Frta	-	0.717	0	0.00	independent var. of ΔT, U, etc.	
	Collector - FRUL	W/m2.C	4.01	0	0.00	independent var. of ΔT, U, etc.	
	Heat Exchanger Effectiveness	-	0.75	1.5	2.25		ST1
	Solar Tank heat loss Coefficient	W/m2.C	0.55	1.5	2.25		ST1, ST2
	Pump Efficiency	-	0.95	1.5	2.25		own, ST1
	Inlet&Outlet Temperature Diff	°C		1.10	1.21	uΔT=0.6C/54.44C (outlet set temp)	own, ST1
Resource	Solar (ir)Radiation	%		3.59	12.85	see 'Solar Resource Statistics'	NREL
	COMBINED UNCERTAINTY (%)			5.46			

Reference List

PV1 Didier Thevenard, Sophie Pelland, Estimating the uncertainty in long-term photovoltaic yield predictions, Solar Energy, Volume 91, May 2013, Pages 432-4 Link

ST1 Emmanouil Mathioulakis, George Panaras, Vassilis Belessiotis, Uncertainty in estimating the performance of solar thermal systems, Solar Energy, Volume 8 Link

ST2 E. Mathioulakis, K. Voropoulos, V. Belessiotis, Assessment of uncertainty in solar collector modeling and testing, Solar Energy, Volume 66, Issue 5, August Link

Appendix A-43. Solar hot water system uncertainty

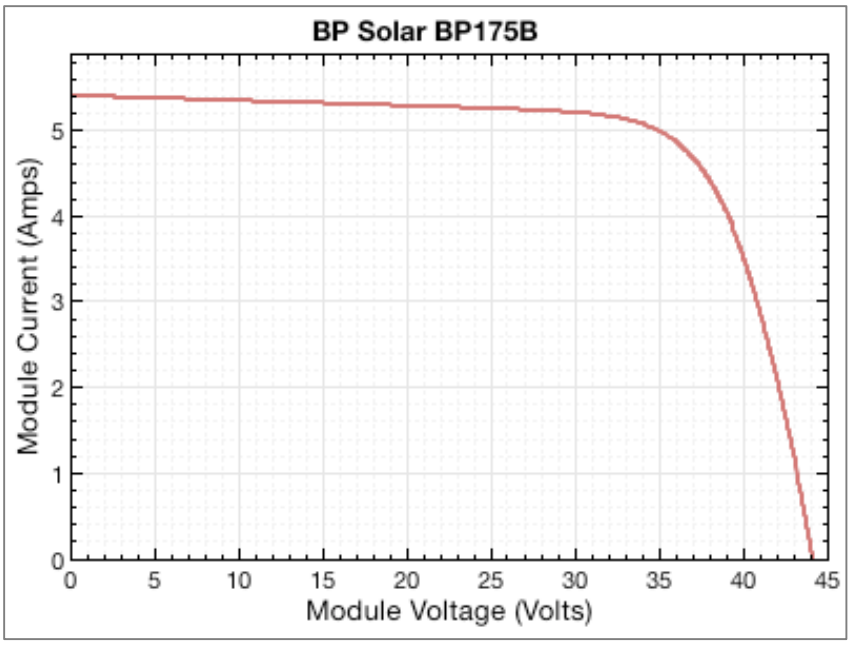

Appendix A-44. SPVS module (BP Solar BP175B) characteristic curve

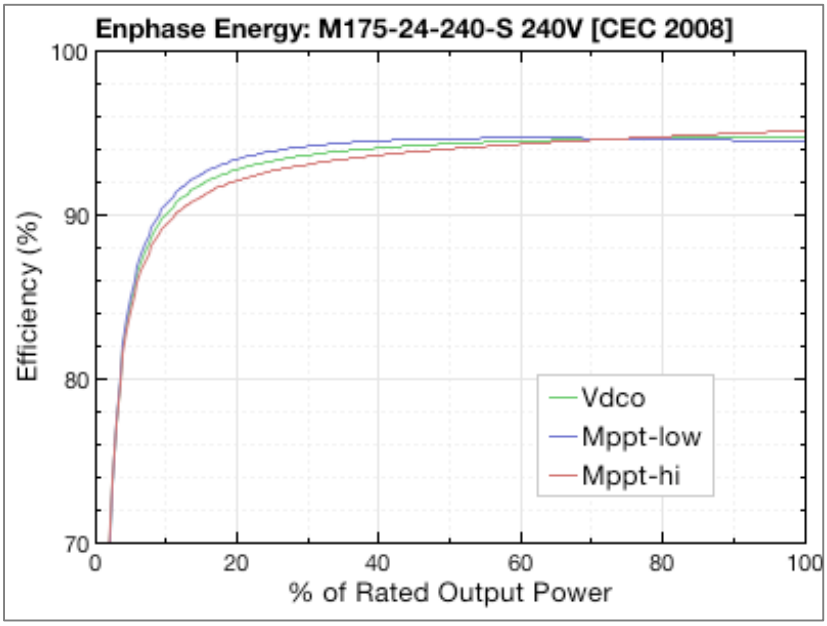

Appendix A-45. SPVS Module inverter (Enphase Energy M175) characteristic curve

Instrument and model	Manufacturer	Website	Purpose of equipment	Calibration Information (if applicable)	Quantity
Hobo U10	Onset Computer, Inc.	http://www.onsetcomp.com/	Measure indoor temperature and humidty and data logger	Riverside Energy Efficiency Laboratory (REEL) TAMU	8
Hobo Energy Logger	Onset Computer, Inc.	http://www.onsetcomp.com/	Logger for submeter data from the house electrical panel	Onset Computer, Inc.	1
Watt Node Pulse	Continential Control Systems	http://www.ccontrolsys.com	Power measurement of heat pump and ERV	Continential Control Systems	2
Hobo 20	Onset Computer, Inc.	http://www.onsetcomp.com/	Water level and temperature gauge	Onset Computer, Inc.	1
E-series 55	Badger Meter, Inc.	http//badgermeter.com	Water flow meter	Badger Meter, Inc.	1
Web Energy Logger	Phil Malone	http://welserver.com	Embedded 1-wire data logger	Maxim Semiconductor, Inc.	1
1-wire temperature system	Maxim semiconductor, Inc.	http://welserver.com	Ten sensors monitoring roof and solar thermal system	Maxim semiconductor, Inc. And REEL	10
Enphase 175-24	Enphase Energy, Inc.	http://enphase.com	Photovoltaic monitoring system	Enphase Energy, Inc.	1
H8053-0100 Enercept	Veris, Inc.	http//veris.com	Whole building energy monitoring	Veris, Inc.	1
Smart reader Plus 9	ACR Systems, Inc.	http://www.acrsystems.com	Two channel digital input logger, one for WBE and water flow	ACR Systems, Inc.	2

Appendix A-46. Equipment list for the study presented herein